A brief introduction to the basics of NMR spectroscopy and selected examples of its applications to materials characterization

Alberto Tampieri,[1] Márk Szabó,[2] Francisco Medina Cabello,[1] Henrik Gulyás[2,3*]

[1] DEQ, etsEQ, Universitat Rovira i Virgili, Avinguda dels Països Catalans 26, 43007, Tarragona, Spain.
[2] XiMo Hungary Ltd., 1045 Budapest, Berlini utca 47-49.
[3] Fundació, Universitat Rovira i Virgili, Avinguda dels Països Catalans 18, 43007, Tarragona, Spain.

*Corresponding author.

Abstract

Nuclear magnetic resonance (NMR) spectroscopy is an analytical technique that gives information on the local magnetic field around atomic nuclei. Since the local magnetic field of the nucleus is directly influenced by such features of the molecular structure as constitution, configuration, conformation, intermolecular interactions, etc., NMR can provide exhaustive information on chemical structure, which is unrivaled by any other analytical method. Starting from the 1950's, NMR spectroscopy first revolutionized organic chemistry and became an indispensable tool for structure elucidation of small, soluble molecules. As the technique evolved, NMR rapidly conquered other disciplines of chemical sciences. When the analysis of macromolecules and solids also became feasible, the technique turned into a staple in materials characterization, too.

All aspects of NMR spectroscopy, including technical and technological development, as well as its applications in natural sciences, have been growing exponentially since its birth. Hence, it would be impossible to cover, or even touch on, all topics of importance related to this versatile analytical tool. In this tutorial, we aim to introduce the reader to the basic principles of NMR spectroscopy, instrumentation, historical development and currently available brands, practical cost aspects, sample preparation, and spectrum interpretation. We show a number of advanced techniques (pulse sequences) relevant to materials characterization. Via a limited number of examples from different fields of materials science, we illustrate the immense scope of the technique in the analysis of materials.

Beyond our inherently limited introduction, an ample list of references should help the reader to navigate further in the field of NMR spectroscopy.

Keywords: Nuclear Magnetic Resonance Spectroscopy, Liquid-Phase NMR, Solid-State NMR, Pulse Sequences, MAS NMR, Dynamic Nuclear Polarization, Materials Characterization, Operando NMR

Contents

1 - Introduction

Nuclear magnetic resonance (NMR) spectroscopy is a non-destructive analytical technique that makes use of magnetic fields to obtain qualitative and quantitative information on gaseous,[1] liquid or solid samples.

The NMR phenomenon was firstly experienced on molecular hydrogen by Rabi et al. in 1939,[2] for which he was awarded a Nobel prize in Physics in 1944, while Bloch and Purcell were awarded one in 1952 for the development of methods to apply NMR to the analysis of liquids and solids. Since then the theoretical understanding of NMR has greatly increased. Also, current generation machines make use of incredibly powerful magnets[3] combined with very fast and precise electronics and mechanics.[4] These advances substantially improved the analysis resolution, and nowadays NMR methods can differentiate between analogous nuclei with very similar substituents (*e.g.* stereoisomers and conformers). In addition, complex pulse techniques were developed, allowing the user to obtain very specific information,[5] and for this Ernst and Wüthrich were awarded a Nobel prize in 1991 and 2003, respectively. Thanks to these, modern NMR methods give information that is hard to obtain by any other analytical tool, such as complete structure elucidation, distances between nuclei, torsional angles, and molecular dynamics.

Nowadays, NMR spectroscopy is a widespread analytical technique,[6] used in industry from composition and quality control to online process monitoring, in academia from structure elucidation and purity determination of organic compounds to the study of inorganic complexes, in medicine from protein and metabolic studies to magnetic resonance imaging (MRI).

An ever-growing branch of NMR spectroscopy is material characterization.[6] The technique is particularly suitable for the task as it can be applied to both soluble and insoluble solids, to crystalline and amorphous materials, to inorganic and organic solids and composites of the two. It provides structural and spatial information, and it can distinguish between different structures of a polymorph.

In this review we will briefly explain the theoretical background of NMR spectroscopy, we will give practical information on sample preparation and data analysis, and we offer a glimpse of the available spectrometers in terms of brands, capacity, and cost aspects. We will describe the method's capabilities in material characterization via a limited selection of relevant examples.

2 - Basic concepts

Nuclear magnetic resonance (NMR) **spectroscopy** is a technique that provides information on the local magnetic fields around atomic nuclei.[7]

Protons and neutrons are spinning nucleons characterized by a **nuclear spin quantum number** (*m*) , a fundamental property just like charge or mass, which can assume the value of -½ or ½ according to their magnetic behavior. Protons and neutrons combined form atomic nuclei, whose magnetic characteristic is described by the **nuclear spin** (*I*). *I* = 0 when all the opposite *m* are paired, while it corresponds to an integer multiple of ½ when the number of protons and/or neutrons are odd. *I* indicates the **total number of spin**

states that a nucleus can assume (equivalent to 2*I*+1), each of which has its own spin quantum number *m* in the range [-*I*, -*I*+1, …, *I*-1, *I*]. Nuclei with *I* = 0 have only one spin state, therefore they are said to be **magnetically inactive** and cannot be directly detected by NMR experiments.

The different spin states of a nucleus are degenerate, but the energy level split when the nucleus is immersed in a magnetic field B_0 (**nuclear Zeeman effect**). Nuclei populating different states will have different alignments to the magnetic field. However, their **magnetic moment vectors** will all precess around the direction of the magnetic field, with an equal angular frequency called **Larmor frequency** (ω). ω depends on the gyromagnetic ratio γ, a constant characteristic of a nuclide, and the external magnetic field. ν, the Larmor linear frequency, can be derived from the angular one.

^{1}H is by far the most studied nucleus by NMR, and will, therefore, be used as an example. ^{1}H nuclei are composed by single protons, thus their $I = ½$ and only two spin states α (parallel to the magnetic field, $m = ½$) and β (antiparallel, $m = -½$) are possible (Figure 1).

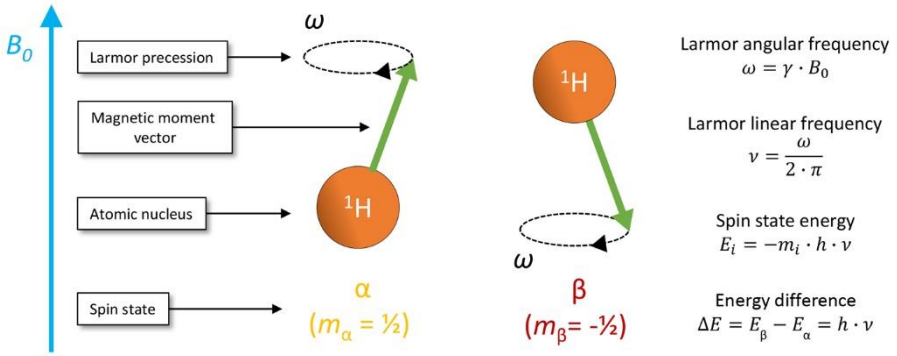

Figure 1. ^{1}H nuclei spin states description and related formulas.

Although the magnetic moment vectors of nuclei of the same state all precess with the same ω and same alignment in a magnetic field B_0, their precessions are out of phase (Figure 2). Therefore, all of their magnetic moment vectors are randomly oriented around the direction of B_0. For this reason, the resulting **net nuclear magnetizations** (M_α and M_β) are parallel to the magnetic field. The non-degeneration of states in a magnetic field will make the states whose magnetic vectors point the same direction as the field more stable and populated. As a result, the overall net nuclear magnetization (M) will also point to the direction of the magnetic field.

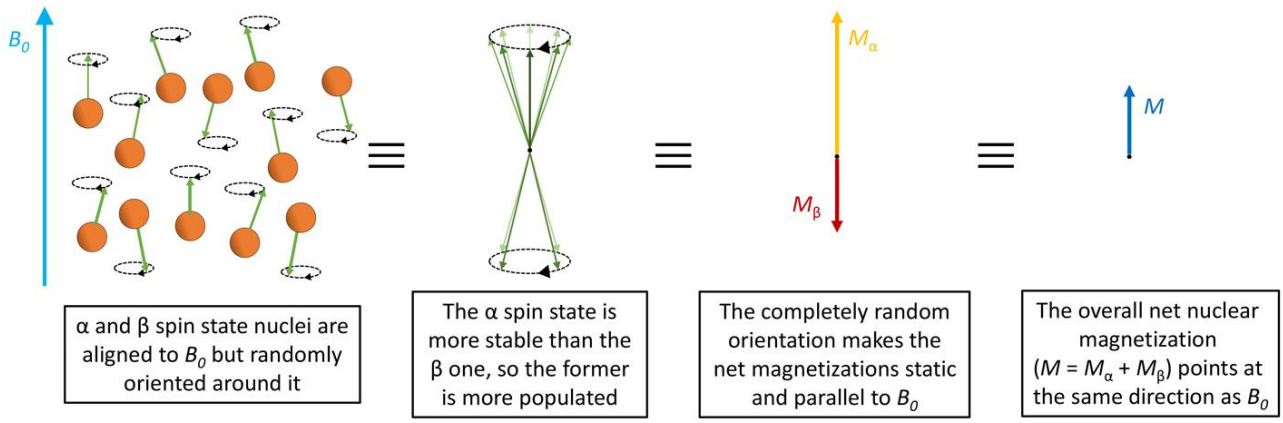

Figure 2. Net nuclear magnetization of ^{1}H nuclei in an external magnetic field (B_0). The populations are exaggeratedly different for explanatory purposes.

If nuclei immersed in B_0 are irradiated with a second magnetic field B_1, weaker than B_0 and perpendicular to it, oscillating at a frequency that matches the ω of the precession, **magnetic resonance** happens (Figure 3). The irradiation will bring phase coherence to the magnetic moment vectors. Therefore,

the net magnetization is perturbed and *M* will tilt, oscillating at *ω* as well. In addition, *M* will start rotating around the rotating axis of B_1 with an **angle of rotation** (θ) that depends on the strength of the pulse and its width.

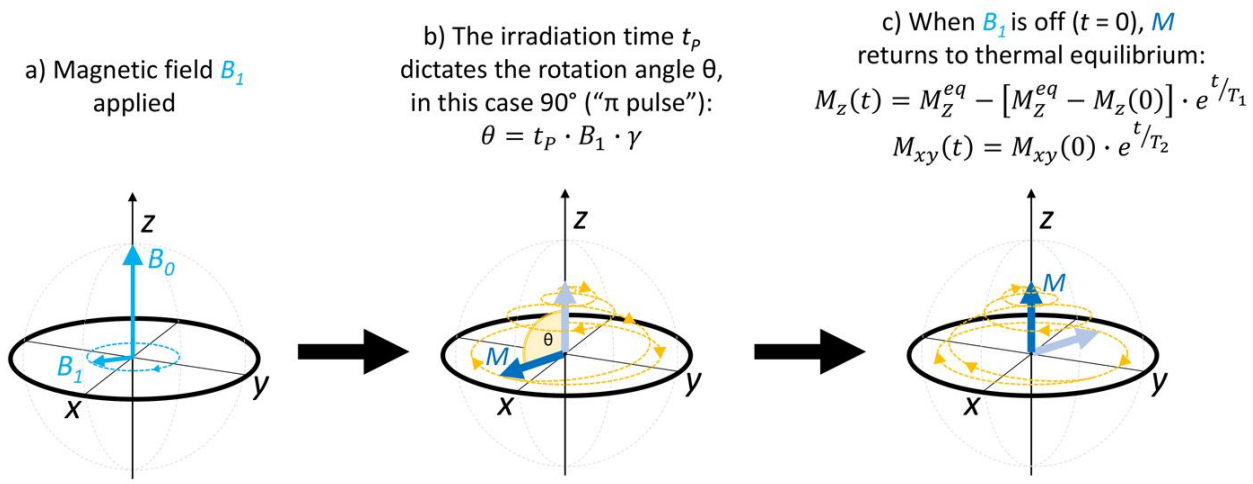

Figure 3. a) Magnetic field B_1 generated by an electromagnetic pulse; b) *M* oscillation and rotation at resonance; c) relaxation.

When the irradiation is interrupted, the nuclear magnetization will undergo **relaxation** (Figure 3). *M* will recover its original *z* component (**longitudinal relaxation**) and lose its oscillating *x* and *y* components (**transversal relaxation**). Each process is associated to a **time constant**), T_1 and T_2 respectively.

Every nuclide with $I \neq 0$ has a unique *γ*, which means that at a given B_0 resonance will occur at different frequencies for different nuclides (*i.e.* the Larmor frequency of ^{1}H will be different from the one of ^{13}C, but also from the one of ^{2}H). Moreover, while the Larmor frequency of bare nuclei of an nuclide will be constant at a given B_0, in natural chemical environment, that is, in molecules, the Larmor frequency of a given nucleus will also be influenced by electron density around it. The greater the electron density, the smaller the perceived magnetic field, an important phenomenon called shielding, and characterized by the so-called **shielding constant** (*σ*) (Figure 4). Accordingly, nuclei of the same nuclide in different molecular environments will have a different *ΔE* and will resonate at slightly different frequencies (Figure 4.a). The phenomenon has a great practical importance. Since the Larmor frequency depends on the molecular environment, it will give information on the molecular structure. In practice, the Larmor frequencies of the nuclei of the studied nuclide are referenced to the Larmor frequency of that nucleus in a reference molecule (*e.g.* tetramethylsilane (TMS) in the case of the ^{1}H nuclide). The difference between the Larmor frequency of a nucleus and the reference Larmor frequency, normalized to B_0, is the **chemical shift** (*δ*) , expressed in **parts per million** (ppm) (Figure 4.b). The nuclei chemical shift is one of the important spectral characteristics that can be used for structure elucidation.

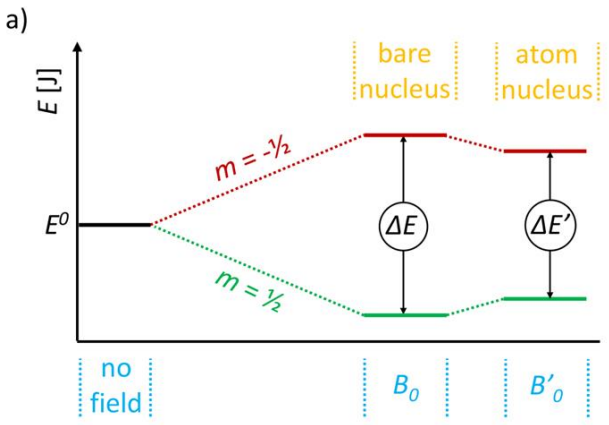

b)

Magnetic field percieved by a shielded nucleus

$$B'_0 = B_0 \cdot (1 - \sigma)$$

Resonance frequence of the shielded nucleus

$$\nu' = \nu \cdot (1 - \sigma)$$

Energy difference between states

$$\Delta E' = \Delta E \cdot (1 - \sigma)$$

Chemical shift

$$\boldsymbol{\delta_x[ppm] = \frac{\nu'_x - \nu'_{REF}\ [Hz]}{B_0\ [MHz]}}$$

Figure 4. a) Energy difference of ^{1}H nuclei states in a magnetic field for a bare nucleus and a shielded atom nucleus; b) Relevant physical quantities related to the phenomenon.

3 - Current generation machines

NMR analysis is performed using **NMR spectrometers**. The spectrometers are used to irradiate the nuclei (with $I \neq 0$) of a sample immersed in a strong magnetic field, to detect the sample's **resonance frequencies** and to measure the **intensities** of the corresponding signals.

In order to collect data on different nuclides, and on differently-shielded nuclei of the same nuclide, the possibility to modify the strong magnetic field B_0 and/or the irradiation frequency of B_1 during the analysis is a requirement. The traditional approach was the use of a **continuous-wave** (CW, referred to the continuous irradiation of the sample) **technique**, varying either the frequency of B_1 (frequency-sweep mode) or B_0 (field-sweep mode).[7] Considerable improvements were made with the development of the **Fourier transform-NMR** (FT-NMR) **technique**. The sample is immersed in a strong, static B_0, and the irradiation B_1 is monochromatic. However, the irradiation time is very short, a pulse length is in the order of microseconds. Thus, for the uncertainty principle the resulting irradiation is actually polychromatic, with frequencies covering a range in the order of kHz around the operating one. This way, all of the differently-shielded nuclei of the irradiated nuclides in the sample resonate at the same time. FT-NMR is much more efficient than the CW techniques, with the acquisition times reduced to seconds. FT-NMR spectrometers are the state-of-the-art machines (Figure 5.a).

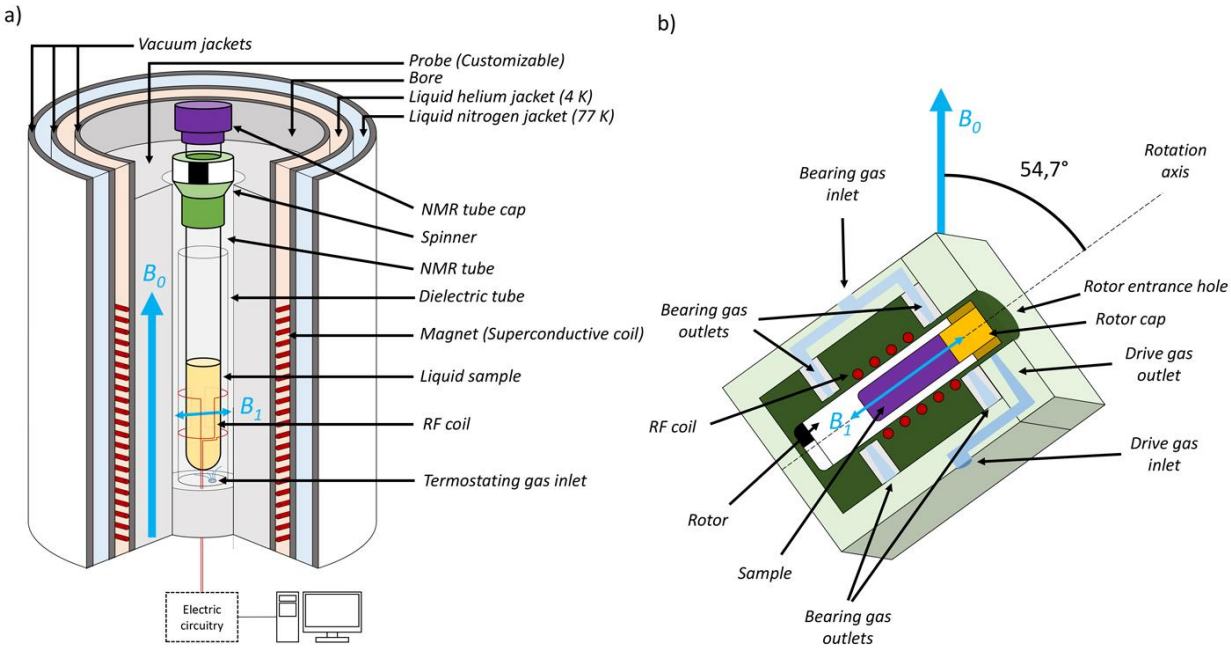

Figure 5. a) Representation of an FT-NMR spectrometer; b) Representation of the inside of a MAS probe's stator.

One of the fundamental elements of an FT-NMR spectrometer is the **magnet**. An important characteristic of a magnet is its **field strength**.[7] An advantage of FT-NMR over CW techniques is the magnets do not need the magnetic field B_0 to change over time. This makes it possible to use **superconductive** coils, which can create extremely strong magnetic fields that are static. Superconductive magnets are solenoids made of metals or metal alloys that under a certain temperature exhibit zero electric resistance. This allows to build powerful magnets with a relatively small size. Up to date, the highest field operative NMR spectrometers make use of 28.2 T superconductive magnets.[8] While T (Tesla) is the SI unit for a field strength, for FT-NMR magnets it is common to describe it as a frequency in MHz, which corresponds to the resonance frequency of ^{1}H nuclei under the specific nominal B_0 (in this case, 28.2 T = 1200 MHz). A high B_0 is usually

desirable, as it increases the difference between Larmor frequencies of different nuclei, resulting in improved separation of the signals (higher **resolution**), and increases the energy difference between spin states, resulting in improved **sensitivity**. Nevertheless, in recent times **low-field benchtop (or desktop) FT-NMR spectrometers** have also been developed.[9] Such spectrometers are much smaller and cheaper than the high-field ones, as they use **permanent magnets** instead of the expensive superconductive ones. The power supply is single phase local power. Permanent magnets provide a magnetic field generated by the internal structure of the magnet itself. On the one hand no consistent electric power and cooling are required, on the other hand the fields permanent magnets can generate are rather low. New generation permanent magnets are based on samarium-cobalt or neodymium alloy (Nd-Fe-B). Using such magnets 90 MHz is the limit field strength, and they are also less stable.

Indeed, the second fundamental characteristic for an FT-NMR magnet is its **field stability**.[7] The generated magnetic field tends to drift over time, therefore a method to maintain B_0 stable is needed in order to obtain consistent analytical results. The field is stabilized by electronically creating a small secondary magnetic field that balances B_0. This technique is called **locking**. To do this, a reference is required. The lock substance is usually an internal reference (*e.g.* the solvent in liquid samples). The lock substance must give rise to an intense NMR signal for a nucleus that has a very different Larmor frequency from the ones in exam (*e.g.* ^{2}H of a deuterated solvent in ^{1}H NMR spectroscopy). Before analysis the lock resonance frequency is found and it is modulated by modifying the secondary magnetic field until it matches with a frequency provided by a reference frequency generator, and then kept constant over time.

Finally, the third important characteristic of an FT-NMR magnet is its **field homogeneity**.[7] If identical nuclei in the sample perceive a different B_0, they will resonate at different frequencies and the resulting signal will be broader, affecting resolution. In high resolution NMR the change in B_0 across the sample cannot exceed ppb levels. Unfortunately, there are many causes of field inhomogeneity: imperfections of the main magnet or the NMR tube, the presence of magnetizable objects in the spectrometer environment, even the sample itself could be magnetized or contain swimming solid particles, creating deviations to the magnetic field. One technique to improve field homogeneity in liquid phase NMR (lpNMR) is **spinning** the sample. When the sample is spun very fast on its axis, the inhomogeneity in the active sample region is averaged out. However, this technique comes with some complications (*e.g.* spinning sidebands), and therefore at present it is often avoided. On the other hand, **shimming** is fundamental to obtain a good quality spectrum. With this more complex technique, multiple electric circuits called shim coils are used to adjust B_0 in several directions to obtain a 3D-homogeneous magnetic field. Nowadays shimming, together with locking, can be done automatically using the developed algorithms.

The irradiation of the sample is operated by another fundamental element of a FT-NMR spectrometer, the **transmitter coil**. The axis of the transmitter coil is oriented perpendicularly to B_0.[4] The transmitter coil is connected to a radio frequency oscillator, which generates alternating current in the coil. When this happens, an oscillating magnetic field B_1 (linearly polarized on the axis) is formed. This linearly polarized magnetic field can be decomposed into two counter-rotating circularly polarized magnetic fields. If the linear frequency of the linearly polarized magnetic field matches a linear Larmor frequency ν, then one of these two components will oscillate at the correspondent Larmor frequency ω, making resonance happen. The possibility of generating pulse sequences led to the development of various techniques that provide exhaustive information on a variety of structural aspects of the analyte.

The signal is revealed by a **receiver coil**.[4] The receiver coil detects the changes in the sample magnetization by means of Faraday induction. The temporary oscillation of M on the coil axis induces alternated current to pass through the coil, which is then used to elaborate the signal. Normally, in modern high-field FT-NMR spectrometers the same **radio frequency** (RF) **coil** is used both as transmitter and receiver.

RF coils are available in different sizes and shapes, and can be tuned to specific frequencies. The RF coils are shaped so that they can accommodate the sample inside them. The coils are inside the **probe** (probehead), together with other elements (*e.g.* gradient coils, designed to induce a spatial dependence of the effective magnetic field).[4] RF coil's **tuning** and **matching** set the frequency of maximum sensitivity and minimize power wastes. If an RF coil is used at a frequency it is not tuned for, it will result in inefficient B_1 field, hence, loss of sensitivity, and in extreme cases it can even damage the hardware. Modern probeheads are equipped with external motors that perform Automatic Tuning and Matching (ATMA). Usually, two or three RF coils are present in a probehead, nested inside one another, with the inner one possessing a higher

sensitivity for the higher filling factor. As proton is the most analyzed nucleus, usually the inner one is tuned to ^{1}H (and to ^{2}H, for the lock), whereas the outer one is tuned to frequencies of other commonly analyzed nuclei such as ^{13}C and ^{15}N. Probeheads with such a configuration are called "inverse" probeheads, as opposed to "direct" probeheads in which the inner coil is tuned for the less abundant nucleus. Of course, a different number of coils can be used. They may be nested differently, or be tuned to different nuclei (^{11}B, ^{19}F, ^{31}P, *etc.*), and they can also be broadband. The choice between different probeheads has to be made according to the nature of the nuclei to be analyzed, and the types of NMR experiments to be performed.

The probe is placed into an empty central cavity of the spectrometer called **bore**, and it can be changed for other probes with different features if needed. In addition to irradiation and signal receiving, the probe has some further functions. For instance, it is the place where spinning of the sample would happen, generated by an air stream. Furthermore, the probe is insulated from the rest of the instrument, allowing **temperature control** of the analysis by flowing a gas at the desired temperature. In **cryoprobes**,, nowadays widespread in NMR spectroscopy, the RF coils are cooled by a stream of cold He to reduce the signal noise arising from them (sensitivity factor can be up to 5x).[10] This poses a challenge: to establish a high temperature gradient between the sample (at room or controlled temperature) and the RF coils (few K) while keeping the two in close contact for ensuring a high filling factor. This is achieved by applying high vacuum to the probe, and separating the elements with a thin dielectric tube. As the maintenance cost of He cooled probeheads are high, N_2 cooled ones are also an option. These are cheaper but their sensitivity factor compared to room temperature probeheads is only around 2.5x.

The probe structure highly depends on what the spectrometer is supposed to analyze with it. For instance, solids are usually rapidly spun around an axis tilted of 54,7°, also known as magic angle, to the direction of B_0.[11] **Magic angle spinning** (MAS) allows to cancel the effects of some strong internuclear interactions, which cause signal broadening, on the NMR spectra of solid samples, greatly improving resolution. For this operation, MAS probes require additional elements such as a stator with a settable spinning angle, which contains a rotor that in turn contains the solid sample (Figure 5.b). The rotor has a cap whose geometry causes fast spinning when a gas stream blows on it. The RF coil also has to be tilted, and it is placed inside the stator around the rotor.

Sample insertion happens from the top of the bore. For liquid samples, when the airflow above the probe is on, the sample can be inserted. Floating on cushion of air, the airflow will gently drop the sample in the probehead slot. Sample introduction could be manual or automatic, with an optional **sample changer** that may be convenient purchasing for routine users. For solid samples, sample insertion and ejection happens through a pipe.

The last fundamental elements of FT-NMR spectrometers are the **computer** and all the **electric circuitry** that allow the user to control all the aforementioned components, and to acquire and elaborate the produced NMR signal.[4,12] The irradiation time is commonly set to apply a 90° pulse to obtain the best sensitivity. After the irradiation time, and a short delay due to temporary repercussions of the pulse on the RF coil, the voltage oscillation caused by Faraday induction on the RF coil is received (Figure 6). This signal, exponentially decreasing in time as a result of nuclei relaxation, is called **free induction decay** (FID, or time-domain spectrum). For the sake of signal digitalization, the FID is sampled at properly set regular time intervals, and registered for a defined **acquisition time**. After acquisition, a **delay time** is applied before starting another **cycle**. The delay length depends on the time the nuclei need to properly relax after irradiation. The pulse sequence is generally repeated multiple times and the resulting spectra summed to obtain a final spectrum. The signal-to-noise ratio can be improved by increasing the **number of scans**.

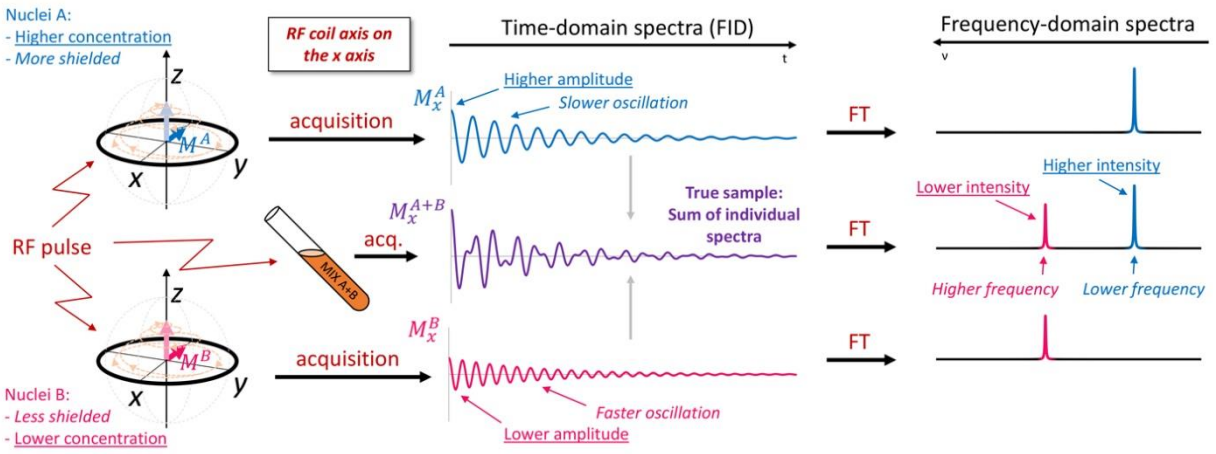

Figure 6. Acquisition sequence: nuclei relaxation after resonance, FID acquisition, and Fourier transform to the final frequency-domain spectrum. In the middle the spectra of a sample that includes nuclei A and B of the same nuclide are shown, but with a different concentration and differently-shielded; on top and bottom the individual spectra of the single components can be seen.

The FID shapes are influenced by the characteristics of the nuclei they originate from. For instance, nuclei concentration influences the FID amplitude, while the nucleus ω dictates the FID's linear oscillation ν (Figure 6). The collective FID signal includes the individual FID signals of all the nuclei in the sample. The collective FID can be mathematically manipulated with the Fourier transform to obtain a frequency-domain spectrum. In this spectrum the signals corresponding to sets of equivalent nuclei are separated in different peaks whose corresponding frequencies and intensities (peak areas) reflect the characteristics of the relative FID.

In addition to spectroscopy, other NMR methods such as imaging and relaxometry have been applied to material characterization.[13–15] Equipment for such methods have also been successfully miniaturized to mobile systems for outdoor analysis.[14]

4 - Brands

Historically, three companies should be credited with the development and marketing of NMR spectrometers, the US company Varian, the Japanese company JEOL, and the German Bruker, with the last two being the only companies currently active on the market of high-field NMR spectrometers.

In 1948 the Varian brothers, Russell H. and Sigurd F. Varian, together with W. W. Hansen and E. L. Ginzton founded the high-tech company **Varian** Associates in the Silicon Valley. By the early fifties the potential of nuclear magnetic resonance for structure elucidation had become obvious,[16] and the company rapidly embarked upon the development of NMR spectrometers. The first 30 MHz equipment, HR-30, was sold in 1952 and by 1959 they released the first 100 MHz equipment, HR-100. These spectrometers were based on continuous-wave sweep methods and on electromagnets. In 1961, Varian marketed the legendary A-60, specifically for organic chemistry applications ("A" stood for "analytical").[17]

In the sixties the company intensively researched into superconducting magnets, computer assistance, and with Richard Ernst, who was employed by the company between 1963-1968, the FID generation – Fourier transformation technology. It is worth noting that Varian's research on the application of FT-NMR was so ahead of time that the seminal paper[18] from Ernst and Anderson was twice rejected by their peers.[19] In 1972, they also marketed CFT-20 for ^{13}C experiments, an equipment that clearly demonstrated the utility of Fourier transformation outside the field of ^{1}H NMR spectroscopy. With Ernst as Varian consultant, the company contributed to the development of 2D NMR techniques, as well.[20] It is worth noting that for his contribution to the development of FT-NMR and 2D experiments, Ernst was awarded the Nobel Prize in Chemistry in 1991.

Soon after the fruitful decades summarized above, mostly due to management mistakes, Varian's NMR business started to slow down. One of the principal reasons for the decline was that the management stopped the research led on the development of high-field magnets, considering "very high-field" NMR non-

profitable. By the time this erroneous business decision had been changed, Varian lost momentum and had to rely on an external company, Oxford Instruments, to acquire high-field superconducting magnets for its NMR instruments. In 1999 Varian Associates spun off its NMR business into Varian Inc. A decade later, in 2010 to be exact, **Agilent Technologies** acquired Varian Inc. However, on the 14th of October 2014, Agilent announced that it was exiting the NMR business, putting an end to 60 years of revolutionary research and development. As Agilent exited the business in 2014, a significant number of Varian NMR spectrometers are still in active use, considering that Agilent had roughly the 20% of the market at the time.[21]

In 1949 Japanese scientists Kenji Kazato and Kazuo Ito founded Japan Electron Optics Laboratory Company, Limited in Tokyo, which was renamed in 1961 as **JEOL**, Limited. The company's first commercial product was a transmission electron microscope, but soon they entered the NMR business by launching JNM-1, the first Japanese NMR spectrometer. Over the seventy-year history of JEOL, nuclear magnetic resonance has remained a staple of the Analytical Instruments segment of the company. Their current product line includes the JNM-ECZ series, the entry level equipment JNM-ECZS with ultra-compact chassis, and the high-end model JNM-ECZR offering high expandability.[22] These FT-NMR spectrometers can be acquired with up to 800 MHz low-cryogen-consumption superconducting magnets, the so-called JJ series. It is worth mentioning that JEOL's one-year-hold 400 MHz magnet, the JJYH 400, principally requires helium refilling only once a year. JEOL had also researched heavily into zero boil off magnets, and in 2013 they marketed ZB 400, in which the evaporated helium gas is re-liquified to minimize the helium loss.[23] As of 2019, ZB 600 is also offered to JEOL's customers.

Among the three companies, **Bruker** is the youngest. Bruker-Physik AG was founded in 1960, Karlsruhe, Germany, by university professor Dr. Günther Laukien and four associates. The name of the company originates from one of the associates, Emil Bruker. The first important achievement of the company was the fully transistorized NMR spectrometer HFX-90 marketed in 1967.[24] Shortly after another landmark was reached, in 1972 Bruker launched its first "FT-only" instrument, WH-90. In the following period Bruker played an important role in the development of multidimensional NMR spectroscopy, in collaboration with Ernst, who drifted away from Varian and started to work with Bruker.[25] Bruker also played a key role in the improvement of probe technology by developing and implementing cryogenic probes in their instruments. In the 2010's the company launched the world's first solid-state dynamic nuclear polarization-enhanced NMR system (DNP-NMR).

Importantly, Bruker also remained committed to the development of ultra-high-field magnets. The first 800 MHz magnet was developed by 1995, the first 900 MHz instrument by 2001, and in 2009 they sold the first 1 GHz NMR spectrometer, Avance 1000, to the Centre de Resonance Magnétique Nucléaire à Très Hauts Champs (CRMN) in Lyon, France.[26] At the end of 2018 Bruker successfully energized the first 1.1 GHz instrument, the Ascend 1.1 GHz. The company announced the achievement at the 60th Experimental Nuclear Magnetic Resonance Conference in April 2019.[27] The advance from 1 GHz (23.5 Tesla) to 1.1 GHz (25.9 Tesla) had been hindered for years due to limitations in the physical properties of low temperature superconductor (LTS) materials used in the fabrication of superconducting magnets. The breakthrough was achieved based on high temperature superconductors (HTS) discovered in the 80's, which allowed the development of new LTS-HTS hybrid magnet technologies. The first 1.1 GHz spectrometer has been delivered to the Structural Biology Department at St. Jude's Children Research Hospital in Memphis, Tennessee, US.[28] Based on this technology Bruker has developed 1.2 GHz magnets. The company announced in August 2019 that the first 1.2 GHz spectrometers were successfully energized.[29] Clients who have already ordered 1.2 GHz spectrometers include the Magnetic Resonance Center and Department of Chemistry, University of Florence, Italy; ETH, Zürich, Switzerland; the Max Planck Institute for Biophysical Chemistry in Göttingen, Germany; and the Leibniz-Forschungsinstitut for Molecular Pharmacology in Berlin, Germany.

It should be noted that the aforementioned three companies were the key players, but not the exclusive participants in the early history of NMR spectrometers. Companies such as Perkin Elmer or Trüb-Täuber certainly deserve honorable mentions for their early contribution.[25,30]

While high resolution NMR spectroscopy will certainly continue driving the progress in both Physical and Life Sciences, it seems that modern low-field NMR, *i.e.* **benchtop NMR**, is also becoming a hot topic. In the past decade several companies started to offer benchtop NMR spectrometers for the analysis of liquid samples. The measurable nuclei include ^{1}H, ^{13}C, ^{19}F, ^{31}P, and more. The number of available pulse sequences is also rapidly growing (1D, COSY, TOCSY, JRES, DEPT, HETCOR, HMQC, HMBC, HSQC, etc.). These

spectrometers are perfectly capable of a broad range of routine applications, such as elucidation of simple structures, purity control, reaction kinetics, etc. Since benchtop NMR instruments are directly setup in the laboratory, and they are very easy to use, they can certainly boost productivity in research, education, and industrial production alike. Nevertheless, it has to be noted that benchtop and high-field instruments serve very different purposes, with the applicability of the former to material characterization being much more limited. Benchtop instruments apply only to the lpNMR analysis of small molecules (*e.g.* molecular solids and material additives) and some polymeric systems, and only in case the resolution at low-fields allow to obtain the desired degree of information.

Some of the notable benchtop models are summarized in Table 1.

Company	Brand	Nuclei	Operating frequency (^{1}H)	Resolution	2D Pulse sequences
Magritek	Spinsolve 60 Carbon	^{1}H, ^{19}F, ^{13}C	60 MHz	< 0.5 Hz	yes
Thermo Fisher	picoSpin 80	^{1}H, ^{19}F, ^{13}C, ^{31}P	82 MHz	1.2 Hz	yes
Nanalysis	NMRready-60Pro	^{1}H, ^{7}Li, ^{11}B, ^{13}C, ^{19}F, ^{31}P	60 MHz	< 1 Hz	yes
Oxford Instruments	Pulsar	^{1}H, ^{19}F, ^{13}C, ^{31}P	60 MHz	< 0.5 Hz	yes

Table 1. Examples of benchtop NMR spectrometers available on the market in 2019.

5 - Sample preparation

5.1 - Liquid phase NMR spectroscopy (lpNMR)

lpNMR is the NMR analysis of liquid samples, suitable for the analysis of liquid and solid analytes. In material characterization, liquid analytes for lpNMR spectroscopy could be materials that melt at relatively low temperatures and liquids absorbed in a material; solid analytes could only be materials that can be dissolved in detectable amounts and without using aggressive conditions that could destroy the NMR tube.

For **liquid samples**, the solution could be prepared either with the **neat liquid** itself,[31] or by **mixing it with a specific solvent**. NMR spectroscopy is an inherently insensitive technique because it relies on the small energy difference between nuclear spin states immersed in a magnetic field B_0. Thus, the analyte demand is high. Usually NMR experiments are performed on solutions. For instance, this is preferable when the analyte is available in **little quantities**, or when the sample has a **high viscosity**, as it would be difficult to introduce it in the NMR tube and, more importantly, the viscosity brings anisotropicity in the interaction between active nuclei, causing peak broadening and thus lowering the resolution.

For **solid samples** a **dissolution is required**. In addition to the considerations made for solutions of liquid samples, for solids the maximum concentration is also limited by **solubility**. Indeed, particles in supersaturated solutions would create inhomogeneities in B_0, generating broad peaks and making the spectrum hard to interpret.

The **sample preparation** usually starts with its **purification**. For instance, if a solid is to be analyzed, then it might be good to heat it up or put it under vacuum to remove all the moisture and/or the solvents it might contain. If the spectrum of a pure component is needed, chromatography could help removing impurities. This step is meant to eliminate the sources of unnecessary NMR signals that would only complicate the determination. However, if the objective is to analyze a sample as a whole, this step, of course, should be avoided.

The sample should then undergo **dissolution**. The right amount of sample is put in a vial, and the right amount of solvent is added and mixed until the sample is completely homogenous. The **amount of sample** affects the **concentration** in the final solution. The lower limit is the detection one, the upper limit the solubility/miscibility one; the right amount in this range depends on the abundance of the analyzed nucleus, on the field strength, etc. and again on the quantities available, as well as the viscosity of the resulting solution. The **amount of solvent** determines the **volume** of the final solution. This in turn will

determine the level of filling of the NMR tube which, as discussed later on, has an influence on the results. If for example the analyses are determinations of multiple analogous samples for quality controls, then these amounts should be optimized. For a single determination, a good starting point could be 1 to 50 mg in 0,6 to 0,8 mL of solvent, then going up with the concentration if this is not enough. For larger molecules (*e.g.* polymers) the quantities are likely going to be higher.

^{1}H NMR solvents are usually **deuterated**. The analysis could also be performed with traditional solvents,[32] but the solvent NMR peaks would be so broad and intense that they could cover the sample ones. Deuterated solvents minimize the intensity of the solvent ^{1}H peaks, although they do not erase it completely and in ^{1}H spectra the **solvent residual peaks** can be observed.[33] D_2O, $CDCl_3$ and DMSO-d6 are the most commonly used NMR deuterated solvents. Moreover, the solvent ^{2}H nuclei can be used as the internal reference for the lock. For the NMR spectroscopy of other nuclei, deuterated solvents might still be a good choice for the lock, otherwise a normal solvent could be used.

The choice of a solvent is done by assessing the best combination of advantages and disadvantages:
- **Solubility/Miscibility**: the solvent should be capable of dissolving/mixing the quantity of sample required for the analysis. In case the sample is especially hard to dissolve/mix, a mixture of solvents can be used.
- **Reactivity**: the solvent should not react with the species in solution, or degrade at the analysis conditions.
- **Thermal behavior**: the solvent should not boil, or freeze, at the analysis conditions.
- **Viscosity**: the solvent should have the lowest viscosity possible at the analysis conditions.
- **Frequencies of its signals**: the solvent resonance frequencies should not overlap with the analytes' signals.
- **Cost**: the prices of different deuterated solvents vary greatly, even in the case of considerable structural similarities (*e.g.* $CDCl_3$ is significantly cheaper than CD_2Cl_2). The price will also heavily depend on the degree of deuteration. These factors are worth considering when the solvent is chosen.
- **Purity**: the solvent should be as pure as possible, because impurities are not distinguishable from the sample and might generate signals overlapping with the analytes ones. Also, in case the solvent is deuterated, it should have the highest degree of deuteration possible. In addition, the solvent should be the least hygroscopic possible, as it would capture moisture. Solvents containing water would have a lower purity, the water could possibly react with the analyte under the conditions of the analysis, and it is a source of labile protons, which in certain cases can lower the degree of deuteration of the solvent.

When the sample is dissolved, the **addition** of other substances could be performed. An example is a **concentration standard**,[34] a known substance added in known quantities to compare the peaks area and obtaining the concentrations of the analytes in solution.

Another commonly added substance is a **calibration reference**: a spectrum includes all the differently-shielded nuclei of the same nuclide in the sample, but a chemical shift reference is required to set the zero on the spectrum scale. The most common reference is **tetramethylsilane** (TMS) for ^{1}H, ^{13}C and ^{29}Si.[35] In case TMS is insoluble in the sample's solvent (*e.g.* it is insoluble in water) another calibration reference is required (*e.g.* DSS and TSP in water). Alternatively, it is possible to introduce in the NMR tube a **capillary** containing the desired calibration reference in a suitable solvent, which is then included in the analysis although physically separated by the sample. In addition, calibration references are required for the analysis of other nuclei, as well (*e.g.* $CFCl_3$ for ^{19}F, or 85% HPO_3 for ^{31}P).[7] These **primary references** could be added to the sample, or the purchased solvent can already contain them. Although the scales on spectra are still centered based on primary references, nowadays it is common to set the zero making use of **secondary references**, which species whose signals frequencies differ of constant amounts from the ones of a primary reference.[36] A secondary reference could be for example the solvent residual peak for the analyzed nuclide, or even the lock frequency itself. Even though these methods are more practical, they are not always reliable, especially in certain chemical environments or at different temperatures when the difference in frequencies is not constant anymore.

The obtained solution can now be put into an **NMR tube**, the specific container for lpNMR. First of all, the appropriate tube for the analysis should be chosen. Normal NMR tubes have a 5 mm diameter, but other sizes are available. NMR tubes range from economy tubes to high quality ones which, according to the spectrometer field strength, have different precision degrees of camber, concentricity and roundness: the higher the field strength, the more the internal tube volume has to resemble a perfect cylinder for a good shim. NMR tubes can be designed for analysis under atmospheric conditions, or for samples with high pressure, low pressure or inert atmosphere.

NMR tubes are usually made of **borosilicate glass**. This means that the tube itself will give rise to signals in ^{11}B and ^{29}Si NMR. For the former the issue can be solved by switching to quartz NMR tubes, for the latter the situation is trickier, but good results can still be achieved by software manipulation or by using PTFE tube liners, which are silicon-free and good also for corrosive samples. Finally, the NMR tube that has been chosen should be clean internally and externally, and must not show any scratch, crack or deformations. Imperfections create distortions to the magnetic field and, more importantly, if the tube is damaged it might break during analysis, possibly damaging the instrument.

Once the NMR tube has been chosen, the solution can be transferred into it. While doing it, a **filtration** could be performed to remove solids (*e.g.* particles, dust). Usually, the filtration is carried out in a Pasteur pipette packed with little cotton or glass wool. At this stage there is also the possibility to place a a plug (*e.g.* silica or alumina) on top of the wool to selectively retain some species from the sample. Of course, more specific filters can be used instead.

The NMR tube should be closed with a **cap**. The normal cap is made of polyethylene and does not insulate the sample from the environment. For air sensitive samples the NMR tube can be filled inside a glovebox and closed by a flame seal or by using a Young valve, which also allows connection to Schlenk lines. If the sample needs **degassing**, this can be done previously on the solvent, or before closure by substituting the unwanted gas with an inert or by using the Freeze-Pump-Thaw technique.[37]

The closed NMR tube should be **labeled** with a marker on the glass close to the cap. The sample is then inserted in a **spinner**, and the spinner is properly placed on the NMR tube with the help of a **depth gauge**, specific for the instrument. Depth and sample volume influence the analysis. If the sample volume is centered in the depth gauge, the sample will be correctly placed in the center of the probe coil, the field inhomogeneities are minimized and the shim required will be short. A small volume sample could also make the shim difficult. Finally, the tube should be **wiped externally** to remove contaminants. It is now ready to be analyzed.

NMR spectroscopy is a **nondestructive technique**, meaning that the analytes are not consumed or destructed by the analysis and therefore can be recovered at the end of it. It is fundamental at this stage to properly **clean** the tube before using it for later analyses to avoid contaminations. As NMR tubes are thin, cleaning them can be time consuming. Specific glassware for doing it is commercially available (NMR tube cleaners).[38] The tube should be rinsed multiple times with appropriate solvents, then dried with dry air or nitrogen and finally be left in the oven to keep it dry. More aggressive chemical solutions could be used if needed as long as they do not damage the tube (*e.g.* chromosulfuric acid could be a good choice).

5.2 - Solid state NMR spectroscopy (ssNMR)

ssNMR is the NMR analysis of solid samples, suitable for the analysis of solid analytes. Because of the nature of the sample and that of the analysis, lpNMR is operationally simpler than ssNMR and the spectra are easier to interpret. In the analysis of material, analytes that could be analyzed with ssNMR are all the solids that cannot be dissolved, and also all the solids for which valuable information on the structure would be lost by dissolving them.

As for lpNMR, sample preparation could start with the **purification** of the sample with analogous considerations (*e.g.* drying to remove moisture). ssNMR sample preparation includes no dissolution, but another step has to be carried before the sample is ready for analysis: the **grinding**. The lower the grain size of the sample, the better it will be packed. This step is of fundamental importance: the presence of empty spaces in the rotor would make it unbalanced and this could potentially end up in destroying the rotor at high-speed, as well as the probe. In case grinding does not apply, a filler could be used, as long as it does not interfere with the analysis and is inert.[39]

Indeed, including external species in the sample might alter it, therefore the use of additives is not always desirable. When this is not possible, some issues could arise: the absence of a deuterated solvent deprives the instrument of an intense and sharp signal for the lock, thus the strong field would drift over time, complicating also the shimming. Using a calibration reference or to quantify the NMR spectrum is more complicated compared to lpNMR. However, in the vast majority of the analyses these problems are by no mean an obstacle.

Regarding the **lock**, external field-frequency lock probes have been developed,[40] although normally substitution methods are used, which consist in performing an experiment with the reference in between normal experiments).[35] For example, ^{79}Br ssNMR experiments on KBr are often performed with this purpose, and the obtained frequency is used for the lock.[39] This way the drift is not controlled via secondary field-sweep as in lpNMR, but it is reset from time to time to the same value. In any case, it has to be noted that the peaks linewidth in ssNMR is inherently broader than the one in lpNMR, therefore in many cases the lock can be unnecessary as the result would not be appreciable. The same applies to the **spectrum zero set**, some secondary references have been proposed, such as adamantane or glycine for ^{13}C and ammonium chloride for ^{15}N, again used with substitution methods.[41,42] But again, having a standard δ scale is not as fundamental as in lpNMR, and often the zero is set on one of the spectrum peaks. As for **quantification**, low resolution and the use of techniques that alter the peaks for improving sensitivity and qualitative information make ssNMR not particularly suitable for quantification. Nevertheless, its usefulness has been proved over the years. For example, the injection of a constant, synthetic signal providing a standard area (*e.g.* ERETIC) has become especially popular.[34,43]

Once the material has been properly grinded, it can be loaded into a **NMR rotor**, the specific container for ssNMR. The appropriate rotor for the analysis has to be chosen.[11,44–46] Rotors are available in different sizes: the higher the volume, the more sample can be put and the better the signal-to-noise ratio is. However, as the rotor has to be completely filled, the available quantity might limit the volume. Also, smaller rotor can reach higher spinning rates, which may result in significantly better resolution. Another important factor is the rotor material (ZrO_2, Si_3N_4, polymer, *etc.*) that makes it more or less apt for the analysis spinning rate, temperature, *etc.* As for NMR tubes, the choice of the rotor has to be done taking into account the elements the rotor is made of.

The **rotor filling** has to be performed very carefully to avoid rotor unbalance. Although it is possible to do it directly, it is recommendable to use **specialized tools** such as funnels and packing tools. These tools make it easy to correctly fill the rotor and minimize damages and scratches on it. The funnel and the rotor should be assembled, and a bit of powder should be loaded. The packing tool can be now inserted in the rotor and be used to tap gently on the sample to pack it, as tapping too hard might damage the rotor. This procedure should be repeated until the rotor is completely full, pre-spinning the sample at low speed for better packing if applies. If the rotor is not full, it will not be balanced during spinning and thus the spinning speed cannot be stabilized. The rotor filling of samples that are not in the form of powder (*e.g.* semisolid materials) might require a sample-specific procedure.[47]

A number of **rotor inserts** are available.[48] Lower and upper **spacers** are inserted respectively before and after the grinded sample and are particularly useful for high resolution ssNMR as they improve shimming and radio frequency inhomogeneity, and when a very little quantity of sample is available. The filling and assembling procedures for these inserts involve screws to tighten and can be aided by the use of a magnifying lamp. This procedure is more complex than the described general one and would be provided by the commercial supplier of the inserts. Another type of inserts are **sealable glass inserts**, useful for air-sensitive or liquid-containing or melting samples. The insert can be filled with samples through a necking entrance and sealed, then removing the unused part to make the insert fit the rotor.

The loaded rotor is finally closed with a **cap**. Some rotors are open on both sides of the cylinder and require a lower cap together with the upper one. The upper cap has a particular geometry to induce rotation. This part is easily deformed when the cap is inserted, so this operation has to be performed carefully. A deformed as well as a not properly inserted cap, might not spin or not spin properly or pop off the rotor during analysis. A soft utensil could be used to close the rotor, although specialized tools to insert the cap are also commercially available. Rotor caps have different materials (ZrO_2, Kel-F, Vespel, *etc.*) which gives them different properties (temperature range, mechanical durability, grip, *etc.*).

The sample is now ready for analysis. In some cases, it is required to **draw a line** on the lower edge of the rotor with a specific marker. This mark is used by the instrument to reveal the frequency the rotor is spinning.

After analysis, the cap is **removed** and the sample collected. Even at room temperature analysis, the spinning is likely to cause heating of the rotor, thus it should be handled with care. The different thermal expansion coefficient of cap and rotor can be used to facilitate cap removal. Again, specific tools to properly remove the cap are available.

When the sample is collected, the rotor and cap should be thoroughly **cleaned**. The cleaning in this case should be both chemical (with the use of suitable solvents) and physical (scrubbing with a cotton swab), and the units should be wiped dry avoiding scratches.

6 - Practical information

The prepared sample can be inserted in the NMR spectrometer for analysis. Benchtop low-field NMR spectrometers could be kept in the lab, and the analysis could be performed **on-site**; for high-field NMR the sample has to be transported to another place, as the spectrometer require a dedicated **NMR room**. The site the spectrometer operates in has to fulfill all the requirements provided by the manufacturer for room dimensions, floor vibration, environmental magnetic field, the range of humidity and temperature and their stability over time, *etc*.[49,50] These requirements have to be met not only for proper NMR spectrometer operation, but also for safety reasons.

Operating NMR spectrometers pose a series of **hazards** that can be avoided with proper precautions. First of all, public access is restricted in the area the spectrometers are positioned. This area should be and highlighted with appropriate **warning signs.** NMR spectrometers are **surrounded in all directions by a magnetic field** whose intensity decays with distance. It is common to place a **line** with tape or painting on the floor to indicate the area surrounding the spectrometer where the field reaches 5 Gauss. No conclusive scientific evidence has indicated that exposure to NMR magnetic field has a direct effect on the body, yet it could indirectly harm people by influencing objects in the area. More specifically, **peacemakers** could be influenced by magnetic fields, possibly causing lethal failure: people having one implanted must not enter the >5 Gauss area, and should not enter the NMR room at all. The same applies for people who have **ferromagnetic implants or prostheses**. Moreover, no **loose ferromagnetic object** should enter the NMR room, as they would be attracted towards the spectrometer and turn into projectiles, possibly hurting people and damaging objects on the way. Finally, magnetic data storage media and credit cards might be affected by the magnetic field, too. Modern NMR magnets are **highly shielded**, thus the >5 Gauss area is decreased (*e.g.* for a 300 MHz magnet it is inside the tank of the magnet itself). Shielding can also improve the stability of the magnetic field.

A second type of hazard is posed by the **cryogenic substances** contained by the spectrometer, liquid He and N_2. In the remote chance that the spectrometer spontaneously undergoes **magnet quench**, as temperature rises the magnet superconductivity would be lost and the current would dissipate heat. This causes liquid He to boil off immediately, releasing a vast volume of gaseous He very fast and **displacing O_2**. The people inside the lab should immediately leave the NMR room. As a preventive measure, the NMR room must be equipped with a **ventilation system** to counteract the inherent normal-rate O_2 displacement, which is the consequence of the natural He and N_2 evaporation of an operating NMR spectrometer: N_2 and He in the spectrometer are liquids at the boiling point and as such are subjected to evaporation. For this reason, over time the liquids will evaporate progressively from the spectrometer and have to be replaced. **Liquid N_2 filling** is commonly performed weekly, while **liquid He filling** is performed less often (months). In both cases, proper safety equipment (face mask and thermal gloves) should be used.[49]

To conclude the safety section, it should be noted that many of the deuterated solvents used in NMR are either harmful or toxic. Besides, the NMR tube containing them break very easily and should be handled with care.

While for benchtop NMR spectrometers the machine is already set up for the available experiments and the software can be used by any user with some practice, for high-field NMR spectrometers the care of an **expert NMR specialist** is required.[51] Once the spectrometer is first assembled, it is cooled down and energized. Since then the machine is not turned off unless needed, so the NMR specialist performs cryogens filling periodically and takes care of the strength, stability and homogeneity of the field. The NMR specialist is in charge of changing the probe,[52] of performing NMR experiments, of helping the users in results interpretation and suggesting them more complex experiments to obtain the desired information, as well as training them. Indeed, depending on the laboratory policies, experienced users are often allowed to submit samples on their own and control the computer for simple experiments for which the instrument has already been set up.

The **procedure** to perform an NMR experiment depends on what NMR spectrometer and software are used, which experiment is performed, and how much is up to the user. For this, the step-by-step procedure should be discussed with the NMR specialist. In any case, for **lpNMR** a synthetic and generic procedure is the following:[53] the user takes control of the computer connected to the spectrometer, input the sample information and select the experiment in the dedicated software. The sample is then introduced. It might be necessary to perform probe's coils tuning and matching. The lock is performed on the input deuterated solvent and the shim is performed to homogenize the field, then the experiment is run and the FID is acquired and transformed into spectrum. According to the result, this cycle can be reiterated by manually performing lock and shim until the output spectrum reaches the desired quality. At the end of the cycle, a spectrum with the selected number of scans is obtained. The procedure for **ssNMR** is analogous, with some differences such as the necessity of setting magic angle and field locking with an analysis of a KBr sample.[54]

In both cases, once the analysis is over the sample can be ejected from the spectrometer and the collected sample can be recovered for further analysis or use. The final spectrum acquired can be phased, baseline corrected, the peaks selected and integrated for data analysis. It is possible to send the FID in a file to the users, and a number of software are available for the users to carry out data analysis independently. Examples of such software are Mnova, ACD Labs, CcpNMR, Sparky, *etc.*

7 - Costs

Although the purchase of a high-field NMR equipment is often individually negotiated, and may slightly depend on such circumstances as the buyer's country, type of organization (business or academy), *etc.*, the approximate price of a **300 MHz Bruker spectrometer** (Ascend magnet, Avance Neo console) is 350.000 €. The corresponding **400 MHz spectrometer** costs 480.000 €, while a **800 MHz** equipment is priced over 3.5M €.[55,56] The price of the **probe** is an additional cost, which can be higher than 100.000 € for advanced probes.[57,58] **Cryoprobes** in this sense are particularly expensive for both price and operational costs. **Benchtop NMR spectrometers** are much cheaper and a 60+ MHz spectrometer would cost around 60.000 €.

The **operational costs** of high-field NMR spectrometers are considerable. Some of the cost factors are the **rent** of an appropriate room, **hiring trained personnel** (NMR specialist), regular **N_2 refill** (ca. 40 L weekly for a 300 MHz Bruker spectrometer) and regular **He refill** (ca. 50 L every quarter for a 300 MHz Bruker spectrometer). These can add up to as much as 80.000 € yearly. However, the price highly depends on **He availability** on the market, with shortages being a major issue in the field.[59,60]

As for the **consumables**, lpNMR analyses make use of NMR tubes and deuterated solvents. The cost of an **NMR tube** depends on the quality of the tube, the NMR field strength and the material it is made of. A normal 5 mm NMR tube for a benchtop spectrometer could cost around 1 $, an economy one for a 300 MHz spectrometer around 4 $ and for a 700 MHZ one around 15 $.[61] A precision one for a 300 MHz could cost around 10 $, for a 1000 MHz one around 40 $ and a quartz one for a 300 MHz around 35 $. NMR caps are very cheap (6 $x100). The cost of the **deuterated solvent** depends on the deuteration degree (50 g of 99.8 atom % d of $CDCl_3$ vs 99.96 % is 28.10 € vs 134.00 €), the content of the calibration reference (50 g 99.8 atom % d of $CDCl_3$ containing 0.03% (v/v) TMS is 29.30 €), if it is anhydrous or not (50 g 99.8 atom % d of $CDCl_3$ anhydrous is 41.80 €) and the type of solvent.[62] **Rotors** for ssNMR and caps are much more expensive than NMR tubes, with prices up to over 1000 € depending on sizes and materials.[61] Finally, spectrometers come with a **software** from the producer, but for independent data analysis the price of the software license has to be considered.

As a conclusion, although high-field NMR spectrometers in certain research areas of materials science, chemistry, biochemistry and medicine are indispensable, key to further scientific progress, the instrument prices and the costs could be prohibitive for many research entities or companies willing to use NMR techniques for materials characterization. Low-field benchtop NMR equipment is an alternative that should not be overlooked in the limited cases it could apply to materials characterization. In other cases, a solution for non-routine user is to run analyses via external companies/universities possessing high-field NMR spectrometers, at a moderate price.

8 - Data analysis

NMR analysis allows the identification of the chemical compounds present in the sample, since the spectra can contain information on most aspects of the chemical structure, such as constitution, configuration, conformation, as well as on nanostructural aspects of the analyzed substances. The signals in the spectra recorded under appropriate conditions also hold meaningful quantitative information.

8.1 - lpNMR spectrum analysis

lpNMR frequency-domain spectra have higher resolution and are easier to interpret than ssNMR spectra. To each resonance signal corresponds a peak in the spectrum, whose position is determined by its resonance frequency and expressed as the **chemical shift** (δ) (Figure 7.a).[7] δ is more practical than absolute frequency as the domain of the NMR spectrum since, unlike resonance frequency, it is independent from the magnetic field strength B_0 of the spectrometer. That is, the chemical shifts of the signals in the spectrum of a given sample will always be the same, independently of the spectrometer (and B_0) used for the analysis. On the other hand, since with increasing B_0 the difference between resonance frequencies will increase, using stronger B_0 for the analysis will result in greater resolution, less peak overlapping.

δ expresses the **shielding** operated by electrons on the nucleus local magnetic field. Hence, δ is indicative of the chemical environment of the nucleus. It may suggest nearby substituents, and the structure of the functional group, moiety the nucleus belongs to. (Figure 7.b).

More than one nucleus could have the same δ (or be **isochronous**). This will happen if the nuclei are **chemically equivalent**, that is, they have identical molecular environment, or they are chemically inequivalent, but the different molecular environments accidentally result in identical δ. Naturally, the chemically equivalent nuclei not only have identical δ in the NMR spectrum, but they also have identical chemical behavior, reactivity. The identical molecular environment of the chemically equivalent nuclei can be the result of molecular symmetry, or conformational flexibility, when fast rotation around a sigma bond renders certain nuclei indistinguishable. Typical example of the latter case is the chemical equivalency of the three CH_3 protons in organic molecules.

In the case when the chemical equivalency is the result of molecular symmetry, the chemically equivalent nuclei can be **homotopic** or **enantiotopic** (Figure 7.c). Homotopic nuclei can be interconverted by a rotation around a C_n axis of the molecule or around a sigma bond in case the rotation is fast enough on the **NMR timescale**. Replacing any of the homotopic nuclei with a chemical moiety would result in the same new molecule. Enantiotopic nuclei can be interconverted by reflection with a σ plane of symmetry of the molecule, but they cannot be interconverted by any rotation of the molecule. Replacing enantiotopic nuclei with a chemical moiety would result in the enantiomers of the new molecule.

Chemically inequivalent nuclei can be **diastereotopic** or **heterotopic**. In both cases, no symmetry element of the given molecule can interchange the nuclei. However, the replacement of diastereotopic nuclei with a chemical moiety would result in diastereomers, while the replacement of heterotopic protons with a chemical moiety would result in constitutional isomers.

Molecules in solution could have different conformations, thus chemically equivalent nuclei might not be so after conform. However, if the conformations interconvert rapidly enough on the NMR timescale, the molecular structure detected by the instrument is averaged out to the most symmetrical one and the chemical equivalence between nuclei of that structure is observed. If the interconversion is too slow (*e.g.* at low temperature, higher field, more viscous solvent) the different conformations would give rise to different sets of signals.

In common experimental conditions, NMR spectroscopy can distinguish between diasteroisomers, but not between enantiomers. If enantiomers are to be distinguished, an element that differently interacts with the two enantiomers should be used in the analysis to resolve the signals (*e.g.* an optically active agent, solvent, reactant, *etc.)*.[63,64]

Ideally, the integral of the NMR signal, that is, the area under the peak in the spectrum is proportional to the **concentration** of the nuclei in solution (Figure 7.d). **Integration** of the peaks gives information on the **relative concentration** of the nuclei. ^{1}H NMR analysis of a $CDCl_3$ solution of equimolar amounts of $CHBr_3$ and CHI_3 will give rise with two peaks with different δ but identical intensity. Adding equimolar amounts of CH_2Cl_2

to this solution, the spectrum of the sample will display a third signal, and the intensity of protons signal from the CH_2 moiety will be the double of the intensity of the signals of the CH protons. The situation is the same when the different nuclei belong to the same molecule. In the ^1H NMR spectrum of CH_2ClCCH_3 the proportion of the areas under the signals of CH_2 and CH_3 protons will be 2 to 3. Comparison of these areas with the ones of the peaks of a **concentration standard** allows the determination of the nuclei **absolute concentration**. In real systems, the **integration accuracy** is limited by various factors, such as peaks superposition, low signal-to-noise ratio, H-D exchange and considerable differences in longitudinal relaxation times (T_2).

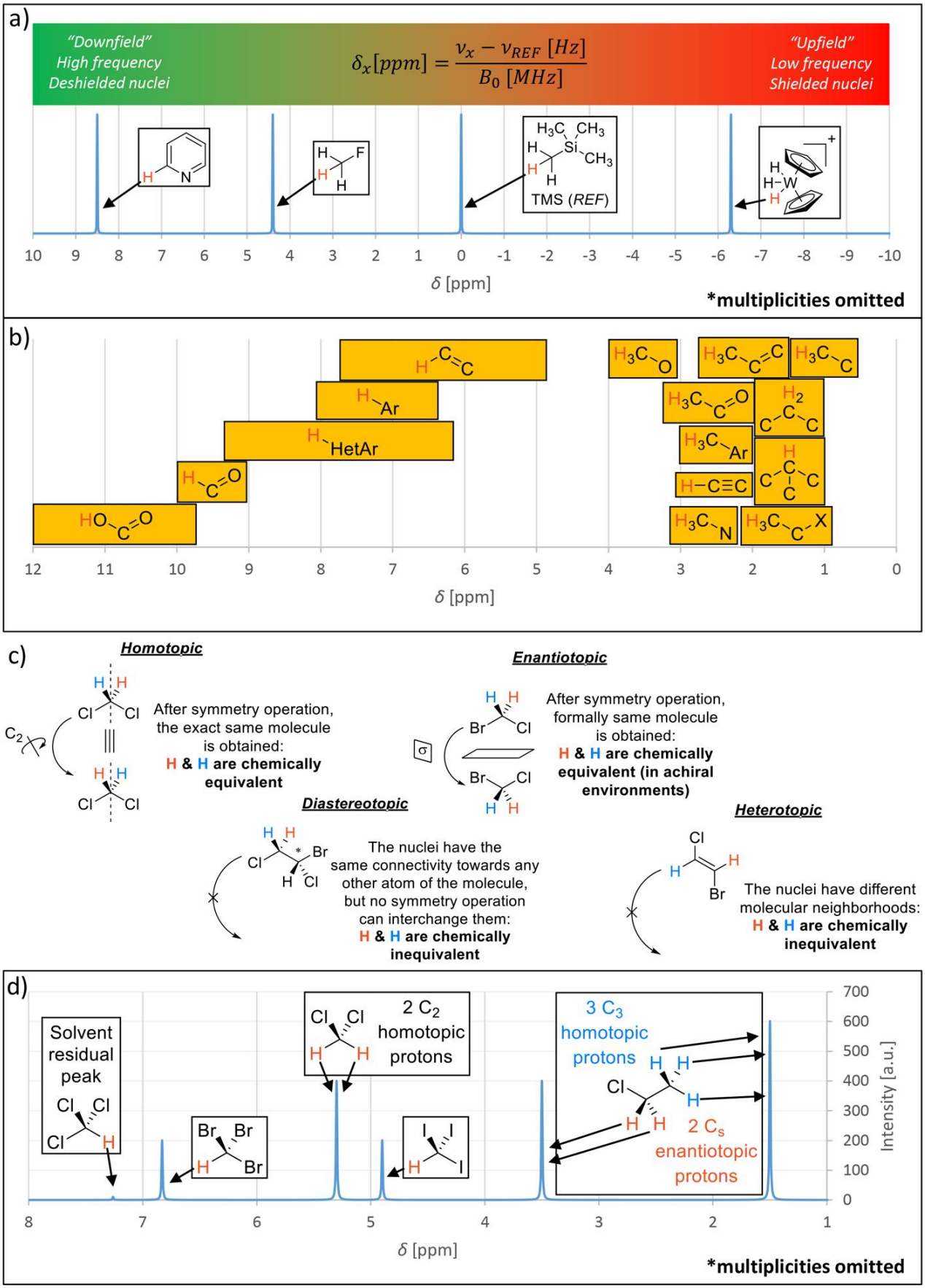

Figure 7. a) δ-based frequency-domain spectrum; b) ^{1}H NMR δ table; c) NMR nuclei chemical equivalence; d) quantitative ^{1}H NMR.

The magnetic field experienced by magnetically active nuclei is not only influenced by their electrons but also by other nearby magnetically active nuclei. **J-coupling** is a type of shift in the resonance frequency of a nucleus arising from interaction with nearby nuclei through covalent bonds. The nearby nuclei will polarize the spins of the bonding electrons which in turn will perturb the energy levels of the nucleus. These interactions cause **signal multiplicity**, because the shift depends on the relation between the spin states of the interacting nuclei: given a proton A in its spin state, according to the spin state of a second proton B interacting with it the local magnetic field might either increase or decrease. As the spectrum takes into account all the nuclei in solution, statistically half of protons A interact with protons B whose spin states match and the half with opposite spin states, because α and β states have almost the same population (small energy difference). This means that the original peak (**singlet**) is split in a **doublet** of peaks whose relative areas are 1:1 (Figure 8.a), even though both actually represent the same kind of proton. If proton A interacts with multiple equivalent protons B, then the peak will be split in a **multiplet** of peaks whose relative areas are set by the **Pascal's triangle**, which takes into account all of the spin state combinations and merges those which cause the same shift. If proton A interacts with more sets of equivalent protons, each set induces an **independent** signal splitting. If proton A interacts with other nuclides with $I = ½$ the same exact rules apply, while nuclides with $I > ½$ will split the signal into peaks according to the number and probability of their spin states. Coupling between nuclei other than protons works the same way. The general rule is that n nuclei with nuclear spin I induces the peak of nuclei it is coupling with to split in $2nI+1$ peaks. However, nuclei that relax very fast in theory should induce splitting, but in practice no splitting is observed.

As the signal splits due to J-coupling, the center of the multiplet will mark the δ of the signal. The peaks of a multiplet are equidistant from each other, and the distance between them is called **coupling constant** (J). The coupling constant is given in Hz. It is independent from B_0, hence, under the same experimental conditions (solvent, concentration, temperature, *etc.*) it will always be the same. The value of the coupling constant depends on the number of bonds between the coupling nuclei, diminishing when the number of bonds increases. In the case of ^{1}H-^{1}H couplings, the most often observed interactions are the ones between germinal protons (two-bonds distance, $^2J_{H\text{-}H}$) or vicinal protons (three-bonds distance, $^3J_{H\text{-}H}$). Constants for protons 4 bonds away ($^4J_{H\text{-}H}$) or more are usually too small to be determined (<1 Hz). As J-coupling is a mutual interaction, the same coupling constant is observed in the multiplets of the two coupling nuclei ($J_{AB} = J_{BA}$) (Figure 8.b). This feature of the spectrum has great practical importance since it allows to recognize which nuclei are structurally close to each other, which can greatly facilitate structure elucidation. The value of the coupling constant also depends on geometry, including conformational geometry. If the geometry readily changes, for instance due to free rotation around σ bonds, the average coupling constant can be observed in the spectrum. Certain structural features, such conjugated π-electron system and specific geometries, may allow the observation of long-range couplings, $^4J_{H\text{-}H}$, $^5J_{H\text{-}H}$, *etc.*

It is also important to note that chemically equivalent nuclei also couple between them, but the coupling usually does not cause signal splitting in the spectrum (*e.g.* ^{1}H NMR signal of CH_2Cl_2 is a singlet). However, there are exceptions. Nuclei that display the same coupling behavior (**isogamous coupling**) are called **magnetically equivalent**. All the magnetically equivalent nuclei are also chemically equivalent, but the opposite is not true. Magnetically equivalent nuclei couple in the same way with each and every other magnetically active nucleus in the molecule that relax slow enough and are close enough for the coupling to happen (Figure 8.c). Limited molecular motion (*e.g.* unsaturated systems) may prevent isogamous coupling of chemically equivalent nuclei. Magnetically equivalent nuclei couple between them, but this coupling is not observed directly. Chemically equivalent but magnetically inequivalent visibly couple between them, multiplying the peaks and greatly complicating the spectra.

The signal splitting due to J-coupling will occur in accordance with the above rules only if the chemical shift of the coupling nuclei is sufficiently different with respect to the coupling constant, that is, if $\Delta\nu/J > 10$. This type of coupling is called **first-order** J-coupling. If the resonance frequencies of the coupling nuclei are relatively close compared to the value of the coupling constant, $\Delta\nu/J < 10$, then the coupling is **second-order** and deviates from normal rules. The most visible second-order effect is the perturbation of the spin states populations, which changes the multiplets relative areas. This makes the peaks of coupled signals **slant** toward each other (Figure 8.d). Other second-order effects are **deceptively simple spectra**, with nuclei that are not magnetically equivalent appearing as they are, and **virtual coupling**, with nuclei that do not couple

appearing as they do. In all of these cases, *J*s and also *δ* cannot be obtained directly from the spectrum, and mathematical analysis of the spectral data is required.[65]

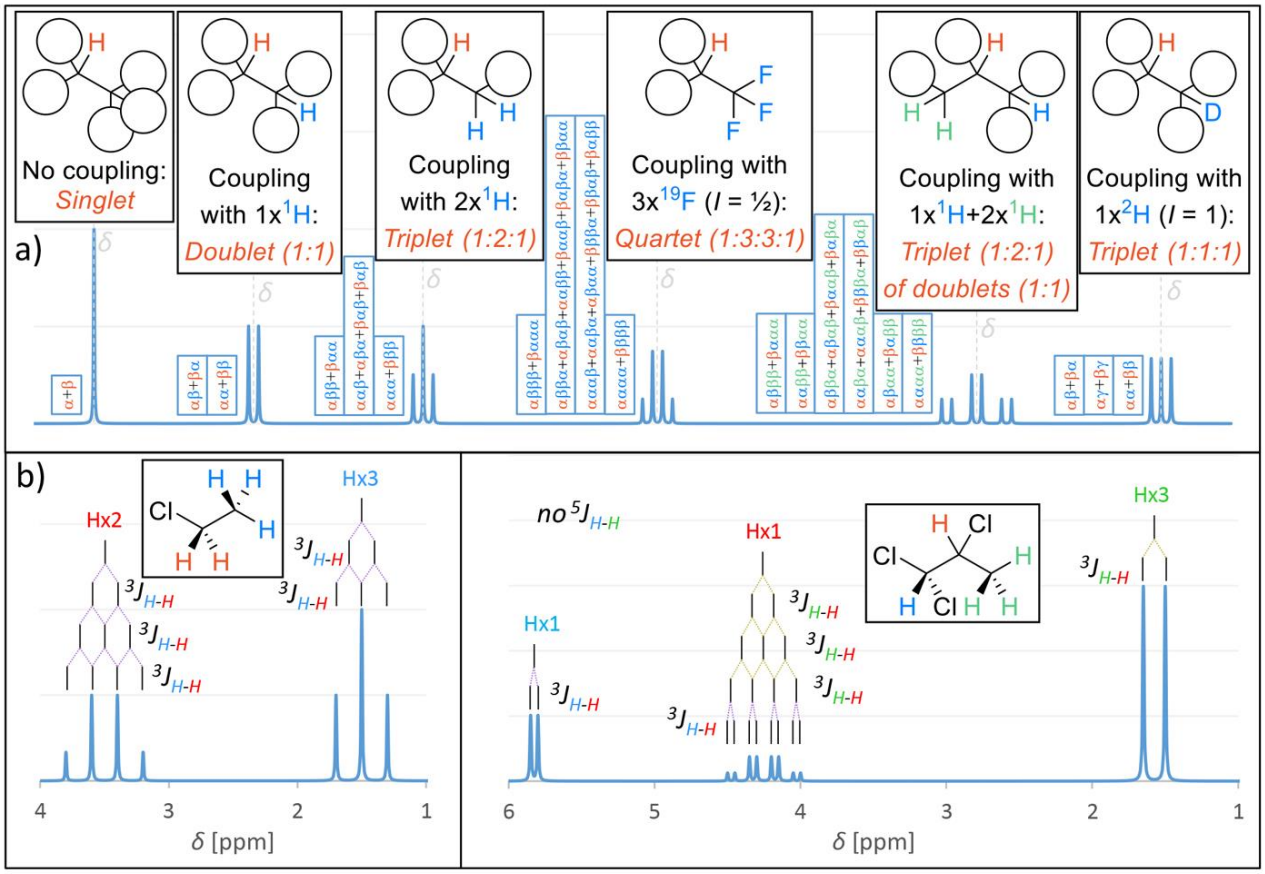

c)

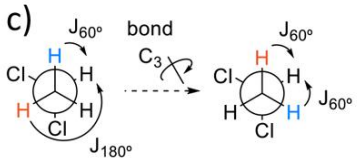

H & H are chemically equivalent and magnetically equivalent: the nuclei may couple differently with the H, but fast bond rotation averages out both chemical shift and coupling constant.

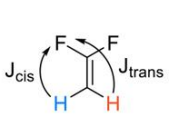

H & H are chemically equivalent but magnetically inequivalent: the nuclei couple differently with one F or the other all the time, as rotation is prevented by the double bond.

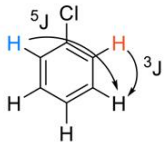

H & H are chemically equivalent but magnetically inequivalent: the rigid ring does not allow rotation. Very common situation in aromatic systems.

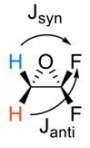

H & H are chemically equivalent but magnetically inequivalent: the cyclic structure does not allow rotation.

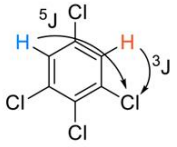

H & H are chemically equivalent and magnetically equivalent: the rigid ring does not allow rotation but Cl relax very fast and does not couple.

d)

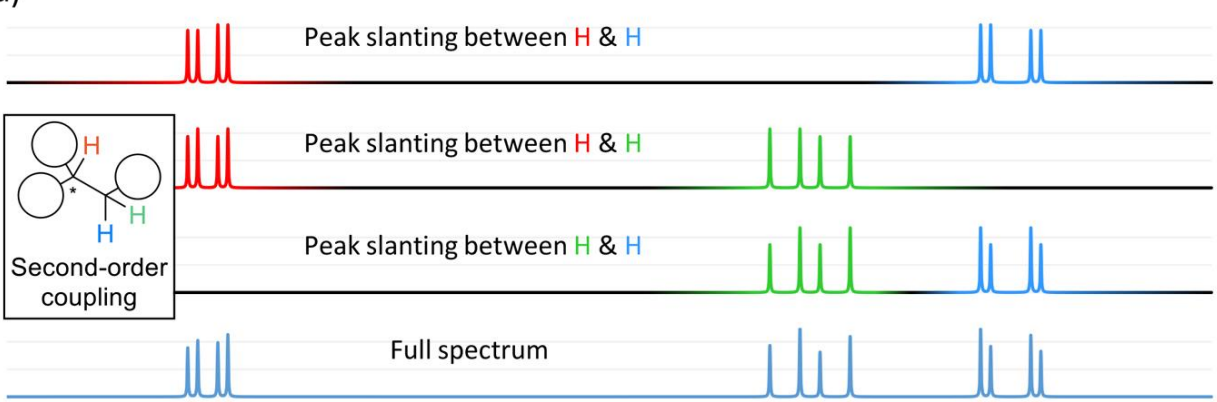

Figure 8. a) Signal multiplicity; b) Coupling constants; c) NMR nuclei magnetic equivalence; d) Slanting as a second-order effect.

Analysis with **complex pulse sequences** provide spectra that provide additional information contain considerable additional information, in comparison with common NMR spectra. Complex pulse sequences consist of multiple pulses, consecutive and/or simultaneous, with a variety of irradiation times and/or orientations, which are designed to have characteristic effects on the spectrum, which in turn can be attributed to specific characteristics of the molecular structure.

Spin decoupling involves the continuous use of certain pulse sequences (*e.g.* WALTZ-16) to irradiate the sample at specific frequencies, leading to spin saturation of the nuclei resonating at those frequencies The spin saturation makes those nuclei invisible to NMR, neither their signal nor their J-coupling interaction will be detected (Figure 9.a). **Heteronuclear decoupling** cancels the J-splitting operated by nuclei of nuclides different from the one under examination. This implies the use of at least a second RF coil, as the operating frequencies are usually very different. To remove all of the couplings from the nuclide, irradiation over a broad range of frequencies is required (**broadband decoupling**). The most popular application of this technique is $^{13}C\{^{1}H\}$ broadband decoupling, that simplifies complex ^{13}C spectra and improves S/N ratio by obtaining intense singlets out of multiplets and by also giving rise to a phenomenon called nuclear Overhauser effect (nOe). Broadband decoupling does not apply to **homonuclear decoupling**, as it would remove not only the all of the couplings between peaks but the peaks as well. Nevertheless, decoupling at very specific frequencies would remove only the correspondent peak and its J-coupling interaction. Indeed, beside simplifying spectra, decoupling can help pinpointing J-couplings between signals, which gives insights on bond vicinity of the corresponding nuclei. In any case, obtaining a broadband homonuclear decoupled spectrum is still possible by means of more complex pulses sequences.[66]

The **nuclear Overhouser effect** (nOe) is an enhancement of signal intensities caused cross relaxation between nuclei magnetic dipoles. Combination of energy levels for a pair of $I = ½$ nuclei (X and Y) lead to an energy diagram with 4 states (Figure 9.b). To simplify the explanation, let us consider that there is no J-coupling between X and Y, but nOe between J-coupling nuclei works basically the same way. Having saturated the spin states of X via spin decoupling, when the irradiation stops, the system will undergo a series of transitions to reestablish the equilibrium populations between states W_1^Y is a single-quantum transition between states of α^Y and of β^Y. The population difference of these states is not affected by saturation and this will therefore not be an operative relaxation pathway. W_1^X is also a single-quantum transition, which reverses the saturation without changing the population difference between α^Y and of β^Y. Therefore, the relative peak area will not be affected and no nOe can be observed. W_2 is a double-quantum transition that increases this population difference and produces a positive nOe. Conversely, the zero-quantum transition W_0 decreases the population difference and results in a negative nOe. W_1^X, W_2 and W_0 operate at the same time, and the dominant one will determine the overall nOe. If **molecular motion** is relatively fast on the NMR timescale, typical for small molecules and low viscosity samples, then W_2 will dominate. If molecular motion is relatively slow, typical for large molecules, viscous samples and solids, then W_0 will be dominant. In case of middle sized molecules (at MW of *ca.* 1000 g/mol), the so called nOe zero-crossing can happen. At this point, despite the close spatial proximity, no nOe can be observed. In this case, despite the close spatial proximity, no nOe can be observed. If the distance is large between nuclei (usually at a distance $r > 4\text{-}5$ Å)) the nOe becomes negligible, independently of the sign and the MW, as it decays at a rate of r^{-6}.

nOe is used, for example to recognize or prove space vicinity between protons. The most common way to visualize a nOe spectrum is the so called difference method, subtracting the normal spectrum from the spectrum of the NOE experiment. This method suffers from some drawbacks, such as difficulties with cancelling unaffected signals and with evaluating small enhancements. Due to these drawbacks, had been developed the **Double Pulsed Field Gradient Spin Echo nOe** (DPFGSE-nOe),[5] a complex pulse sequence that provides higher quality nOe spectra. It is worth noting that nOe is also used to intensify the ^{13}C signals in $^{13}C\{^{1}H\}$ spectra. The polarization transfer from the more abundant ^{1}H to ^{13}C nuclei further increases the S/N ratio, at expense of losing the quantitative information normally derives from the relative intensity of the signals. nOe has the signs swapped for nuclei with negative gyromagnetic ratios (*e.g.* ^{15}N), and it does not

take place for nuclei that preferentially relax through mechanisms other than the dipole-dipole mechanism, such as quadrupolar relaxation of most $I > ½$ nuclei.

Another useful tool is the **insensitive nuclei enhancement by polarization transfer** (INEPT) technique.[67] INEPT uses a complex pulse sequence to trigger **selective population inversion** (SPI) in a system of two J-coupled nuclei. Considering two $I = ½$ nuclei, X and the less abundant Y, with their transitions ν_X^1, ν_X^2, ν_Y^1 and ν_Y^2 (Figure 9.c), by irradiating selectively ν_X^1 the intensity of the transitions ν_Y^1 and ν_Y^2 will be greatly increased and decreased, respectively. This already allows to increase the S/N ratio, but making the peak symmetric via subtraction of the same spectra but in opposite direction, then refocusing and decoupling increase the S/N ratio to values higher than decoupling alone, although the pulse sequence is more complex. **Distortionless enhancement by polarization transfer** (DEPT) adds a ^{1}H pulse with a varying angle to a Y{^{1}H} INEPT sequence. According to the angle, the signals of the Y spectrum s will appear as positive, negative or null, depending on the number of ^{1}H attached to X. This can be very helpful in structure elucidation,[68] and it is mostly applied to the interpretation of ^{13}C spectra (Figure 9.d). The use of 90° and 135° DEPT are adequate to establish the number of protons on the carbon atoms of the molecule. With 90° DEPT, only the carbon atoms of CH moieties will have positive intensity. With 135° DEPT, both the CH and the CH_3 carbons will have positive intensity, while the CH_2 carbons will appear as negative signals. It is important to emphasize that INEPT and DEPT techniques only work when ^{1}H-^{13}C ^1J is present, thus quaternary carbons do not have signals in these spectra. DEPT is commonly used also to analyze other nuclei such as ^{15}N, ^{29}Si, etc.

In general, a great number of complex pulse sequences have been developed to obtain different specific information from the analyzed sample solution.[5] For instance, **pulse field gradient NMR** (PFG NMR) experiments make use of gradient coils, in addition to the RF coil, to apply a magnetic field gradient to the sample.[69] Nowadays every modern probehead is equipped with gradient coils. PFGs are used in order to obtain cleaner spectra, and to avoid phase cycling. One of the main applications of PFGs is **diffusion ordered spectroscopy** (DOSY). In DOSY, a first gradient pulse modifies the magnetic field experienced by nuclei according to their spatial position in the sample, causing dephasing of the magnetic moment vectors (loss of net magnetization); a second refocusing pulse restores the net magnetization, but only if the nuclei do not move in the sample. Therefore, the intensities of the observed signals will depend on the diffusion of the molecules. The diffusivity (D) of a molecule can be determined from the decay (ψ) of the intensity of its signals with increasing gradient field strength (g), obtained by repeating the same experiment multiple times at different gs. The determined diffusivity D gives information on the size of the molecules in solution.

In the last 30 years it has become increasingly common to acquire **2D-NMR spectra** (Figure 9.e).[5] These useful spectra are generated from a series of independent 1D-NMR spectra, whose pulse sequences share the same structure. First, the nuclei are excited by one or more RF pulses in the **preparation** step. Next, in the **evolution** step, the nuclei are allowed to interact for a time t_1. This phase is usually followed by a **mixing** step in which one or more RF pulses are applied. Finally, the signal **acquisition** is carried out, in the course of a t_2 time interval. This sequence is repeated multiple times gradually increasing t_1, leaving enough time between experiment so that all the nuclei will relax. The 1D-NMR t_2 FIDs are plotted over t_1, the function is Fourier transformed along t_1 and t_2 to F_1 (FT(t_1)) and F_2 (FT(t_2)). The obtained 2D-NMR spectra are usually visualized as contour (stains in a 2D graph, F_1 vs F_2) or stacked plots (2D peaks in a 3D graph, F_1 vs F_2 vs signal intensity). The significate the 2 dimensions depends on the type of pulses applied. In ***J*-resolved 2D spectroscopy** the second dimension is a J-coupling one,[70] meaning that overlapping peaks are dispersed over this dimension depending on their J-splitting pattern. Indeed, an advantage of all 2D-NMR experiments is the **improved resolution**, as signals are spread over a 2D space and peaks that overlap in a 1D spectrum can be resolved in virtue of their different characteristics. **2D correlation spectroscopy**, the biggest family of 2D-techniques, highlight correlations between the signals of F_1 and F_2, based on interactions between nuclei, facilitating peaks assignation. For example, among the most performed 2D-experiments is the **homonuclear correlation spectroscopy** (COSY) for highlighting J-coupling between protons and identify the protons usually 3 bonds away from each other (*i.e.* F_1 and F_2 are two identical 1D ^{1}H-NMR spectra and the stains in a contour plot show which signals correspond to ^{1}Hs that are at most 3 bonds away). The **nuclear Overhauser effect spectroscopy** (NOESY) and its heteronuclear analogue (HOESY) highlight nOe between nuclei. nOes can reveal the spatial proximities and thus can help solving structure elucidation problems (*e.g.* differentiating between isomers) or even provide the 3D structure (*i.e.* F_1 and F_2 are two identical 1D ^{1}H-NMR spectra and stains/peaks reveal protons that are spatially close). The **heteronuclear single-quantum correlation**

spectroscopy (HSQC) reveals $^{1}J(X\text{-}^{1}H)$ couplings. In its most typical application, F_1 and F_2 are 1D ^{13}C- and ^{1}H-NMR spectra, respectively, and the 2D spectrum indicates the directly bound protons and carbons. The **heteronuclear multiple-bonds correlation spectroscopy** (HMBC) identifies $^{2}J_{(X\text{-}1H)}$ and $^{3}J_{(X\text{-}1H)}$ couplings, typically between proton and carbon nuclei 2 and 3 bonds away from each other.

Several so called **pure shift techniques**, which help to suppress *J*-couplings in the 1D ^{1}H spectrum and several ^{1}H detected 2D techniques, have been developed.[71]

At present, 2D-NMR techniques represent a well-established field, they are commonly used for structure determination. However, they do have some disadvantages, limitations. An obvious drawback is the longer acquisition times, deriving from the fact that multiple 1D scans are required to obtain a 2D spectrum. Since the time to analyze multiple samples is considerable, the application of 2D-NMR spectrometry to dynamic systems, unstable analytes, online or operando analyses, etc. is significantly limited.

To overcome the limitations of the classic 2D techniques in terms of time efficiency, **ultrafast 2D** (UF-2D) NMR spectroscopy has been developed.[72,73] Using UF-2D, due to spatial encoding, the series of experiments required to generate a 2D NMR spectrum is reduced to a single experiment only. However this approach suffers of some drawbacks, among which is low sensitivity. Over the years, the technique has evolved. Pulse sequences have been improved, multiscan strategies have been developed and hyperpolarization techniques have been implemented.[74,75] Importantly, both conventional and UF-2D NMR techniques can be performed on benchtop NMR spectrometers, as well.[76,77]

Analogously to 2D-NMR, 3D-NMR techniques can show correlation between three 1D NMR spectra. A 3D NMR spectrum could be represented as a 3D cubic spectrum, or as 2D spectra that are slices of the 3D spectrum, as well as a collection of restricted-window 2D spectra recorded at different positions of the remaining 1D spectrum (also called strips). 3D (and higher dimensional) NMR experiments have mostly been applied in the field of structural biology, but they have importance to materials' characterization too. The time required for an experiment increase exponentially with dimensionality, which can be detrimental in the analysis of samples with limited chemical stability. Therefore, with multidimensional techniques, such aspects as the sampling method and data processing become very important in order to decrease the overall analysis time (e.g. **nonuniform sampling**, NUS).[78–80] **Polarization-enhanced fast-pulsing techniques** (*e.g.* BEST, SOFAST) are complementary to these sampling approaches, as they enhance sensitivity and reduce acquisition times.[79] The ultrafast approach could also be adapted to 3D NMR, either with a UF-3D single scan experiment or a hybrid UF-2D vs. 1D NMR.

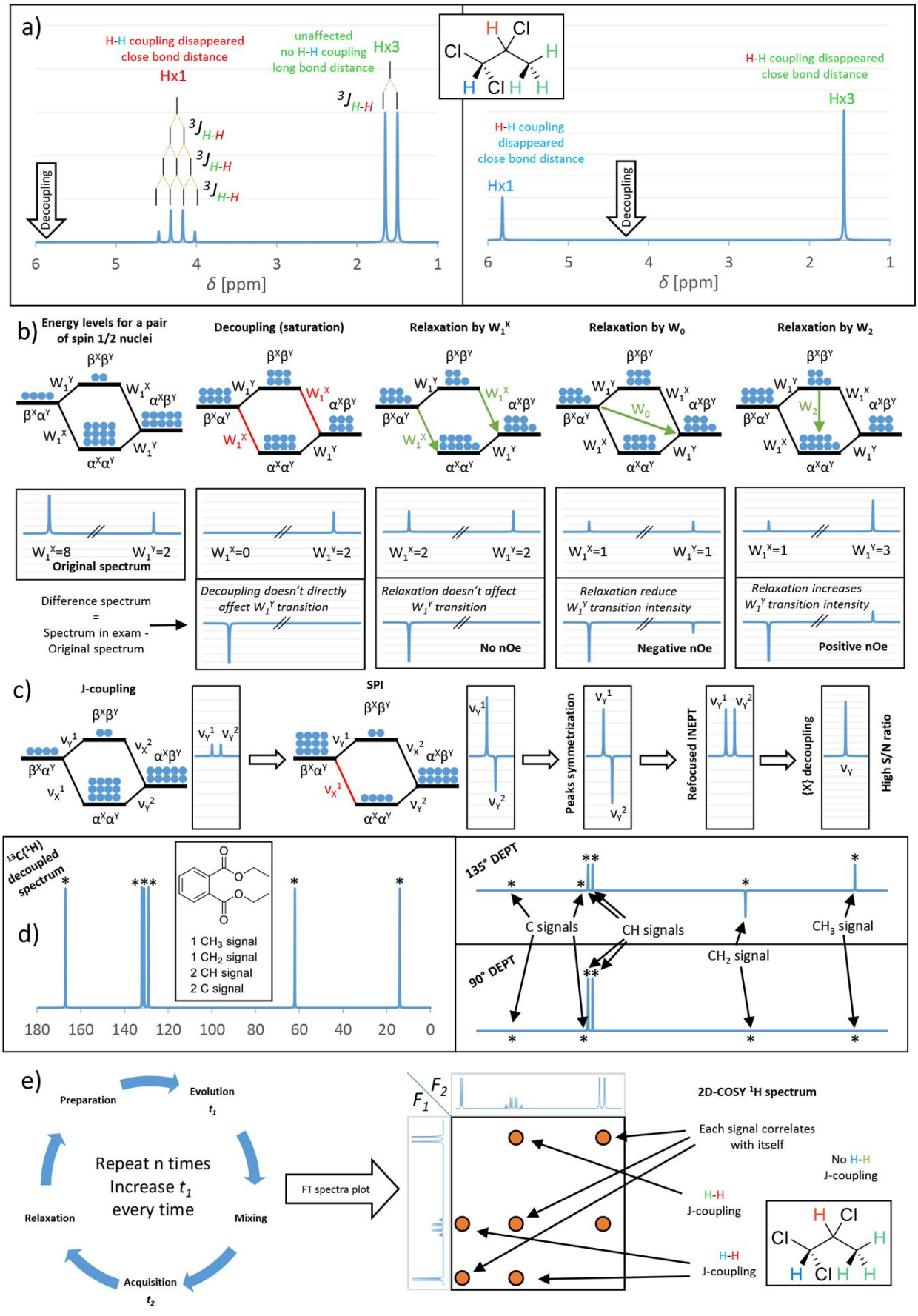

Figure 9. a) Decoupling; b) nOe spectrum; c) INEPT spectrum; d) DEPT spectrum; e) 2D-NMR contour spectrum.

8.2 - ssNMR spectrum analysis

Solid-state NMR (**ssNMR**) spectra are recorded and interpreted similarly to the lpNMR spectra. The qualitative and quantitative concepts of the spectra, such as the chemical shift, the area under the NMR resonance signal, etc., are analogous to those in the lpNMR, too. Nevertheless, the **restricted mobility** of the nuclei in the solid sample highlights interactions that are **averaged out** in lpNMR as a result of the isotropic tumbling of molecules, which on one hand has a negative effect on the resolution and requires numerous expedients obtain meaningful spectra. On the other hand, it provides insights into the solid-phase structure and dynamics.

While in lpNMR, fast rotations around sigma bonds may result in **chemical equivalence** of certain nuclei, in ssNMR molecular motion usually is strongly restricted, and the number of signals can multiply, although some rotations might still occur at relatively high temperatures.[7,81] Moreover, in lpNMR the chemical shift of a signal is averaged by the rapid random motion of molecules in solution, but it actually assumes different values according to the nuclei orientation with respect to B_0. The non-spherically symmetric electron distribution has an influence on the shielding and it is commonly described with a **chemical shift tensor** (Figure 10.a).[82] In ssNMR the reorientations do not happen, resulting in **chemical shift anisotropy** (CSA). As a consequence, in single crystals, a discrete set of signals appears in the spectra depending on the number of nonequivalent nuclei in the unit cell and the crystal orientation.[83] In powders (the most common sample form in ssNMR) orientations of the crystallites are random and the signal will appear as a broad peak with a characteristic shape. The symmetry of the chemical shift tensors will define the shape of the signals (Figure 10.a).

Magic angle spinning (MAS) is an NMR technique that has been developed to improve resolution in ssNMR by means of averaging CSA and eliminating powder patterns. For the overall axially symmetric CSA of a single crystal, the anisotropy can be averaged to zero if the CSA long axis is inclined at the magic angle with respect to B_0. The obtained δ is called isotropic chemical shift (δ_{ISO}). For polycrystalline powders this is not possible, but by spinning the sample at the magic angle the average CSA looks like an ellipsoid whose long axis is oriented at the magic angle, even when the CSA is not axially symmetric.[81] The **spinning rate** to narrow a peak must have a frequency higher than the spectral window the broad peak occupies. At low spinning rates, the broad peak collapses in multiple peaks. In addition to the isotropic δ_{ISO} peak, **spinning sidebands** also appear, as a result of the incomplete averaging of the CSA ellipsoid at slow spinning speeds (Figure 10.b). Spinning sidebands can be easily identified as their distance is always a frequency that is an integer multiple of the spinning frequency. Hence, spinning sidebands change in number and position at different rates, while the δ_{ISO} peaks does not, and they can be suppressed by techniques such as TOSS or SELTICS.[84] Although the presence of spinning sidebands is usually undesired, they can give useful information for the determination of CSA parameters.[81]

Over time, technological solutions have been developed to increase MAS spinning rates and improve spectrum quality. **Ultrafast MAS** probes have been developed,[85] nowadays probes that can spin at rates higher than 100 kHz have become commercially available,[86,87] and experiments utilizing spinning rates as high as 140 kHz have been reported.[88] The spinning rate is limited by the speed of sound. For this, in some cases specific gases different from air are used (*e.g.* the speed of sound in He gas is about 3 times higher than air). It is also to be considered that an increase in spinning rate requires corresponding decrease in the rotor size. This means that the quantity of the analyte is very little, which has a negative impact on the absolute sensitivity of the analysis. Moreover, sample preparation for ultrafast MAS experiments takes longer, and the available temperature range for the analysis is narrower (-50/50 °C vs -100/200 °C).[89] Nevertheless, this technique has numerous of advantages, notably, the higher RF efficiency, the possibility of using low-power complex sequences, and its particular efficiency in reducing peak broadening. Indeed, ultrafast MAS has contributed greatly to the development of ^{1}H ssNMR, notoriously less studied than its lpNMR counterpart. Mapping the local environment of hydrogen atoms is extremely desirable in materials science, as they are often present in high quantity and they have high isotopic abundance and sensitivity to NMR. lpNMR methods are based on the high resolution (in the order of 1 Hz) of the ^{1}H spectrum. However, in ssNMR we have to overcome the obstacle of broad signals due to the strong ^{1}H–^{1}H homonuclear **dipolar coupling** (in the order of kHz). Ultrafast MAS improves ^{1}H spectral resolution, simplifying experiments such as correlation spectroscopy and internuclear distance measurements.[90]

In lpNMR, dipolar coupling is averaged out by fast molecular tubling, as the effects of the dipolar coupling decay rapidly with the distance between nuclei. In ssNMR, because of the restricted motion the dipolar coupling constant may assume a value that could be relatively high as compared to the nuclide chemical shift range. Moreover, each pair of spins in the solid establish a dipolar coupling, whose constant depend on the length of the internuclear vectors and the angle that it makes with B_0. Given the amount of nuclei in a solid sample, a great number of coupling constants are experienced at the same time, transforming the narrow peaks typical of lpNMR into broad ones. If the only source of peak broadening was the dipolar coupling between only two sets of I = ½ nuclei for the whole powder sample, the peak would have what is called a **Pake doublet** shape (Figure 10.c). The peak splitting arises from the different spin pairings and the broadening from the different orientations of the internuclear vectors.

Dipolar coupling can be either heteronuclear or homonuclear. For instance, in the ^{13}C spectra of organic molecules, most of the times ^{1}H are the only active nuclei ^{13}C can couple with, considering that the low abundance of ^{13}C makes its homonuclear coupling negligible. In this case to obtain a cleaner spectrum it may be necessary to remove the effects of the ^{1}H-^{13}C dipolar coupling. One way to remove this is **heteronuclear dipolar decoupling**, which works in an analogous way to the lpNMR one of J-coupling.[91] Even so, peak broadening by homonuclear coupling and heteronuclear coupling with nuclei different than the decoupled one would still be present. Complete dipolar decoupling would afford peaks whose shape is given by CSA, indeed this technique is generally coupled with MAS. MAS itself reduces the effects of heteronuclear dipolar coupling although its effectiveness is limited, especially at low spinning rates. Homonuclear dipolar coupling can be removed by MAS only for nuclei with low γ (*e.g.* ^{13}C and ^{15}N), while for ^{1}H and other high γ nuclei the coupling constants are too high and **homonuclear dipolar decoupling** is required to achieve satisfactory spectrum resolution.[92] Other strategies are also possible, such as proton dilution with deuterium atoms[93] and ultrafast NMR.[94] Homonuclear dipolar decoupling is achieved by the combination of MAS with special RF pulses, usually referred to as **CRAMPS** (combined rotation and multi-pulse spectroscopy).[95] In general, the ^{1}H CRAMPS approach provides results of higher resolution and higher reliability than MAS-only results,[96] although it has been recently demonstrated that ultrafast MAS may provide spectra with ^{1}H line widths comparable to the ones obtained with state of the art homonuclear decoupling schemes under optimal conditions.[97] The traditional CRAMPS experiment is performed at slow spinning rates (*ca.* 10 kHz) for the rotor period to be long compared to the multiple-pulse cycle, therefore there is no need to use expensive probeheads capable of fast MAS. Over the years, various methods have been presented that are applicable at faster MAS frequencies (up to 65 kHz).[98] Acquiring a spectrum with the CRAMPS technique is usually electronically demanding, as very short hard pulses have to be applied.

2D and multidimensional techniques can also be applied to the analysis of static and rotating solids. For instance, **spin diffusion** experiments afford information on homonuclear spin-pair dipolar connectivities;[99] the use of radio frequency driven dipolar recoupling (RFDR) pulses could shorten the mixing time.[100] **Double quantum/single quantum** (DQ/SQ) correlation experiments (*e.g.* BaBa)[101] include the excitation of DQ coherences and generally better separate the overlapped cross peaks as compared to SQ/SQ experiments. These techniques are especially useful when coupled with ultrafast MAS (*e.g.* in the study of ^{1}H-^{1}H dipolar couplings).[90] 3D versions of these experiments have also been developed.[102] They are also compatible with UF-2D analyses.[103] As for the coupling of different nuclei, **heteronuclear correlation** (HETCOR) experiments are used.[104] Unlike J-coupling-based techniques used in lpNMR, such as HSQC, HMBC, etc., HETCOR in ssNMR is based on dipolar coupling. J-coupling is present in ssNMR too, and it may show some anisotropicity because of the reduced motion, but the order of magnitude of the constants is usually lower than in the case of dipolar coupling. 2D-correlation spectroscopy based on J-coupling is possible, although less common.[105]

As in lpNMR, in ssNMR it is common to use polarization transfer to improve the signal-noise ratio in the spectra of low-abundance nuclei: this is achieved with a technique called **cross polarization** (CP).[106] By applying simultaneously two RF pulses B_{1I}^{+} and B_{1S}^{+} whose frequencies brings about the resonance of the I nuclei in a sample as well as the rare S ones, and whose pulse strengths makes the frequency of M_I and M_S rotations equal in their own rotating frames, the **Hartman-Hahn conditions** are met and the two nuclei can mutually exchange magnetization. After an optimized RF pulse width (or contact time), I is decoupled while the S spectrum is acquired. All of the S nuclei that undergo dipolar coupling with I will increase their polarization and experience an increase in the area of the respective peaks. As a slightly imprecise pulse can

have a radical effect on the Hartman-Hahn matching, a ramped contact pulse could be preferred to make it it less susceptible to instrumental imprecisions. CP is generally coupled with MAS (CP-MAS) to obtain peaks that are both intense and sharp. CP-MAS is often used when recording ^{13}C spectra, exploiting ^{1}H natural abundance. Moreover, as ^{1}H relaxes faster than ^{13}C, the relaxation time is reduced to the one of ^{1}H, **reducing the time of the experiments** too. CP-MAS is commonly used for other nuclei such as ^{15}N and ^{29}Si. CP works well for rigid systems, whereas in mobile systems heteronuclear dipolar couplings are averaged by molecular motions. Combination of CP with nOe or refocused-INEPT could enhance the intensity of the signal of mobile components.[107] One of the main problems of CP in systems such as ^{13}C-^{1}H networks is that the contact time has to be optimized considering the slow magnetization increase of ^{13}C not directly bound to ^{1}H, and the decay of ^{1}H magnetization. Under these conditions, different carbons will be polarized differently, therefore CP spectra are usually not quantitative. To solve this issue, **multiple cross polarization** (multiCP) was developed. The introduction of intervals between short CP pulses allows repolarization of ^{1}H and an even polarization of all ^{13}C at the end of the pulse sequence, enabling quantitative CP.[108]

In some cases, traditional polarization methods are not enough to obtain a signal with a satisfactory intensity. A way to greatly increase signals intensities is **dynamic nuclear polarization** (DNP) .[109] DNP is a technique that falls in the category of hyperpolarizations, and it is used also for liquid samples,[74] although the solid state version is most appropriate for material characterization. With this technique, the large polarization of unpaired electrons of radical species contained in the sample is transferred to the nuclei of interest upon saturation of electron paramagnetic resonance (EPR) transitions reached by irradiating the sample with microwaves. The sample is generally prepared by creating a glass-forming matrix with an appropriate solvent in which the polarizing agent is dissolved, and the analyte. Depending on the nuclei to analyze, cross polarization could be used to transfer the enhanced polarization to more diluted spins (indirect DNP). DNP is compatible and often coupled with MAS. **Signal enhancements** obtainable depend in theory on the ratios between the *γ*s of electron spins and nuclei, and in practice are routinely over x20 but can reach several hundreds in some cases, greatly contributing to push NMR sensitivity limits and expand the applicability of the NMR to systems whose analysis was not feasible before. Moreover, DNP can be used for probing **surfaces** selectively.[110] For this, DNP in recent years has attracted considerable attention, although it still is at early stages and far from routine use, mostly because of its complex setup. DNP MAS probes include both rotors for MAS and gyrotrons for microwaves, and in addition most of the analyses are run on samples at cryogenic temperatures, provided by liquid N_2. Nowadays, such probes are commercially available.[111] Systems to reduce the minimum achievable temperatures have been developed, by substituting N_2 with He, which also allows higher MAS frequencies.[112,113] It is important to note that the use of cryogenic MAS probes is not limited to DNP analysis, they can be applied generally in ssNMR analyses as lower temperatures increase the theoretical signal to noise ratio.[114]

Solid-state **Pulse-Field Gradient** (**PFG)** NMR can be used to gather information about mass transfer in porous materials, as it allows the estimation of the diffusion coefficient D of the mobile species.[115] Note that PFG NMR is also used in liquid samples with a similar purpose (cf. Chapter 8.1). It is important to note that the minimum detectable molecular displacement is limited by the transversal relaxation time of the analyzed nucleus, hence limiting the application of the technique to system with a relatively high molecular mobility. With the implementation of spinning, **MAS PFG NMR** improves the transversal relaxation and therefore the applicability of the technique to low mobility systems. Moreover, the improvement in transversal relaxation leads also to the traditional resolution improvement with MAS. On the other hand, with the introduction of MAS the amplitude of the applied gradient is lower, and there is a loss in spatial resolution of the molecular displacement. The probe setup includes two gradient coils on the top and bottom of the MAS stator, for a field gradient aligned to the magic angle. The sample preparation for this type of experiments happens in a sealable glass insert that fits the MAS rotor, which is then sealed. This allows to keep the pressure and prevents the fluid to leave the sample. The additional gravity forces in play with MAS could be expected to have an influence on the results, but no significant effect have been found.

$I > ½$ nuclei in solution do not behave very differently to $I = ½$ nuclei, although their peaks could be broadened by the fast quadrupolar relaxation, and their splitting pattern is different. $I > ½$ nuclei do not have a spherical charge distribution thus if they are located in a solid in which there typically is an electric field gradient, **quadrupolar coupling** arises.[116,117] As a result, the Zeeman splitting, in which transitions share the same ΔE and afford a single peak, is perturbed based on a coupling constant, multiplying the number of

peaks. The coupling constant depends on the coupling orientation with respect to B_0, which makes quadrupolar coupling another source of peak broadenings when working with powders (Figure 10.d). Fortunately, for **first-order quadrupolar coupling** the constant is nullified at the magic angle and simple MAS can remove it from the spectrum. If the first-order quadrupolar coupling constant is high enough, **second-order quadrupolar coupling** is observed, and its constant is nullified by rotation angles different than the magic angle. With the exception of some nuclei with $I = 1$ that are often analyzed with NMR (*e.g.* ^{2}H,[118] or ^{14}N for the high isotopic abundance), in almost all cases quadrupolar nuclei analyzed with NMR have a $I = n/2$. For this, among the peaks in the spectra of quadrupolar nuclei, generally only the peak resulting from the single-quantum **central transition** (CT, $m = ½ \leftrightarrow - ½$) is studied: the CT peak is much sharper than the others because it is not affected by the first-order quadrupolar coupling, while the **satellite transitions** (ST) are broadened by it, sometimes to the point that they become undetectable with strong couplings. Still, the CT peak is affected by second-order coupling, whose broadening is not reduced by MAS, although MAS improves the broadening from the powder pattern. One approach to eliminate this broadening is to physically rotate the sample at different angles, either simultaneously with **double rotation** (DOR, with a rotor inside another rotor) or sequentially with **dynamic-angle spinning** (DAS, with the rotor changing angle).[119] It has to be noted that these two techniques are far from simple, routine use because specialized probe heads are required.

The other, more common approach is to resort to a type of complex pulse sequence known as **multi-quantum combined with MAS** (MQMAS).[119–121] MQMAS is a 2D experiment that affords spectra containing isotropic CTs peaks, free from second-order quadrupolar broadening. The development of this technique was groundbreaking, and made possible the analysis of quadrupolar nuclei without the use of very complex setups such as the ones related to DOR and DAS, which was a very limiting issue in the field, considering that the vast majority of the NMR-active nuclei are quadrupolar and that many elements only have NMR-active isotopes that are quadrupolar. MQMAS refocuses the anisotropies by compensating the residual CT broadening with the ones related to multiple quantum transitions. MQMAS experiments with different coherence level pathways have been developed, but in general they start with excitation of symmetric $m = x/2 \leftrightarrow - x/2$ coherences (xQ) in the first part of the pulse sequence. After an evolution time, a second pulse converts the coherence to the single-quantum one. If the time t_1 and t_2 between and after pulses are properly chosen, in the 2D spectra obtained after FT with respect to these two times the anisotropies related to second-order coupling are averaged out. Nowadays, two MQMAS pulse sequences, **z-filter** and **shifted echo**, are commonly used. To obtain the isotropic projection (broadening-free 1D spectrum) out of the 2D spectra acquired with the two aforementioned experiments a **shearing** transformation has to be applied, which can be performed by spectrum editing tools. The obtainment of the isotropic projection is oftentimes decisive to resolve signals corresponding to nuclei with similar environments. From these spectra additional valuable information such as the quadrupolar constants and the anisotropy parameters for the CT peaks can be obtained. The development of the **split-t_1 method** has removed the need of shearing. MQMAS can be coupled to other techniques (*e.g.* cross polarization, correlation with other nuclei). Multiple-quantum transitions are prohibited, therefore the signals refocusing comes with loss of signal, making MQMAS a relatively insensitive technique. Effort over the years have been put in to enhance sensitivity and expand the technique to nuclei that are hard to analyze. Some strategies that have been developed aim to improve the efficiency of the MQ excitation (*e.g.* FASTER,[122] RIACT)[123] and MQ to CT conversion (*e.g.* FAM,[124] SFAM,[125] SPAM,[126] DFS).[127] Another technique, the **Carr-Purcell-Meiboom-Gill** (CPMG) **echo train acquisition**, can be combined with MQMAS to improve the overall signal-to-noise factor.[128]

Another technique related to MQMAS is **satellite-transition combined with MAS** (STMAS) .[129] STMAS follows the same principles already explained, but instead of exciting multi-quantum transitions, single-quantum STs (which, differently to MQ transitions, are allowed) are excited and then the coherence is converted to the one of the CT. For this, STMAS is quite more sensitive than MQMAS, but it is also very demanding in terms of magic angle setting and spinning stability. Other techniques to analyze $I > ½$ nuclei are the quadrupolar versions of **magic-angle turning** (QMAT) and **phase-adjusted sideband separation** (QPASS) ,[130] created for $I = ½$ nuclei to obtain MAS infinite-speed spectra at moderate speeds and evolved to adapt to quadrupolar nuclei and achieving spinning sidebands separation.

Although the purpose of all the aforementioned techniques is to simplify spectra and facilitate interpretation, there are techniques that allow the reintroduction of a broadening source to obtain additional information:[81] **homo- and heteronuclear recoupling** allows the selective reintroduction of dipolar coupling

for the determination of internuclear distances and 2D-correlation spectroscopy; other techniques **reintroduce CSA**, to obtain information on the structure around the nuclei. **Rotational Echo DOuble Resonance** (REDOR) is a technique that provides a direct measure of short and long-range heteronuclear dipolar couplings, typically between rare spins pairs (*e.g.* ^{13}C-^{15}N).[131] Under certain conditions, the REDOR experiment can also be applied to quadrupolar nuclei.[132] The measured dipolar couplings contain information on internuclear distances and orientations. Although dipolar coupling is partly removed by MAS, it can be recoupled by the application of rotor synchronized pulses on the dipolar coupled spins of the observed nucleus, applied twice per rotor period, with a single π pulse applied to the other nucleus halfway during the sequence. The NMR signal of the observed nucleus is attenuated and the extent is a measure of the dipolar coupling, which yields internuclear distances. The REDOR technique has been applied to many problems from the field of biochemistry[133] to materials science. There are several other techniques related to recoupling of dipolar coupling. With the help of **Transferred-Echo DOuble-Resonance** (TEDOR) , dipolar-coupled spins can be selected from the background by a coherence transfer from one heteronucleus of the spin pair to the other.[134] With the **TRAnsfer of Population in DOuble-Resonance** (TRAPDOR) experiments the dipolar coupling of a quadrupolar and spin ½ (*e.g.* ^{14}N-^{13}C) nuclei can be measured.[135] Although TRAPDOR is an attractive experiment, sometimes it may be of limited use, for example in the case of weak interactions. However, this obstacle can be overcome by using **Rotational-Echo Adiabatic-Passage DOuble-Resonance** (REAPDOR) NMR technique, which combines the simplicity of the REDOR experiments with the adiabatic passages of TRAPDOR.[136]

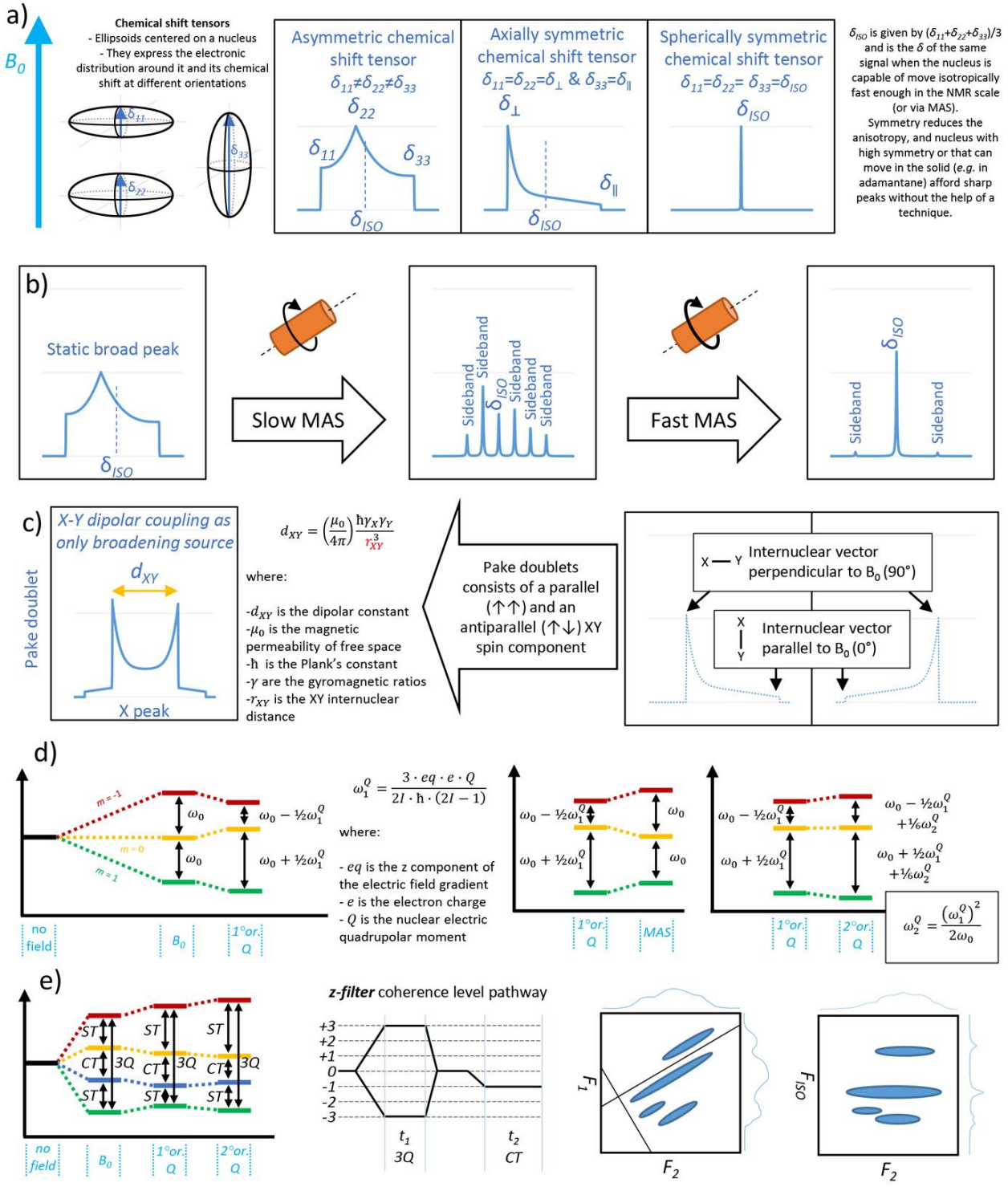

Figure 10. a) Effect of the δ tensor symmetry on spectra; b) peak narrowing by MAS; c) Pake doublet; d) quadrupolar coupling; e) MQMAS of I = 3/2 nuclei.

9 - Capabilities

The majority of elements have $I \neq 0$ NMR active nuclides, and all of them respond qualitatively and quantitatively differently to an NMR experiment. To understand the **capabilities of NMR** to analyze a given nuclide, at least the following 3 factors must be considered: **nuclear spin (*I*)**, **relative sensitivity** and **natural abundance** of the isotope.

NMR active nuclei with an odd number of nucleons have **fractional spins** (I = 1/2, 3/2, 5/2 *etc*.) whilst even mass nuclei have **integer spins** (I = 1, 2 *etc*.). Nuclei with I = 1/2 usually give rise to sharp lines in lpNMR, which rarely exceeds the linewidths a few Hz, whereas the linewidths of I > 1/2 **quadrupolar nuclei** can reach even several MHz. This is due to the fact that quadrupolar nuclei have non-spherical charge distribution and hence **fast T_1 and T_2 relaxation**, making them sometimes impossible to detect. T_1 is determined by two factors: the **nuclear electric quadrupolar moment** (Q) and **molecular symmetry**. Smaller Q nuclei (*e.g*. deuterium or ^{6}Li) are easy-to-analyze nuclei and usually give lines sharp enough to even show J coupling, whilst ^{197}Au and ^{201}Hg yield signals too broad to be observed with a high-resolution NMR spectrometer. The more symmetric the molecule the sharper the signal is (*e.g.* the ^{14}N linewidth of $N^{+}(Me)_4$ (3D symmetry) is less than 1 Hz whereas the one for NMe_3 (2D symmetry) is close to 80 Hz).[137] Fast T_1 relaxation of a quadrupolar nucleus can also cause T_2 broadening of another nucleus coupled to it. To sum up, usually in lpNMR the nuclei of choice are I = 1/2 as they give sharp signal and easily observable J couplings. Other nuclei can be measured, but not with routine techniques and the evaluation of these spectra are not always straightforward. In ssNMR, there are certain techniques with which quadrupolar nuclei, especially with half integer spins, can be easily measured with high resolution, as previously mentioned (*e.g*. MQMAS).[138]

The **sensitivity (*S*)** of a nucleus depends both on I and the gyromagnetic ratio (γ), according to the equation $S = |\gamma|^3 \cdot I \cdot (I+1)$. If γ is low (*i.e.* under the value of ^{15}N), special instrumentation may be required, and the sensitivity will be very low. The **relative sensitivity** of a nucleus is usually given compared to the most popular NMR nucleus, ^{1}H, measured under identical conditions, with the equal number of nuclei.

The **relative receptivity** (R) is the product of relative sensitivity and **natural abundance** of the given isotope. This determines the sensitivity of the NMR experiment and the effect of J-coupling on neighboring nuclei. This is the value based on which the time to measure different nuclei can be compared. While the natural abundance of ^{1}H, ^{19}F and ^{31}P is almost 100 %, two of the most important nuclei in organic chemistry, carbon (^{13}C) and nitrogen (^{15}N) are 1.1 and 0.4 % respectively, and therefore time-consuming to measure (as a higher number of scan will be required). There are certain techniques in 1D NMR which can help to increase the sensitivity, such as INEPT, DEPT or, in the case of positive γ nuclei in proximity of a proton, the nOe effect when using ^{1}H decoupling.

To improve the limits of NMR several **isotope enrichment** techniques are available. In case of molecules with high molar mass and usually small available amounts (*e.g*. proteins), enrichment of ^{13}C and ^{15}N nuclei is a must to study them properly. In other cases, isotope labelling is used to be able to study the structure and/or dynamics of only a certain site of the given molecule.

Nucleus	ν (MHz)*	γ (10^7·rad·T^{-1}·s^{-1})	R (%)**	Comments
^{1}H	500	26.8	100	Most analyzed nucleus
^{19}F	470	25.2	83.4	
^{31}P	202	10.8	6.65	
^{89}Y	24.5	-1.32	1.20 x 10^{-2}	Low γ
^{103}Rh	15.7	-0.846	3.16 x 10^{-3}	Low γ
^{169}Tm	41.4	-2.21	5.64 x 10^{-2}	Low γ

Table 2. Properties of I = ½ nuclei with ~100% natural abundance (*Using a 11.74 T magnetic field, **In a one-pulse NMR experiment, compared to ^{1}H)

Nucleus	ν (MHz)*	γ (10^7·rad·T^{-1}·s^{-1})	Nat. abund. (%)	R (%)**	Comments
^{3}H	533	28.5	0.00	rel.: 121	Highest rel. sens.
^{13}C	125	6.73	1.11	1.77 x 10^{-2}	
^{15}N	50.7	-2.71	0.365	3.85 x 10^{-4}	
^{29}Si	99.3	-5.32	4.70	3.69 x 10^{-2}	
^{57}Fe	16.1	0.866	2.19	7.38 x 10^{-5}	Low γ
^{77}Se	95.3	5.12	7.58	5.25 x 10^{-2}	
^{107}Ag	20.2	-1.09	51.8	3.43 x 10^{-3}	Low γ
^{109}Ag	23.3	-1.25	48.2	4.86 x 10^{-3}	Low γ

^{111}Cd	106	-5.69	12.8	0.121	
^{113}Cd	111	-5.96	12.3	0.133	
^{119}Sn	186	-10.0	8.58	0.444	
^{125}Te	158	-8.50	6.99	2.20	
^{129}Xe	138	-7.44	26.4	0.560	
^{183}W	20.8	1.12	14.4	1.03×10^{-3}	Low γ
^{187}Os	11.5	0.616	1.64	2.00×10^{-5}	
^{195}Pt	107	5.77	33.7	0.336	
^{199}Hg	89.1	4.82	16.8	9.54×10^{-2}	
^{205}Tl	289	15.6	70.5	13.0	
^{207}Pb	105	5.54	22.6	0.207	

Table 3. Properties of some I = ½ nuclei with less than 100% natural abundance.

Nucleus	I	ν (MHz)*	γ (10^7radT^{-1}s^{-1})	Nat. abund. (%)	R (%)**	Q (barns)	Comments
^{2}H	1	76.7	4.11	1.15×10^{-2}	1.45×10^{-4}	2.73×10^{-3}	
^{6}Li	1	73.6	3.94	7.42	6.31×10^{-2}	3.58	
^{7}Li	3/2	194	10.4	92.6	29.2	1.54×10^{3}	
^{10}B	3	53.7	2.88	19.6	0.393	22.1	
^{11}B	3/2	160	8.58	80.4	16.4	754	
^{14}N	1	36.1	1.93	99.6	0.101	5.69	Low γ
^{17}O	5/2	67.8	-3.63	3.81×10^{-2}	1.08×10^{-3}	6.11×10^{-2}	
^{23}Na	3/2	132	7.08	100	9.25	525	
^{27}Al	5/2	130	6.98	100	20.6	1.17×10^{3}	
^{33}S	3/2	28.3	2.06	0.750	1.72×10^{-3}	9.73×10^{-2}	Low γ
^{79}Br	3/2	125	6.72	50.5	3.97	226	

Table 4. Properties of some commonly studied quadrupolar nuclei (I > ½)

9.1 - Organic materials

Organic materials are analyzed by lpNMR and ssNMR. NMR spectroscopy is particularly suitable to analyze organic matter as it is mainly composed by easy-to-analyze nuclei (*e.g.* ^{1}H, ^{13}C, ^{15}N, ^{19}F, ^{31}P).

lpNMR can be used for soluble **organic molecular solids** to determine the type of molecules present in the solid and elucidate their structure,[68] according to the considerations made in data analysis of lpNMR. lpNMR of **polymers** follow the same principles. The monomeric units in a polymer are all enchained to other units in a relatively regular order (without considering chain ends) and therefore correspondent nuclei on different units behave like chemically equivalent nuclei. However, polymers have generally a lower solubility than compared small molecules, if any. Moreover, with increasing molecular size peak broadening also increase. These macromolecules consist of monomeric units whose **mobility is restrained** by the other monomeric units they are covalently bound to. The limited mobility has analogous effects to viscosity and to staticity in solids, and brings about similar peak broadening related to anisotropicity. This is why high temperature often helps resolution, as increases the segmental motion.[139] In any case, the resolution achievable with polymer is typically lower than small molecules and oligomers, and this sometimes can pose a problem in J-constants evaluation.

Nevertheless, lpNMR is an excellent tool for the characterization of polymeric materials, as it gives great information on the polymer chain structure, which in many case has a direct effect on the properties of such materials. Typical information that can be obtained by NMR is: **copolymerization sequence** (alternating, random, block or graft copolymers), **chain ends structures** (and by signal intensity comparison between chain ends and monomeric units, the polymers **average molecular weight**), **regioisomerism** (monomers head-tail enchainment), **cis-trans isomerism**, **tacticity** (isotactic, syndiotactic or atactic polymers) and **branching**.[140] It is not always possible to obtain these information from simple 1D spectra; in case of very

complex macromolecular system it might be needed to resort to 2D or even 3D NMR.[140,141] PFG-NMR could be used to obtain the diffusion coefficient distribution (DCD) of macromolecules, which could be used to obtain a polymer molecular weight distribution (MWD).[142]

Norbornene is an unsaturated bridged bicyclic hydrocarbon. The presence of a double bond makes it suitable for polymerization. Depending on the mechanism of the method applied, the polymerization would lead to different enchainments.[143] For example, **ring opening metathesis polymerization** (ROMP) afford a **polynorbornene** (poly(NBE)) with five-membered saturated hydrocarbon rings which are connected with -HC=CH- units (Figure 11.a). The stereostructure of the polymer is determined by two features, the cis/trans ratio of the double bonds, and the tacticity of the chain, which depends on the relative orientation of adjacent chiral centers. Polymers stereoregularity is an important feature, as it could have a great influence on the material's characteristic.[144] With appropriately designed catalyst structures, very high stereoregularity can be achieved. For instance, Schrock and Hoveyda have shown that Mono-Alkoxide-Pyrrolide (MAP-type) Mo- and W-alkylidenes with small imido and large alkoxide ligands yield *cis, syndiotactic* polymers in the ROMP of norbornene-type substrates.[145]

Since poly(NBE) is organosoluble, lpNMR can be an efficient analytical tool to determine to stereostructure of poly(NBE). The ^{1}H NMR spectrum of a *cis, syndiotactic* poly(NBE) exhibit only one set of signals (Figure 11.b, cis/tras ratio of 60:1). In contrast, the spectrum of an atactic polynorbornene with low cis-selectivity will clearly show the comparable amounts of cis and trans double bonds in the polymer chain (Figure 11.c, cis/tras ratio of 2.5:1).[146] Schrock's study on the stereospecific ROMP of norbornene and tetracyclododecene discusses the NMR characterization of the different stereoisomeric polymers in detail.[147]

It is also worth noting that in the case of norbornene-type substrates the organosolubility of the polymers will greatly depend on the structure. Choosing higher boiling solvents, higher temperatures can be used for the analysis, which can ensure adequate solubility.

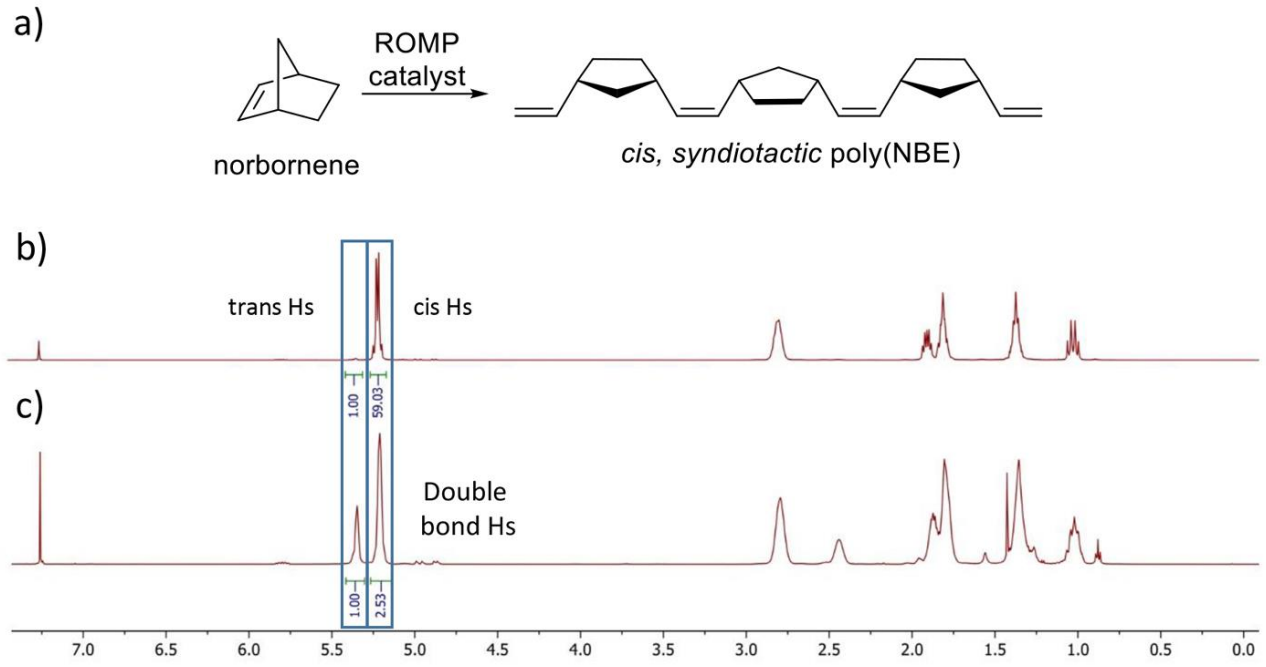

Figure 11. a) Norbornene ROMP scheme; b) ^{1}H-NMR of pure *cis, syndiotactic* poly(NBE); c) ^{1}H-NMR of irregular poly(NBE).

Crosslinking is another important factor that has a profound impact on polymer properties. NMR spectroscopy has emerged as a practical method to obtain crosslink density in a polymeric material, overcoming limitations of other analytical techniques.[148] Crosslinking greatly reduces polymer solubility, which makes it difficult to analyze such materials by lpNMR. However, alternatively, polymer swelling with a suitable solvent allows analysis of some crosslinked polymers without resorting to MAS and other ssNMR methods.[148–150] On the other hand, when crosslinking is not an issue, and the polymer has sufficient solubility,

lpNMR is often the ideal technique for analysis, as it allows simultaneous analysis of the polymer itself and that of small molecules included in the material, such as **residual solvents**, **monomers** (useful to obtain the conversion in polymer syntheses) and **additives**.[151]

Among the practical aspects of lpNMR spectroscopy of polymers, it should be considered that the increase in molecular weight has an influence on the observable **nOe**, which can be even nullified completely (zero-crossing) or change sign. Yet another issue is that the dissolution of a polymer often results in a viscosity increase. Also, **air bubbles** could get trapped in the solution, which would have a negative impact on the analysis and should be removed before analysis (e. g. by sonication). **Isotopic labeling** of initiators, chain transfer agents and quenching agents can provide useful information on chain ends. Labeling catalysts and monomers could give insights into polymerization mechanisms and can assist determining the stereostructure of the polymers.[139,152] The use of a high-field spectrometer is preferred, although it is possible to obtain a number of information on complex polymeric systems even at **low fields**. Chakrapani *et al.* recently highlighted the difference in terms of resolution and sensitivity of analysis at 400, 250 and 60 (low-field) MHz.[153] While more detailed peak information (*e.g.* multiplicity) is lost with peak broadening, systems with signals sufficiently distant from each other on the chemical shift scale still allow to obtain the ratio between areas for compositional analyses. The study showed how it is possible to distinguish signals and quantify the ratio of different polymerization enchainment (1,4-, 1,2- and 3,4-PI), and of the composition in block copolymers (SBS and SIS) and polymer blends (PS/PI and PS/PMMA), with results reflecting the ones obtained with deviation of less than 3% in all cases.

ssNMR can be used to obtain information on insoluble **organic molecular solids**, or when morphology[154] and internal mobility[155] are the information of interest, according to the considerations made in data analysis of ssNMR. Also for polymers, ssNMR could provide the same information of lpNMR for insoluble polymers but with lower resolution due to strong interactions. In addition, ssNMR analysis of polymers provides information on the disposition, mobility and interactions of polymer chains in the solid,[140] which also have an influence in determining material properties. To obtain detailed information it is often necessary to use complex pulse techniques and to record multidimensional spectra.[156,157] DNP could be used for enhance the signals.[158] UF-2D ^{1}H-^{1}H could be used to characterize elastomers.[159] The CRAMPS protocol made it possible to investigate on the **interactions** between drug probe molecules and polymers as the linewidth of the latter becomes significantly narrower compared to MAS only spectra.[160] The technique can also be applied to study molecular structure in powders.[161] 2D versions of CRAMPS can also be used to reveal H-bonds or π–π stacking effects[162] or to even determine exact **intermolecular distances,** thus providing an even more detailed picture of the given system. With the help of spatial proximities obtained from REDOR and REAPDOR experiments, the amorphous blends of tri-p-tolylamine (TTA) and polycarbonate could be characterized based on ^{13}C-^{2}D and ^{13}C-^{14}N dipolar interactions. The results showed that TTA molecules are arranged in such a way as to shield the nitrogen site from the polymer chains.[163] Typical CSA peaks shapes take into account a random orientation of molecules in the solids. Deformation of a polymeric material can induce **orientation** of the chains. This modifies the peaks shapes, and makes the shape dependent on the orientation of the deformation axis to B_0.[164] Different polymer crystalline phases, as well as amorphous phases, can be distinguished. The different phases of different polymers in blends or in block copolymers can also be distinguished, the **domain size** can be estimated and the interfaces between domains studied.[165] Polymers with a **high crosslinking density** cannot be analyzed by lpNMR and require ssNMR analyses.[148,150] MAS PFG NMR can be used to evaluate the diffusion of water in swollen polymers.[166]

ssNMR spectroscopy has been applied to the analysis of organic materials with complex compositions. **Wood** is composed by cellulose, hemicellulose and lignin. Wood and wood products can be analyzed by ssNMR,[167] which can give information on the components, such as cellulose crystallinity or lignin composition, and be used to assess wood degradation. Other examples of complex organic materials that can be analyzed by ssNMR are **fabrics** and **leathers**, that can also have a cultural interest.[168] For instance, ssNMR has been widely applied to the study of silk.[169]

9.2 - Inorganic materials

While lpNMR of inorganic materials has limited application due to the samples insolubility and the loss of important structural information, **ssNMR** is usually the approach of choice.[170,171] All types of inorganic

material can be analyzed by NMR, from metals and alloys,[172] to ceramics[173,174] and minerals,[175] to glasses,[176] cements,[177] carbon allotropes,[178] nanomaterials,[179] inorganic polymers,[180] thermoelectric materials,[181] etc. The chemical shifts and the parameters of their anisotropy, and scalar (J), dipolar and quadrupolar couplings, give important information on nuclei local magnetic fields.[170] The use of complex pulse techniques and multidimensional correlation spectroscopy multiply the information obtainable.[170,182] **NMR crystallography**[183] can be used together with X-Ray Diffraction (XRD) to simplify the determination of crystalline structures, and distinguish between different polymorphs. Moreover, ssNMR is not limited to the study of crystalline samples and works well for amorphous structures, can reveal the local disorder[184] and defects in solids, and can distinguish between polyamorphs.[183] A critical feature of NMR crystallography is that at fast MAS it is possible to study ^{1}H nuclei, which is basically invisible to XRD.[185] ssNMR of inorganic materials can also provide information on the porosity,[186] dynamics,[186] adsorption,[187] and interfaces.[188] The technique is also applicable to high-temperature analyses.[189] Various types of hydroxyls without fast chemical exchange were identified with **CRAMPS** in fully hydrated silica networks.[190] Due to the better resolution, strongly hydrogen-bonded and weakly hydrogen-bonded hydroxyl groups physisorbed water and non-hydrogen-bonded silanols sites could be distinguished in the hydrated silica gel. A CRAMPS based method has been employed in the characterization of the hydrogen bonding network of P-OH, NH groups and H_2O in organically templated titanium phosphate.[191] Exact location of protons in Keggin heteropolyacids could be determined with REDOR and DFT calculations.[192] There are several **recoupling** studies of zeolites, in which, amongst others, the oxygen chemical environments could be distinguish with ^{17}O-^{27}Al and ^{17}O-^{31}P dipolar couplings.[193] REDOR was also applied in one of the recently most researched field, lithium-ion batteries.[194] ^{6}Li-^{7}Li measurements has been used to compare the ionic conductivity in $Li_6BaLa_2M_2O_{12}$ (M = Ta, Nb). The results indicate that the Nb phase has a higher overall ionic conductivity, as well as a higher activation energy for lithium ion hopping than the Ta counterpart in the range of 247-350 K. In porous materials, **PFG NMR** could be used to study the in-pore diffusion, which may be used as a tool to estimate tortuosity[195] and pores sizes.[196] Thanks to increased resolution, **MAS PFG NMR** could be used f to study the selective diffusion of fluids mixtures,[197] and of a single component in different local environments.[198] Other NMR methods based on the decay due to diffusion in the susceptibility-induced internal field gradients (DDIF) could also be used for pores characterization.[199,200] ^{27}Al SQ/DQ NMR could provide information on the local Al environments in microporous solids.[201] **Xenon** is a noble gas present in multiple isotopes, among which two are NMR active: ^{129}Xe and ^{131}Xe. The former is a relatively easy-to-analyze I = ½ nucleus with a wide chemical shift range. The chemical shift of this highly-polarizable nucleus is very susceptible to the physical and chemical environment it is placed in. For this, ^{129}Xe has been widely applied used as a probe to study solids, in particular porous materialsr.[202] In addition, the magnetization of this isotope can be greatly boosted to obtain hyperpolarized ^{129}Xe (HP-^{129}Xe) via Rb-mediated spin exchange optical pumping and other techniques, extending the technique to materials with lower adsorption capacity.

Nevertheless, oftentimes other spectroscopic techniques are preferred over ssNMR for the characterization of inorganic materials. One of the reasons is that the degree of information obtainable depends on resolution, and because of **peak broadening** it is not always possible to obtain a resolved spectrum unless an expensive, very high field spectrometer is used, or complex pulse techniques are employed, with accurate pulses and angles and stable MAS rates. Spectrum interpretation is often **complicate** and a technique with more straightforward data analysis may be preferred when detailed information is not required. The number of easy-to-analyze nuclei is **limited**, and some of the key nuclei in inorganic chemistry are not in this group, most notably **oxygen**,[203] for which it might be needed to resort to ^{17}O enriched samples,[204] although it has been shown that DNP can be used to enhance natural abundance ^{17}O signals in samples such as magnesium hydroxide,[205] which could be used to probe surfaces.[206] NMR mostly applies to the analysis of diamagnetic nuclei, while the presence of paramagnetic species bring about **paramagnetic shifts** components to the observed chemical shifts, [207] and **paramagnetic broadening** because of the relaxation times reduction.[208] For this, paramagnetic nuclei-containing materials are usually studied by Electron Paramagnetic Resonance (EPR),[209]although the big interest in the NMR study of these materials is pushing research to overcome these difficulties.[210]

Yet, ssNMR is a powerful tool for the characterization of materials containing easy-to-analyze nuclei (^{11}B, ^{27}Al, ^{29}Si, etc.), and for materials in which the local structure has a striking effect on its properties, such

as in advanced materials and solid catalysts. Moreover, the development of new magnets, hardware and techniques is progressively extending the applicability of ssNMR to yet-unexploited nuclei.[174]

HydroTalcites (HTs) are layered double hydroxides, anionic clays with the general formula $[M^{2+}_{1-x}M^{3+}_{x}(HO^{-})_2]^{x+}A^{n-}_{x/n}\cdot m(H_2O)$, where: M^{2+} & M^{3+} are di- and trivalent metals respectively, commonly Mg and Al, organized in brucite-type layers which bear positive charges as a results of Al^{3+} presence in the $Mg(OH)_2$ framework; A^{n-} is an interlayer counteranion, commonly CO_3^{2-}, NO_3^- or halides; H_2O is the hydration water, also present in the interlayers (Figure 12.a).[211] Although HTs are naturally occurring minerals, in chemistry synthetic ones are usually used, easily prepared by coprecipitation of suitable metal salts in basic media. HTs have mostly been applied as absorbent, as ion-exchangers and as solid catalysts with tunable surface basicity. Although the general formula and structure of hydrotalcites had been long known,[212] Sideris *et al.* elucidated the Mg/Al ordering in the layers, and therefore the Mg and Al local structure, which is hard to obtain by any other technique different than ssNMR.[213] Three samples of 19%, 25% and 33% Al-doped HTs were analyzed. In randomly Al distributed layers, 4 hydroxyl local environments are possible (Mg_3OH, Mg_2AlOH, $MgAl_2OH$ and Al_3OH), whereas only the first 2 are possible in the perfectly Al distributed layer (Figure 12.a). Fast ^{1}H MAS NMR spectroscopy almost completely removed dipolar homonuclear coupling and highlighted three ^{1}H local environments, the first ascribable to water, and the other two peaks assigned to Mg_3OH and Mg_2AlOH (Figure 12.b). The spectral assignment was verified by a ^{1}H-^{27}Al TRAPDOR experiment, in which the difference spectra highlighted that one of the two peaks is influenced by Al irradiation and therefore corresponds to Mg_2AlOH (Figure 12.c). The obtained proportions between Mg_3OH and Mg_2AlOH protons closely resemble the ones of ordered structures. A 2D ^{25}Mg triple quantum (TQ) MAS experiment performed on a 33% Al doped HT corroborated the presence of one only Mg local environment which, because of the low asymmetry parameter, should correspond to the highly symmetric $Mg(OMg)_3(OAl)_3$ environment (Figure 12.d). ^{25}Mg is not an easy-to-analyze nucleus because of its low *γ*, low natural abundance and large *Q*. Yet, with the help of 70% ^{25}Mg enrichment in the HT preparation, it was possible to obtain a great deal of information.

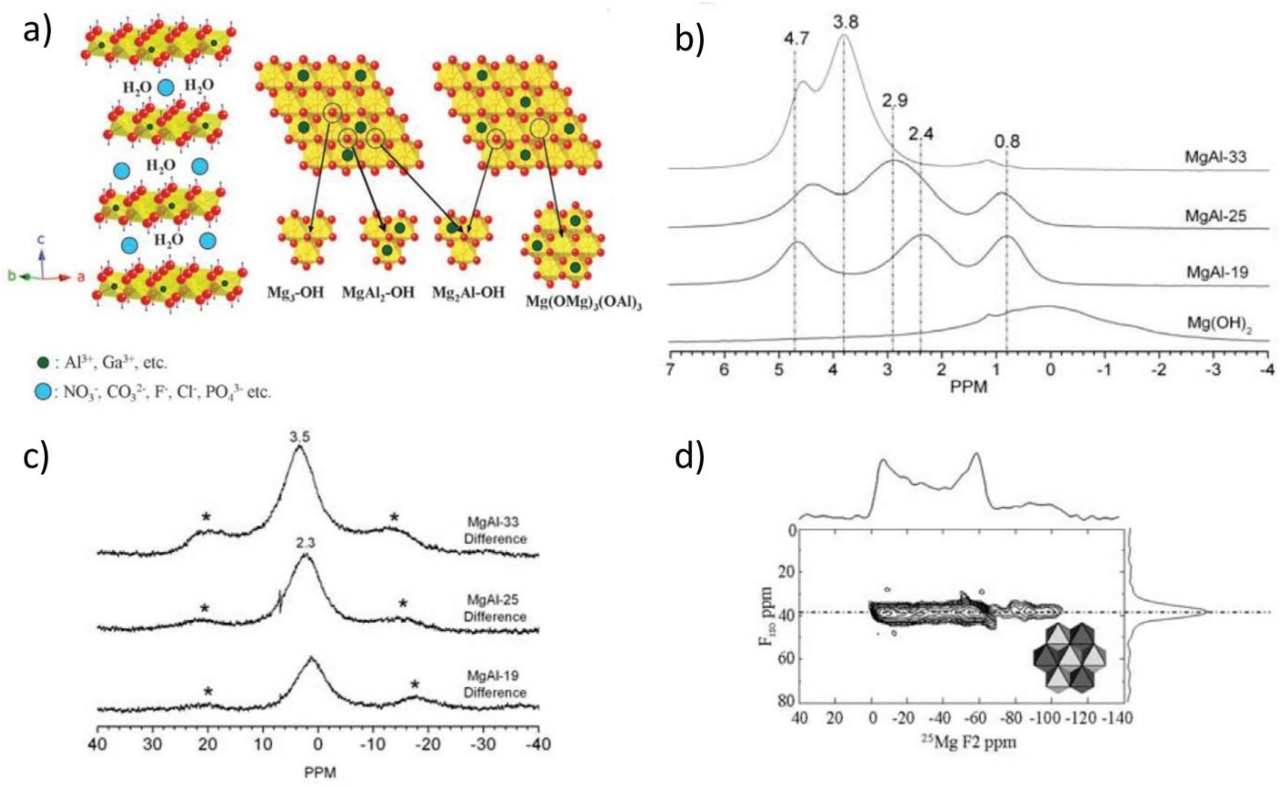

Figure 12. a) 3D HT structure and 2D random and ordered layers of 33% Al-doped HT; b) ^{1}H MAS spectra of HTs and brucite; c) ^{1}H-^{27}Al TRAPDOR/^{1}H MAS difference spectra; d) 2D ^{25}Mg TQ MAS spectrum of 70% ^{25}Mg-enriched 33% Al-doped HT.

When HTs are used as basic catalysts, they are commonly calcined and rehydrated. Calcination causes the collapse of the layered structure and the departure of interlayer water and counteranions as gases. Rehydration of the calcined hydrotalcite with water restores the layered structure (memory effect) and includes HO^-, which increase Brønsted basicity. Abelló *et al.* studied the use of rehydrated HTs in aldol condensations, and compared the structures obtained after rehydration in the gas or in the liquid phases by ^{27}Al ssNMR spectroscopy.[214] In the calcination Al atoms undergo a transition from an octahedral position to a tetrahedral one, while the rehydration partially reverse this transformation (Figure 13.a). The obtained oct/tet ratios are different, indicating that the gas-phase reconstruction is more complete. These results contributed to the proposal of different reconstructed structures obtained, which seem to explain the difference in terms of activity of the two catalysts, with the less-reconstructed structure obtained after liquid-phase rehydration containing more active basic sites on the surface (Figure 13.b).

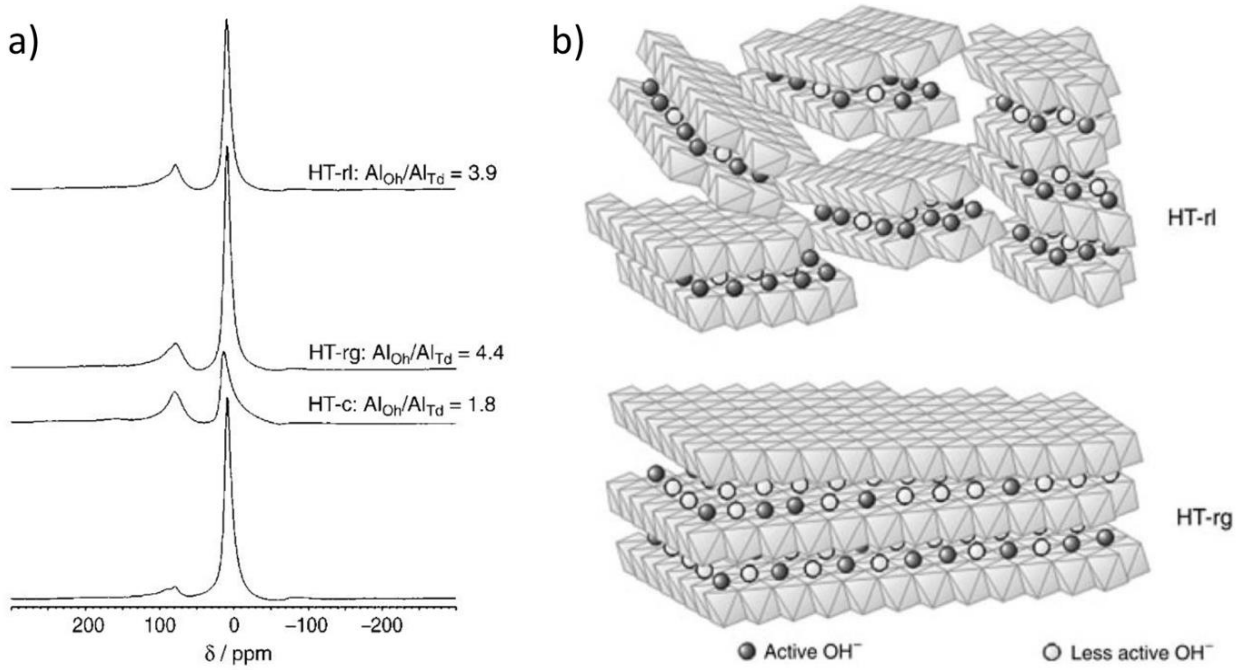

Figure 13. a) ^{27}Al NMR spectra of HTs; b) proposed structures for the differently reconstructed HTs.

9.3 - Organic/inorganic materials

ssNMR has been applied to the characterization of materials including both organic and inorganic matter in their structure, such as composites,[215] nanocomposites,[216] hybrid materials[217] and metal organic frameworks.[218] In this field ssNMR is a useful tool as it allows investigation on the features of both components, as explained in the previous sections, and the interaction between them.

In this category also fall Surface OrganoMetallic Chemistry (SOMC) catalysts,[219,220] heterogeneous catalysts with well-defined active sites on the surface, supported on inorganic materials. SOMC and SOMC catalysis are today well-established concepts, which aim to implement the chemistry of **molecular organometallic compounds** and related **homogeneous catalysis** in the field of **heterogeneous catalysis**. Its main methodology is grafting well-defined, organometallic species on an appropriately pretreated solid surface to form catalytically active **Surface OrganoMetallic Fragments** (SOMFs). The pretreatment of the metal-oxide surface usually consists in decreasing the concentration of the surface hydroxyl groups, which typically serve as an anchor for the organometallic precursor and practically become the ligand of the surface organometallic species. The approach principally allows the synthesis of single-site heterogeneous catalysts, meaning that the catalytically active sites on the surface are expected to be identical. In terms of rational understanding, predictability and designability, it seems to be progressing faster than classical

heterogeneous catalysis. On the other hand, it clearly promotes advances in the field of its older brother, as well.[221,222]

ssNMR spectroscopy can efficiently be used to characterize SOMFs in many cases. For instance, recently, NHC stabilized neutral and cationic W(VI)[223] and Mo(VI)[224] alkylidenes were grafted on partially dehydroxylated silica (SiO_{2-700}) (Figure 14). The novel SOMC catalysts, which proved highly efficient in a variety of olefin metatheses, were characterized by elemental analyses, FT-IR, and MAS ssNMR. In the case of grafted cationic W(VI)-alkylidene **B**, which provided >1.200.000 turnovers in homo-cross metathesis of propylene, the ^{1}H MAS ssNMR spectrum displayed signals at δ = 10.4 ppm, 7.4 ppm and 1.9 ppm, corresponding to the alkylidene signal, the aromatic protons and methyl protons of the molecule, respectively. Similarly, the characteristic alkylidene signals could readily be detected in all SOMFs.

It is important to note that the alkylidene signals usually cannot be observed by ^{13}C CP MAS at their natural ^{13}C abundance. For the full characterization of **A**-**D**, the authors also prepared the corresponding molecular precursors with ^{13}C-enriched neophylidene ligands, and grafted them (Figure 14). DNP has also been used to improve the analyses sensitivity.[225]

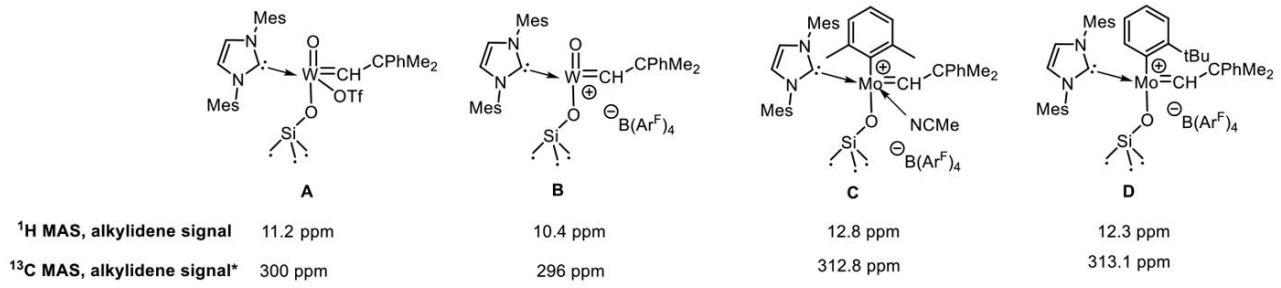

Figure 14. MAS NMR characterization of grafted cationic W(VI) and Mo(VI) alkylidenes, highly efficient catalysts for olefin metatheses.

9.4 - In situ/operando NMR studies

In addition of being applicable to the characterization of a broad range of materials, NMR spectroscopy could be used to investigate the properties and behavior of the material during its use, or its formation. An example of this type of analysis has already been illustrated for the diffusion studies of small molecules in porous materials. **In situ/operando NMR spectroscopy** has evolved over time and it has overcome various of its limits, mostly related to the difficulties in running a process inside an NMR spectrometer during analysis (*i.e.* inlets and outlets implementation to a closed system, high-speed rotation in ssNMR, limited vessels geometries, *etc.*).[226]

NMR spectroscopy is sensitive to **phase changes** in the material. **Crystallization**, a process of forming a solid (generally from a liquid) through nucleation and growth, could be investigated via NMR spectroscopy.[227] In this sense, the analysis of both liquid and solid phases are fundamental to understand the process. For example, in the **formation of zeolites** and other related crystalline porous materials happen in hydrothermal conditions.[228] Given the relatively high temperature and pressure of the process,[229] tubes and rotors for NMR analyses had to be chosen or developed taking into account the compatibility of the material to the physical and chemical conditions, and to not affect the process and the NMR analysis at the same time. Moreover, a crucial parameter of the hydrothermal process is pH, whose measure in an NMR spectrometer is a hard task. For this, molecules such as imidazole and DABCO have been used as NMR pH-meters. A method to analyze both liquid and solids during the same process with alternate acquisition have been recently developed.[230] The so-called **CLASSIC NMR** method is performed with a rotor, as the analysis of a solid in a lpNMR experiment is tough, while the one of a liquid in a ssNMR experiment is reasonably feasible. The method exploits the fact that a solid is visible in a CP experiment while a liquid is not, and that the opposite is true for a direct excitation with a short recycle delay. The method has been applied to the crystallization

of molecular solids such as cocrystals, crystals presenting different polymorphic phases or inclusions.[231] More established is the field of NMR studies of **solid phase transitions**.[232] In this type of analyses it might be necessary the use of an NMR thermometer, such as $Pb(NO_3)_2$,[233–235] as it is important to monitor temperature inhomogeneities in the sample and temperature increments due to frictional heating.

NMR spectroscopy is also sensitive to **chemical changes** in the material. This aspect is particularly important for **heterogeneous catalysts**.[236] In this case, the rotor act as a reactor, with two possible types of set-up: batch or continuous-flow conditions. The batch approach is technologically easier, as no probe/rotor modifications are required. The sample inclusion in the rotor commonly happen by loading of a sealed glass insert containing the pre-activated reaction mixture or by a special rotor design that could be air tight sealed (CAVERN). The continuous-flow approach is more complicated as it requires the implementation of an inlet/outlet on the rotating reactor inside the spectrometer, but it more realistically represents reactors. One of the solid properties that can be elucidated with these methods is the **acidity**, indirectly detected by analyzing probe molecules that interact with the acidic sites. The **catalytically active sites** could be analyzed directly in case they contain NMR-active nuclei. However, oftentimes the active sites on heterogeneous catalysts are not easy-to-analyze nuclei (*e.g.* ^{197}Au), therefore it is common to detect the properties indirectly by analyzing the nuclei of reactants and products, or by using sensitive probes such as laser-hyperpolarized ^{129}Xe. Indirect characterization of the catalyst activity could also be obtained with lpNMR analyses,[237] even with a benchtop NMR spectrometer,[238] by analyzing the reaction products. When not applicable, ssNMR characterization of catalytic materials (*e.g.* porous materials) could be coupled with other in situ techniques, such as FT-IR.[239] **Adsorption** is the initial step of the heterogeneous catalysis cycle, and therefore it is an important process to be monitored. It has been demonstrated that NMR spectroscopy is capable of monitoring the adsorption process over time and at different temperatures.[187] Although it is possible to analyze heterogeneously-catalyzed **polymerization** in an ssNMR rotor,[240] analysis of polymerizations in liquid media are more common.[241] One of the advantages of liquid phase NMR is that the analysis can be performed on polymerizations in situ inside the tube but also on line, and instrumentation for both type of reaction monitoring are commercially available. Not only catalysis can be monitored by NMR spectroscopy, also non-catalytic **heterogeneous reactions**. For instance, a study on the in-rotor hydration of calcium aluminate cement have recently been reported.[242] The data obtained with the CLASSIC NMR method were consistent with the results obtained for calorimetry experiments.

Another active research field is the one of the NMR in situ/operando study of **energy storage materials**, which aim to better understand and upgrade our current technology of electrochemical energy storage and improve sustainability. These energy devices are studied as a whole, inserting the sealed cell into the spectrometer inside the RF coil.[243] This poses a series of technical obstacles. For instance, during cell operation the alternate current of the RF coil and the direct current of the electrochemical circuit could interfere with each other, affecting the electrochemical performance and/or the NMR signal. Another technical limitation is the difficulty in combining the analysis with MAS, which constrains resolution. Even in the case of ex situ analyses, MAS speed cannot be too high to prevent the electrolyte to leak. Nevertheless, this type of analysis has given good insights on the functioning of energy storage materials. **Batteries** are electrochemical cells that release electrical energy after converting the free energy of its constituents via redox reactions.[244] The most important component of these devices is Li, which can be analyzed in both of its isotopes (^6Li and ^7Li), and among the other nuclei that are easy-to-analyze ^1H, ^{19}F and ^{31}P are present. In situ NMR study could provide information for example on the identity and quantities of species in the various components over time upon cycles of charge/discharge, or study the interface between components, or the formation of microstructures. During operation, the metallic anodes tend to modify their structure and form dendrites, which eventually could lead to short-circuiting. Study on the formation and growth of these structures would help understanding how to suppress them.[245] Electrochemical capacitors, or **supercapacitors**, are electrochemical cells that store energy through the formation of an electric double layer at the interface between a liquid electrolyte and a porous carbon electrode.[246] In this case the analysis focuses on the nuclei contained in the electrolyte, with commonly studied nuclei being ^{19}F, ^{31}P and ^{11}B. An NMR analysis could differentiate between bulk and in-pore specie by differences in chemical shift; cyclic voltammetry could change the distribution of charges in the electric double layer. This information could be used for example to study different electrolytes and electrodes and improve the system. A similar type of

analysis setup to the one of energy storage materials could be used to determine the catalytic performances of **electro-catalysts**.[247]

10 - Summary

In this introductory review, we have outlined the basic principles of NMR spectroscopy, one of the most versatile spectroscopic methods developed to date. We have guided the reader through the most important structural features of the spectrometers, and explained the fundamentals of their operation. We have given a glimpse of the most relevant brands and compared the most powerful ultra-high-field spectrometers to the emerging, broadly affordable, low-field benchtop devices. Practical advice on performing the NMR experiments and basic theoretical concepts to analyze the spectra have been provided. Through relevant literature samples, we have introduced some of the most widely used, as well as a few emerging pulse sequences and techniques used in liquid-phase and solid-state NMR spectroscopy. We hope that the very limited number of examples prove sufficient to demonstrate the virtually limitless application to the characterization of practically all kinds of materials, as well as to the in-situ analysis of physical, chemical, and biological processes they can be involved in. In Table 5, we summarize some of the characteristics, advantageous and less favorable, relevant to material characterization by NMR spectroscopy.

Advantages	Drawbacks
Detailed information on nuclei local environment with atomic level resolution.	Not every element has an NMR active isotope.
Broad range of applications.	Rather low sensitivity for any NMR active nucleus.
Non-invasive technique.	Not every NMR active nuclide is easy-to-analyze (low abundance or γ, high Q, *etc.*).
Linear technique, suitable for accurate quantification (below ±1%) under appropriate conditions.	The presence of paramagnetic species in the sample, independently whether they are the analytes of interest or not, can render the analysis difficult.
Sample preparation is relatively simple for most analytes.	Not suitable for ultra-precise quantifications.
Fast analysis in many cases (*e.g.* ^{1}H).	Spectrum interpretation can be demanding.
Highly reproducible results, characteristic to the analyte. Vast amount of literature data.	Relatively complicated technique to perform, especially for complex pulse techniques.
It allows complete molecular structure elucidation, stereostructures, conformations (lpNMR).	The analysis of complex mixtures might be very demanding.
It allows the determination of the morphology of solids, as well as internuclear distances and internal dynamics (ssNMR).	Very cost-intensive technique, for both equipment and operative costs (high-field NMR).
Complex pulse techniques and correlation spectroscopy may unlock information not obtainable by any other analytical technique.	NMR specialist is required (high-field NMR).
Low-field benchtop NMR spectrometers may significantly broaden the number of users.	The affordable low-field NMR provides limited information.

Table 5. Advantages and drawbacks of material characterization by NMR spectroscopy.

11 - Conclusions

After becoming a staple analytical method in chemistry and life sciences, NMR spectroscopy has also proved to be an excellent technique for material characterization. A great variety of materials can be analyzed, from organic solids and polymers in lpNMR to obtain detailed structure elucidation, and ssNMR, to gain information on the solid structures, internuclear distances and internal dynamics, to inorganic materials

and inorganic materials with an organic content, also analyzed by ssNMR. Few analytical techniques for material characterization provide such a great deal of information and has so many applications as NMR spectroscopy. There are aspects of material characterization that are virtually impossible to elucidate without using NMR spectroscopy. Nevertheless, as any technique, NMR spectroscopy also has its limitations, and its applicability to a specific system very much depends on the nature of the sample and the type of nuclei it contains.

NMR spectroscopy is continuously evolving in many aspects, and some of the current limits of the technique are expected to be overcome in the near future, just like modern NMR has overcome its limits in the past. Both resolution and sensitivity will benefit from the development of new, more powerful spectrometers above 1 GHz, improving the applicability of this tool to more complex materials and materials containing elements with low receptivities. Sensitivity might also be improved by the development of new probes, as cryoprobes and DNP probes already did. Improvements in the electronics and mechanics (*e.g.* ultrafast MAS), as well as the development of new complex pulse techniques, should further increase the amount of information obtainable from a material by obtaining simpler and clearer spectra in shorter times. The rapid development of benchtop NMR technology will hopefully make the technique even more accessible and increase its applicability to more systems, which should increase the number professionals knowledgeable about this versatile analytical tool.

Acknowledgements

We thank Dr. Shigetaka Hayano from Zeon Co. for providing us with NMR spectra to demonstrate the application of NMR spectroscopy to analysis of organsoluble polymers. This project has received funding from the European Union's Horizon 2020 research and innovation programme under the Marie Skłodowska-Curie grant agreement No 712949 (TECNIOspring PLUS), and from the Agency of Business Competitiveness of the Government of Catalonia. A.T. gratefully acknowledges his postgraduate scholarship 2018 FI_B 01124 cofunded AGAUR, Government of Catalonia, and ESF, European Union.

References

(1) Jameson, C. J. Chapter 1. Fundamental intramolecular and intermolecular information from NMR in the gas phase. In *Gas Phase NMR*; Jackowski, K., Jaszunski, M., Eds.; New Developments in NMR; Royal Society of Chemistry: Cambridge, 2016; pp 1–51.

(2) Becker, E. D. A brief hystory of nuclear magnetic resonance. *Anal. Chem.* **1993**, *65*, 295A-302A.

(3) Schwalbe, H. New 1.2 GHz NMR spectrometers- New horizons? *Angewandte Chemie (International ed. in English)* **2017**, *56*, 10252–10253.

(4) Webb, A. *Magnetic resonance technology: Hardware and system component design*; New Developments in NMR 7; Royal Society of Chemistry: Cambridge UK, 2016.

(5) Berger, S.; Braun, S. *200 and more NMR experiments: A pratical course*; Wiley-VCH: Weinheim, 2004.

(6) Grant, D. M.; Harris, R. K. *Encyclopedia of nuclear magnetic resonance*; John Wiley: Chichester, New York, 1996-2002.

(7) Macomber, R. *A complete introduction to modern NMR spectroscopy*; Wiley: New York, 1998.

(8) Bruker. Ascend 1.1 GHz: A Technological Milestone. https://www.bruker.com/products/mr/nmr/magnets/magnets/ascend/ascend-11-ghz.html.

(9) Grootveld, M.; Percival, B.; Gibson, M.; Osman, Y.; Edgar, M.; Molinari, M.; Mather, M. L.; Casanova, F.; Wilson, P. B. Progress in low-field benchtop NMR spectroscopy in chemical and biochemical analysis. *Analytica chimica acta* **2019**, *1067*, 11–30.

(10) Kovacs, H.; Moskau, D.; Spraul, M. Cryogenically cooled probes—a leap in NMR technology. *Progress in Nuclear Magnetic Resonance Spectroscopy* **2005**, *46*, 131–155.

(11) Doty, F. D. Solid State NMR Probe Design. In *eMagRes*; Harris, R. K., Wasylishen, R. L., Eds.; John Wiley & Sons, Ltd: Chichester, UK, 2007; p 2042.

(12) Schorn, C. *NMR spectroscopy: Data acquisition*; Wiley-VCH: Weinheim, 2001.

(13) Kimmich, R. *NMR: Tomography, Diffusometry, Relaxometry*; Springer Berlin: Berlin, 2013.

(14) Blümich, B.; Singh, K. Desktop NMR and Its Applications From Materials Science To Organic Chemistry. *Angewandte Chemie (International ed. in English)* **2018**, *57*, 6996–7010.

(15) Rugar, D.; Budakian, R.; Mamin, H. J.; Chui, B. W. Single spin detection by magnetic resonance force microscopy. *Nature* **2004**, *430*, 329–332.

(16) Arnold, J. T.; Dharmatti, S. S.; Packard, M. E. Chemical Effects on Nuclear Induction Signals from Organic Compounds. *The Journal of Chemical Physics* **1951**, *19*, 507.

(17) Shoolery, J. N. The development of experimental and analytical high resolution NMR. *Progress in Nuclear Magnetic Resonance Spectroscopy* **1995**, *28*, 37–52.

(18) Ernst, R. R.; Anderson, W. A. Application of Fourier Transform Spectroscopy to Magnetic Resonance. *Review of Scientific Instruments* **1966**, *37*, 93–102.

(19) Freeman, R.; Morris, G. A. The Varian story. *Journal of magnetic resonance (San Diego, Calif. : 1997)* **2015**, *250*, 80–84.

(20) Aue, W. P.; Bartholdi, E.; Ernst, R. R. Two-dimensional spectroscopy. Application to nuclear magnetic resonance. *The Journal of Chemical Physics* **1976**, *64*, 2229–2246.

(21) Reisch, M. S.; Kemsley, J. Agilent Draws Academics' Ire. *Chemical & engineering news* **2014**, *92*, 17–18.

(22) JEOL. JEOL NMR catalogue 2019. https://www.jeol.co.jp/en/products/category_nmr.html.

(23) JEOL USA. JEOL Resonance Introduces New Zero Boil Off Magnet for NMR Systems. https://www.jeolusa.com/NEWS-EVENTS/Press-Releases/jeol-resonance-introduces-new-zero-boil-off-magnet-for-nmr-systems.

(24) Anklin, C. Spotlight on nuclear magnetic resonance: a timeless technique. https://www.spectroscopyeurope.com/article/spotlight-nuclear-magnetic-resonance-timeless-technique.

(25) Ernst, R. R. Zurich's contributions to 50 years development of Bruker. *Angewandte Chemie (International ed. in English)* **2010**, *49*, 8310–8315.

(26) Laboratory equipment. First 1,000 MHz NMR Installed. https://www.laboratoryequipment.com/news/2009/12/first-1000-mhz-nmr-installed.

(27) PR Newswire. Bruker Announces World's First Superconducting 1.1 Gigahertz Magnet for High-Resolution NMR in Structural Biology. https://www.prnewswire.com/news-releases/bruker-announces-worlds-first-superconducting-1-1-gigahertz-magnet-for-high-resolution-nmr-in-structural-biology-300825288.html.

(28) St. Jude Inspire. World's most powerful Nuclear Magnetic Resonance Spectrometer arrives at St. Jude. https://www.stjude.org/inspire/news/semiconductor-ascend-nmr-spectrometer.html.

(29) Bruker. Bruker Announces World's First 1.2 GHz High-Resolution Protein NMR Data. https://ir.bruker.com/press-releases/press-release-details/2019/Bruker-Announces-Worlds-First-12-GHz-High-Resolution-Protein-NMR-Data/default.aspx.

(30) Bible, R. H. NMR Instrumentation since the Varian A-60. *Appl Spectrosc* **1970**, *24*, 326–331.

(31) Masili, A.; Puligheddu, S.; Sassu, L.; Scano, P.; Lai, A. Prediction of physical-chemical properties of crude oils by 1H NMR analysis of neat samples and chemometrics. *Magnetic resonance in chemistry : MRC* **2012**, *50*, 729–738.

(32) Hoye, T. R.; Eklov, B. M.; Ryba, T. D.; Voloshin, M.; Yao, L. J. No-D NMR (no-deuterium proton NMR) spectroscopy: a simple yet powerful method for analyzing reaction and reagent solutions. *Organic letters* **2004**, *6*, 953–956.

(33) Fulmer, G. R.; Miller, A. J. M.; Sherden, N. H.; Gottlieb, H. E.; Nudelman, A.; Stoltz, B. M.; Bercaw, J. E.; Goldberg, K. I. NMR Chemical Shifts of Trace Impurities: Common Laboratory Solvents, Organics, and Gases in Deuterated Solvents Relevant to the Organometallic Chemist. *Organometallics* **2010**, *29*, 2176–2179.

(34) Giraudeau, P.; Tea, I.; Remaud, G. S.; Akoka, S. Reference and normalization methods: essential tools for the intercomparison of NMR spectra. *Journal of pharmaceutical and biomedical analysis* **2014**, *93*, 3–16.

(35) Harris, R. K.; Becker, E. D.; Cabral de Menezes, S. M.; Granger, P.; Hoffman, R. E.; Zilm, K. W. Further conventions for NMR shielding and chemical shifts (IUPAC Recommendations 2008). *Pure and Applied Chemistry* **2008**, *80*, 59–84.

(36) Hoffman, R. E. Standardization of chemical shifts of TMS and solvent signals in NMR solvents. *Magnetic resonance in chemistry : MRC* **2006**, *44*, 606–616.

(37) Shaver, R.; van Wallendael, S.; Rillema, D. P. A rapid method for degassing samples. *J. Chem. Educ.* **1991**, *68*, 604.

(38) Landrie, C. L.; Marszalek, R. A Durable and Economical NMR Tube Cleaner. *J. Chem. Educ.* **2011**, *88*, 1734–1735.

(39) Taylor, R. E. Setting up13C CP/MAS experiments. *Concepts Magn. Reson.* **2004**, *22A*, 37–49.

(40) Paulson, E. K.; Zilm, K. W. External field-frequency lock probe for high resolution solid state NMR. *Review of Scientific Instruments* **2005**, *76*, 26104.

(41) Morcombe, C. R.; Zilm, K. W. Chemical shift referencing in MAS solid state NMR. *Review of Scientific Instruments* **2003**, *162*, 479–486.

(42) Bertani, P.; Raya, J.; Bechinger, B. 15N chemical shift referencing in solid state NMR. *Solid state nuclear magnetic resonance* **2014**, *61-62*, 15–18.

(43) Ziarelli, F.; Caldarelli, S. Solid-state NMR as an analytical tool: quantitative aspects. *Solid state nuclear magnetic resonance* **2006**, *29*, 214–218.

(44) Turcu, R. V. F.; Hoyt, D. W.; Rosso, K. M.; Sears, J. A.; Loring, J. S.; Felmy, A. R.; Hu, J. Z. Rotor design for high pressure magic angle spinning nuclear magnetic resonance. *Journal of magnetic resonance (San Diego, Calif. : 1997)* **2013**, *226*, 64–69.

(45) Hu, J. Z.; Sears, J. A.; Mehta, H. S.; Ford, J. J.; Kwak, J. H.; Zhu, K.; Wang, Y.; Liu, J.; Hoyt, D. W.; Peden, C. H. F. A large sample volume magic angle spinning nuclear magnetic resonance probe for in situ investigations with constant flow of reactants. *Physical chemistry chemical physics : PCCP* **2012**, *14*, 2137–2143.

(46) Hayashi, S. Sealing Effect of Magic-Angle-Spinning Rotors in Solid-State NMR. *Anal. Sci.* **2009**, *25*, 133–136.

(47) Hisao, G. S.; Harland, M. A.; Brown, R. A.; Berthold, D. A.; Wilson, T. E.; Rienstra, C. M. An efficient method and device for transfer of semisolid materials into solid-state NMR spectroscopy rotors. *Journal of magnetic resonance (San Diego, Calif. : 1997)* **2016**, *265*, 172–176.

(48) König, R.; Scholz, G.; Kemnitz, E. New inserts and low temperature--two strategies to overcome the bottleneck in MAS NMR on wet gels. *Solid state nuclear magnetic resonance* **2007**, *32*, 78–88.

(49) Varian, I. N. s. Installation planning guide: Pub. No. 01-999262-00, Rev. A0305. http://www.emory.edu/NMR/docs/Varian%20NMR%20Installation%20Planning%20Guide%20020406.pdf.

(50) Bruker. Site Planning for AVANCE systems: 300-700 MHz User Guide. Version 005. http://sermn.uab.cat/wiki/lib/exe/fetch.php?media=edifici_fusio:bruker_-_site_planning_for_300-700_mhz_-_z31276.pdf.

(51) Reisch, M. S. A Renaissance For NMRs, Big And Small. *Chemical & engineering news* **2015**, *93*, 19–21.

(52) Bruker. Manual probes: User manual. Version 003. http://www2.chem.uic.edu/nmr/downloads/bruker/en-US/pdf/z31339.pdf.

(53) Bruker. Basic 1D and 2D Experiments: Introduction to 1- and 2-dimensional NMR Spectroscopy. Version 001. http://nmrlab.chem.upenn.edu/pdf%20files/basic_1d_and_2d_experiments.pdf.

(54) Bruker. Solid state NMR Avance solids: User manual. Version 002. https://www.nmr.ucdavis.edu/sites/g/files/dgvnsk4156/files/inline-files/solids.pdf.

(55) *Information from Gábor Csatádi, Bruker's Hungarian sales person, as of June 2019.*

(56) Reisch, M. S. NMR Instrument Price Hikes Spook Users. *Chemical & engineering news* **2015**, *93*, 16.

(57) Mukhopadhyay, R. Liquid NMR probes: Oh so many choices. *Analytical chemistry* **2007**, *79*, 7959–7963.

(58) Spectroscopyonline. Market Profile: NMR Probes **2011**, *26*.

(59) Reisch, M. S. Securing The Future Of NMR. *Chemical & engineering news* **2016**, *90*, 17–18.

(60) Reisch, M. S. Helium supplies are tightening up again. *Chemical & engineering news* **2018**, *96*, 11.

(61) Information gathered on Wilmad-Labglass website (leading manufacturer of NMR consumables), as of July 2019.

(62) Information gathered on Sigma-Aldrich (Merck) website, as of July 2019.

(63) Pérez-Trujillo, M.; Parella, T.; Kuhn, L. T. NMR-aided differentiation of enantiomers: Signal enantioresolution. *Analytica chimica acta* **2015**, *876*, 63–70.

(64) Labuta, J.; Ishihara, S.; Šikorský, T.; Futera, Z.; Shundo, A.; Hanyková, L.; Burda, J. V.; Ariga, K.; Hill, J. P. NMR spectroscopic detection of chirality and enantiopurity in referenced systems without formation of diastereomers. *Nature communications* **2013**, *4*, 2188.

(65) Yadav, L. D. S. *Organic Spectroscopy*; Springer Netherlands: Dordrecht, 2005.

(66) Castañar, L.; Parella, T. Broadband 1H homodecoupled NMR experiments: recent developments, methods and applications. *Magnetic resonance in chemistry : MRC* **2015**, *53*, 399–426.

(67) Derome, A. E. *Modern NMR techniques for chemistry research*; Pergamon Press: Oxford, 1987.

(68) Silverstein, R. M.; Kiemle, D. J.; Webster, F. X. *The spectrometric identification of organic compounds*, 7. ed.; John Wiley & Sons: Hoboken, 2005.

(69) Kay, L. E. Field gradient techniques in NMR spectroscopy. *Current Opinion in Structural Biology* **1995**, *5*, 674–681.

(70) Morris, G. A. Two-Dimensional J -Resolved Spectroscopy. In *Encyclopedia of Magnetic Resonance*; Harris, R. K., Ed.; John Wiley & Sons, Ltd: Chichester, UK, 2007.

(71) Zangger, K. Pure shift NMR. *Progress in Nuclear Magnetic Resonance Spectroscopy* **2015**, *86-87*, 1–20.

(72) Giraudeau, P.; Frydman, L. Ultrafast 2D NMR: an emerging tool in analytical spectroscopy. *Annual review of analytical chemistry (Palo Alto, Calif.)* **2014**, *7*, 129–161.

(73) Gouilleux, B.; Rouger, L.; Giraudeau, P. Ultrafast 2D NMR: Methods and Applications; Annual Reports on NMR Spectroscopy; Elsevier, 2018; pp 75–144.

(74) Kovtunov, K. V.; Pokochueva, E. V.; Salnikov, O. G.; Cousin, S. F.; Kurzbach, D.; Vuichoud, B.; Jannin, S.; Chekmenev, E. Y.; Goodson, B. M.; Barskiy, D. A. *et al.* Hyperpolarized NMR Spectroscopy: d-DNP, PHIP, and SABRE Techniques. *Chemistry, an Asian journal* [Online early access]. DOI: 10.1002/asia.201800551.

(75) Robertson, T. B.R.; Mewis, R. E. Perspective on the Hyperpolarisation Technique Signal Amplification by Reversible Exchange (SABRE) in NMR Spectroscopy and MR Imaging; Annual Reports on NMR Spectroscopy; Elsevier, 2018; pp 145–212.

(76) Singh, K.; Blümich, B. NMR spectroscopy with compact instruments. *TrAC Trends in Analytical Chemistry* **2016**, *83*, 12–26.

(77) Gouilleux, B.; Charrier, B.; Akoka, S.; Felpin, F.-X.; Rodriguez-Zubiri, M.; Giraudeau, P. Ultrafast 2D NMR on a benchtop spectrometer: Applications and perspectives. *TrAC Trends in Analytical Chemistry* **2016**, *83*, 65–75.

(78) Billeter, M.; Orekhov, V.; Arthanari, H. *Novel sampling approaches in higher dimensional NMR*; Topics in current chemistry 316; Springer: Berlin, New York, 2012.

(79) *Fast NMR data acquisition: Beyond the Fourier transform;* Mobli, M.; Hoch, J. C., Eds.; New Developments in NMR no.11; Royal Society of Chemistry: United Kingdom, 2017.

(80) Kazimierczuk, K.; Orekhov, V. Non-uniform sampling: post-Fourier era of NMR data collection and processing. *Magnetic resonance in chemistry : MRC* **2015**, *53*, 921–926.

(81) Laws, D. D.; Bitter, H.-M. L.; Jerschow, A. Solid-State NMR Spectroscopic Methods in Chemistry. *Angew. Chem. Int. Ed.* **2002**, *41*, 3096–3129.

(82) Facelli, J. C. Chemical shift tensors: theory and application to molecular structural problems. *Progress in Nuclear Magnetic Resonance Spectroscopy* **2011**, *58*, 176–201.

(83) Gee, M.; Wasylishen, R. E.; Eichele, K.; Britten, J. F. Phosphorus Chemical Shift Tensors for Tetramethyldiphosphine Disulfide: A 31 P Single-Crystal NMR, Dipolar-Chemical Shift NMR, and Ab Initio Molecular Orbital Study. *J. Phys. Chem. A* **2000**, *104*, 4598–4605.

(84) Antzutkin, O. N. Sideband manipulation in magic-angle-spinning nuclear magnetic resonance. *Progress in Nuclear Magnetic Resonance Spectroscopy* **1999**, *35*, 203–266.

(85) Deschamps, M. Ultrafast Magic Angle Spinning Nuclear Magnetic Resonance; Annual Reports on NMR Spectroscopy; Elsevier, 2014; pp 109–144.

(86) Bruker. Magic Angle Spinning Above 100kHz. https://www.bruker.com/fileadmin/user_upload/1-Products/Magnetic_Resonance/NMR/probes/Solids/04_ENC15_111KHz-MAS-lowres.pdf.

(87) JEOL USA. JEOL RESONANCE Introduces Worlds' Fastest and Smallest Solid State NMR Probe. https://www.jeolusa.com/NEWS-EVENTS/Press-Releases/jeol-resonance-introduces-worlds-fastest-and-smallest-solid-state-nmr-probe-.

(88) Lin, Y.-L.; Cheng, Y.-S.; Ho, C.-I.; Guo, Z.-H.; Huang, S.-J.; Org, M.-L.; Oss, A.; Samoson, A.; Chan, J. C. C. Preparation of fibril nuclei of beta-amyloid peptides in reverse micelles. *Chemical communications (Cambridge, England)* **2018**, *54*, 10459–10462.

(89) Nishiyama, Y. Solid-State NMR Under Ultrafast MAS Rate of 40–120 kHz. In *Experimental Approaches of NMR Spectroscopy*; Soci, T. N. M. R., Ed.; Springer Singapore: Singapore, 2018; pp 171–195.

(90) Zhang, R.; Mroue, K. H.; Ramamoorthy, A. Proton-Based Ultrafast Magic Angle Spinning Solid-State NMR Spectroscopy. *Accounts of chemical research* **2017**, *50*, 1105–1113.

(91) Madhu, P. K. Heteronuclear Spin Decoupling in Solid-State Nuclear Magnetic Resonance: Overview and Outlook. *Isr. J. Chem.* **2014**, *54*, 25–38.

(92) Mote, K. R.; Agarwal, V.; Madhu, P. K. Five decades of homonuclear dipolar decoupling in solid-state NMR: Status and outlook. *Progress in Nuclear Magnetic Resonance Spectroscopy* **2016**, *97*, 1–39.

(93) McDermott, A.E.; Creuzet, F.J.; Kolbert, A.C.; Griffin, R.G. High-resolution magic-angle-spinning NMR spectra of protons in deuterated solids. *Journal of Magnetic Resonance (1969)* **1992**, *98*, 408–413.

(94) Marchetti, A.; Jehle, S.; Felletti, M.; Knight, M. J.; Wang, Y.; Xu, Z.-Q.; Park, A. Y.; Otting, G.; Lesage, A.; Emsley, L. *et al.* Backbone assignment of fully protonated solid proteins by 1H detection and ultrafast magic-angle-spinning NMR spectroscopy. *Angewandte Chemie (International ed. in English)* **2012**, *51*, 10756–10759.

(95) Madhu, P. K. High-resolution solid-state NMR spectroscopy of protons with homonuclear dipolar decoupling schemes under magic-angle spinning. *Solid state nuclear magnetic resonance* **2009**, *35*, 2–11.

(96) Dec, S. F.; Bronnimann, C. E.; Wind, R. A.; Maciel, G. E. Comparison of the 1H NMR analysis of solids by the CRAMPS and MAS-only techniques. *Journal of Magnetic Resonance (1969)* **1989**, *82*, 454–466.

(97) Sternberg, U.; Witter, R.; Kuprov, I.; Lamley, J. M.; Oss, A.; Lewandowski, J. R.; Samoson, A. 1H line width dependence on MAS speed in solid state NMR - Comparison of experiment and simulation. *Journal of magnetic resonance (San Diego, Calif. : 1997)* **2018**, *291*, 32–39.

(98) Brown, S. P. Probing proton–proton proximities in the solid state. *Progress in Nuclear Magnetic Resonance Spectroscopy* **2007**, *50*, 199–251.

(99) Elena, B.; Emsley, L. Powder crystallography by proton solid-state NMR spectroscopy. *J. Am. Chem. Soc.* **2005**, *127*, 9140–9146.

(100) Nishiyama, Y.; Zhang, R.; Ramamoorthy, A. Finite-pulse radio frequency driven recoupling with phase cycling for 2D (1)H/(1)H correlation at ultrafast MAS frequencies. *Journal of magnetic resonance (San Diego, Calif. : 1997)* **2014**, *243*, 25–32.

(101) Saalwächter, K.; Lange, F.; Matyjaszewski, K.; Huang, C.-F.; Graf, R. BaBa-xy16: robust and broadband homonuclear DQ recoupling for applications in rigid and soft solids up to the highest MAS frequencies. *Journal of magnetic resonance (San Diego, Calif. : 1997)* **2011**, *212*, 204–215.

(102) Reddy, G. N. M.; Malon, M.; Marsh, A.; Nishiyama, Y.; Brown, S. P. Fast Magic-Angle Spinning Three-Dimensional NMR Experiment for Simultaneously Probing H-H and N-H Proximities in Solids. *Analytical chemistry* **2016**, *88*, 11412–11419.

(103) André, M.; Piotto, M.; Caldarelli, S.; Dumez, J.-N. Ultrafast high-resolution magic-angle-spinning NMR spectroscopy. *The Analyst* **2015**, *140*, 3942–3946.

(104) Mao, K.; Pruski, M. Directly and indirectly detected through-bond heteronuclear correlation solid-state NMR spectroscopy under fast MAS. *Journal of magnetic resonance (San Diego, Calif. : 1997)* **2009**, *201*, 165–174.

(105) Massiot, D.; Fayon, F.; Deschamps, M.; Cadars, S.; Florian, P.; Montouillout, V.; Pellerin, N.; Hiet, J.; Rakhmatullin, A.; Bessada, C. Detection and use of small J couplings in solid state NMR experiments. *Comptes Rendus Chimie* **2010**, *13*, 117–129.

(106) Burum, D. P. Cross Polarization in Solids. In *eMagRes*; Harris, R. K., Wasylishen, R. L., Eds.; John Wiley & Sons, Ltd: Chichester, UK, 2007; p 57.

(107) Zhang, R.; Mroue, K. H.; Ramamoorthy, A. Hybridizing cross-polarization with NOE or refocused-INEPT enhances the sensitivity of MAS NMR spectroscopy. *Journal of magnetic resonance (San Diego, Calif. : 1997)* **2016**, *266*, 59–66.

(108) Johnson, R. L.; Schmidt-Rohr, K. Quantitative solid-state 13C NMR with signal enhancement by multiple cross polarization. *Journal of magnetic resonance (San Diego, Calif. : 1997)* **2014**, *239*, 44–49.

(109) Lilly Thankamony, A. S.; Wittmann, J. J.; Kaushik, M.; Corzilius, B. Dynamic nuclear polarization for sensitivity enhancement in modern solid-state NMR. *Progress in Nuclear Magnetic Resonance Spectroscopy* **2017**, *102-103*, 120–195.

(110) Rossini, A. J.; Zagdoun, A.; Lelli, M.; Lesage, A.; Copéret, C.; Emsley, L. Dynamic nuclear polarization surface enhanced NMR spectroscopy. *Accounts of chemical research* **2013**, *46*, 1942–1951.

(111) Rosay, M.; Blank, M.; Engelke, F. Instrumentation for solid-state dynamic nuclear polarization with magic angle spinning NMR. *Journal of magnetic resonance (San Diego, Calif. : 1997)* **2016**, *264*, 88–98.

(112) Matsuki, Y.; Nakamura, S.; Fukui, S.; Suematsu, H.; Fujiwara, T. Closed-cycle cold helium magic-angle spinning for sensitivity-enhanced multi-dimensional solid-state NMR. *Journal of magnetic resonance (San Diego, Calif. : 1997)* **2015**, *259*, 76–81.

(113) Bouleau, E.; Saint-Bonnet, P.; Mentink-Vigier, F.; Takahashi, H.; Jacquot, J.-F.; Bardet, M.; Aussenac, F.; Purea, A.; Engelke, F.; Hediger, S. *et al.* Pushing NMR sensitivity limits using dynamic nuclear polarization with closed-loop cryogenic helium sample spinning. *Chemical science* **2015**, *6*, 6806–6812.

(114) Concistrè, M.; Johannessen, O. G.; Carignani, E.; Geppi, M.; Levitt, M. H. Magic-angle spinning NMR of cold samples. *Accounts of chemical research* **2013**, *46*, 1914–1922.

(115) Kärger, J.; Freude, D.; Haase, J. Diffusion in Nanoporous Materials: Novel Insights by Combining MAS and PFG NMR. *Processes* **2018**, *6*, 147.

(116) Ashbrook, S. E.; Duer, M. J. Structural information from quadrupolar nuclei in solid state NMR. *Concepts Magn. Reson.* **2006**, *28A*, 183–248.

(117) Man, P. P. Quadrupole Couplings in Nuclear Magnetic Resonance, General. In *Encyclopedia of Analytical Chemistry*; Meyers, R. A., Ed.; John Wiley & Sons, Ltd: Chichester, UK, 2006; p 685.

(118) Mizuno, M. Solid-State 2H NMR Studies of Molecular Motion in Functional Materials. In *Experimental Approaches of NMR Spectroscopy*; Soci, T. N. M. R., Ed.; Springer Singapore: Singapore, 2018; pp 341–364.

(119) Freude, D. Quadrupolar Nuclei in Solid-State Nuclear Magnetic Resonance. In *Encyclopedia of Analytical Chemistry*; Meyers, R. A., Ed.; John Wiley & Sons, Ltd: Chichester, UK, 2006; p 126.

(120) Amoureux, J.-P.; Pruski, M. MQMAS NMR: Experimental Strategies and Applications. In *eMagRes*; Harris, R. K., Wasylishen, R. L., Eds.; John Wiley & Sons, Ltd: Chichester, UK, 2007; p 1659.

(121) Gan, Z. Perspectives on high-field and solid-state NMR methods of quadrupole nuclei. *Journal of magnetic resonance (San Diego, Calif. : 1997)* **2019**, *306*, 86–90.

(122) Vosegaard, T.; Kehlet, C.; Khaneja, N.; Glaser, S. J.; Nielsen, N. C. Improved excitation schemes for multiple-quantum magic-angle spinning for quadrupolar nuclei designed using optimal control theory. *Journal of the American Chemical Society* **2005**, *127*, 13768–13769.

(123) Wu, G.; Rovnyak, D.; Griffin, R. G. Quantitative Multiple-Quantum Magic-Angle-Spinning NMR Spectroscopy of Quadrupolar Nuclei in Solids. *J. Am. Chem. Soc.* **1996**, *118*, 9326–9332.

(124) Colaux, H.; Dawson, D. M.; Ashbrook, S. E. Investigating FAM-N pulses for signal enhancement in MQMAS NMR of quadrupolar nuclei. *Solid state nuclear magnetic resonance* **2017**, *84*, 89–102.

(125) Koczor, B.; Rohonczy, J. A novel pulse scheme for multiple quantum excitation, SFAM to enhance the sensitivity of MQMAS experiments. *Solid state nuclear magnetic resonance* **2016**, *74-75*, 1–9.

(126) Amoureux, J. P.; Delevoye, L.; Steuernagel, S.; Gan, Z.; Ganapathy, S.; Montagne, L. Increasing the sensitivity of 2D high-resolution NMR methods applied to quadrupolar nuclei. *Journal of magnetic resonance (San Diego, Calif. : 1997)* **2005**, *172*, 268–278.

(127) Kentgens, A.P.M.; Verhagen, R. Advantages of double frequency sweeps in static, MAS and MQMAS NMR of spin I=3/2 nuclei. *Chemical Physics Letters* **1999**, *300*, 435–443.

(128) Lefort, R.; Wiench, J. W.; Pruski, M.; Amoureux, J.-P. Optimization of data acquisition and processing in Carr–Purcell–Meiboom–Gill multiple quantum magic angle spinning nuclear magnetic resonance. *The Journal of Chemical Physics* **2002**, *116*, 2493–2501.

(129) Gan, Z. Isotropic NMR Spectra of Half-Integer Quadrupolar Nuclei Using Satellite Transitions and Magic-Angle Spinning. *J. Am. Chem. Soc.* **2000**, *122*, 3242–3243.

(130) Hung, I.; Gan, Z. A magic-angle turning NMR experiment for separating spinning sidebands of half-integer quadrupolar nuclei. *Chemical Physics Letters* **2010**, *496*, 162–166.

(131) Gullion, T.; Schaefer, J. Rotational-echo double-resonance NMR. *Journal of Magnetic Resonance (1969)* **1989**, *81*, 196–200.

(132) Fyfe, C. A.; Mueller, K. T.; Grondey, H.; Wong-Moon, K. C. Dipolar dephasing between quadrupolar and spin-12 nuclei. REDOR and TEDOR NMR experiments on VPI-5. *Chemical Physics Letters* **1992**, *199*, 198–204.

(133) Toke, O.; Cegelski, L. REDOR Applications in Biology: An Overview. In *Encyclopedia of Magnetic Resonance*; Harris, R. K., Ed.; John Wiley & Sons, Ltd: Chichester, UK, 2007; p 196.

(134) Hing, A. W.; Vega, S.; Schaefer, J. Transferred-echo double-resonance NMR. *Journal of Magnetic Resonance (1969)* **1992**, *96*, 205–209.

(135) Grey, C. P.; Eijkelenboom, A. P.A.M.; Veeman, W. S. 14N Population transfers in two-dimensional 13C・14N・1H triple-resonance magic-angle spinning nuclear magnetic resonance spectroscopy. *Solid state nuclear magnetic resonance* **1995**, *4*, 113–120.

(136) Gullion, T. Measurement of dipolar interactions between spin-12 and quadrupolar nuclei by rotational-echo, adiabatic-passage, double-resonance NMR. *Chemical Physics Letters* **1995**, *246*, 325–330.

(137) Claridge, T. D. W. *High-resolution NMR techniques in Organic Chemistry*, 3. ed.; Elsevier: Amsterdam, 2016.

(138) Fernandez, C.; Pruski, M. Probing quadrupolar nuclei by solid-state NMR spectroscopy: recent advances. *Topics in current chemistry* **2012**, *306*, 119–188.

(139) Cudby, M.E.A.; Willis, H. A. The Nuclear Magnetic Resonance Spectra of Polymers. *Annual Reports on NMR Spectroscopy Volume 4*; Annual Reports on NMR Spectroscopy; Elsevier, 1972; pp 363–389.

(140) Matyjaszewski, K.; Möller, M. *Polymer science: A comprehensive reference*; Elsevier: Amsterdam, 2012.

(141) Rinaldi, P. L. Polymer Characterization by 3D Solution NMR. In *NMR Spectroscopy of Polymers in Solution and in the Solid State*; Cheng, H. N., English, A. D., Eds.; ACS Symposium Series; American Chemical Society: Washington, DC, 2002; pp 94–122.

(142) Guo, X.; Laryea, E.; Wilhelm, M.; Luy, B.; Nirschl, H.; Guthausen, G. Diffusion in Polymer Solutions: Molecular Weight Distribution by PFG-NMR and Relation to SEC. *Macromol. Chem. Phys.* **2017**, *218*, 1600440.

(143) Janiak, C.; Lassahn, P. G. The Vinyl Homopolymerization of Norbornene. *Macromol. Rapid Commun.* **2001**, *22*, 479–493.

(144) Baugh, L. S.; Canich, J. A. M. *Stereoselective polymerization with single-site catalysts*; CRC Press: Boca Raton, 2008.

(145) Flook, M. M.; Jiang, A. J.; Schrock, R. R.; Müller, P.; Hoveyda, A. H. Z-selective olefin metathesis processes catalyzed by a molybdenum hexaisopropylterphenoxide monopyrrolide complex. *Journal of the American Chemical Society* **2009**, *131*, 7962–7963.

(146) *The poly(NBE) NMR spectra are courtesy of Shigetaka Hayano from Zeon Corp.*

(147) Autenrieth, B.; Schrock, R. R. Stereospecific Ring-Opening Metathesis Polymerization (ROMP) of Norbornene and Tetracyclododecene by Mo and W Initiators. *Macromolecules* **2015**, *48*, 2493–2503.

(148) Whittaker, A. K. NMR Studies of Cross linked Polymers; Annual Reports on NMR Spectroscopy; Elsevier, 1997; pp 105–183.

(149) Mathur, A. M.; Scranton, A. B. Characterization of hydrogels using nuclear magnetic resonance spectroscopy. *Biomaterials* **1996**, *17*, 547–557.

(150) Ando, I.; Asakura, T. *Solid state NMR of polymers*; Studies in physical and theoretical chemistry 84; Elsevier: Amsterdam, New York, 1998.

(151) Rinaldi, P. L. Tutorial on Solution NMR of Polymers. In *NMR Spectroscopy of Polymers: Innovative Strategies for Complex Macromolecules*; Cheng, H. N., Asakura, T., English, A. D., Eds.; ACS Symposium Series; American Chemical Society: Washington, DC, 2011; pp 37–63.

(152) Cheng, H. N.; English, A. D. Advances in the NMR Spectroscopy of Polymers: An Overview. In *NMR Spectroscopy of Polymers: Innovative Strategies for Complex Macromolecules*; Cheng, H. N., Asakura, T., English, A. D., Eds.; ACS Symposium Series; American Chemical Society: Washington, DC, 2011; pp 3–20.

(153) Chakrapani, S. B.; Minkler, M. J.; Beckingham, B. S. Low-field 1H-NMR spectroscopy for compositional analysis of multicomponent polymer systems. *The Analyst* **2019**, *144*, 1679–1686.

(154) Bryce, D. L. NMR crystallography: structure and properties of materials from solid-state nuclear magnetic resonance observables. *IUCrJ* **2017**, *4*, 350–359.

(155) Schwoerer, M.; Wolf, H. C. *Organic molecular solids*; Wiley-VCH: Weinheim, 2007.

(156) Schmidt-Rohr, K. *Multidimensional Solid-State NMR and Polymers*; Elsevier Science: Burlington, 2012.

(157) Spiess, H. W. Polymer Dynamics and Order from Multidimensional Solid State NMR. In *Encyclopedia of Magnetic Resonance*; Harris, R. K., Ed.; John Wiley & Sons, Ltd: Chichester, UK, 2007; p 1655.

(158) Le, D.; Ziarelli, F.; Phan, T. N. T.; Mollica, G.; Thureau, P.; Aussenac, F.; Ouari, O.; Gigmes, D.; Tordo, P.; Viel, S. Up to 100% Improvement in Dynamic Nuclear Polarization Solid-State NMR Sensitivity Enhancement of Polymers by Removing Oxygen. *Macromolecular rapid communications* **2015**, *36*, 1416–1421.

(159) Rouger, L.; Yon, M.; Sarou-Kanian, V.; Fayon, F.; Dumez, J.-N.; Giraudeau, P. Ultrafast acquisition of 1H-1H dipolar correlation experiments in spinning elastomers. *Journal of magnetic resonance (San Diego, Calif. : 1997)* **2017**, *277*, 30–35.

(160) Domján, A.; Manek, E.; Geissler, E.; László, K. Host–Guest Interactions in Poly(N -isopropylacrylamide) Hydrogel Seen by One- and Two-Dimensional 1 H CRAMPS Solid-State NMR Spectroscopy. *Macromolecules* **2013**, *46*, 3118–3124.

(161) Elena, B.; Pintacuda, G.; Mifsud, N.; Emsley, L. Molecular structure determination in powders by NMR crystallography from proton spin diffusion. *Journal of the American Chemical Society* **2006**, *128*, 9555–9560.

(162) Brown, S. P.; Schnell, I.; Brand, J. D.; Müllen, K.; Spiess, H. W. An Investigation of π−π Packing in a Columnar Hexabenzocoronene by Fast Magic-Angle Spinning and Double-Quantum 1 H Solid-State NMR Spectroscopy. *J. Am. Chem. Soc.* **1999**, *121*, 6712–6718.

(163) Kesling, B.; Hughes, E.; Gullion, T. 13C–14N REAPDOR and 13C–2D θ-REDOR NMR on a blend of tri-p-tolylamine and bisphenol-A-polycarbonate. *Solid state nuclear magnetic resonance* **2000**, *16*, 1–7.

(164) Dybowski, C. Characterization of Materials with NMR Spectroscopy. In *NMR Spectroscopy of Polymers: Innovative Strategies for Complex Macromolecules*; Cheng, H. N., Asakura, T., English, A. D., Eds.; ACS Symposium Series; American Chemical Society: Washington, DC, 2011; pp 135–160.

(165) Spiess, H. W. 50th Anniversary Perspective : The Importance of NMR Spectroscopy to Macromolecular Science. *Macromolecules* **2017**, *50*, 1761–1777.

(166) Alam, T. M.; Childress, K. K.; Pastoor, K.; Rice, C. V. Characterization of free, restricted, and entrapped water environments in poly(N -isopropyl acrylamide) hydrogels via 1 H HRMAS PFG NMR spectroscopy. *J. Polym. Sci. Part B: Polym. Phys.* **2014**, *52*, 1521–1527.

(167) Maunu, S.L. NMR studies of wood and wood products. *Progress in Nuclear Magnetic Resonance Spectroscopy* **2002**, *40*, 151–174.

(168) Lambert, J. B.; Wu, Y.; Santiago-Blay, J. A. High-Resolution Solid State NMR Spectroscopy of Cultural Organic Material. In *Modern Magnetic Resonance*; Webb, G. A., Ed.; Springer International Publishing: Cham, 2016; pp 1–22.

(169) Asakura, T.; Tasei, Y. NMR Studies on Silk Materials. In *Experimental Approaches of NMR Spectroscopy*; Soci, T. N. M. R., Ed.; Springer Singapore: Singapore, 2018; pp 297–312.

(170) Fitzgerald, J. J. *Solid-State NMR Spectroscopy of Inorganic Materials* 717; American Chemical Society: Washington, DC, 1999.

(171) Hanna, J. V.; Smith, M. E. Recent technique developments and applications of solid state NMR in characterising inorganic materials. *Solid state nuclear magnetic resonance* **2010**, *38*, 1–18.

(172) van der Klink, J. J.; Brom, H. B. NMR in metals, metal particles and metal cluster compounds. *Progress in Nuclear Magnetic Resonance Spectroscopy* **2000**, *36*, 89–201.

(173) Hatfield, G. R.; Carduner, K. R. Solid state NMR: Applications in high performance ceramics. *J Mater Sci* **1989**, *24*, 4209–4219.

(174) Lapina, O. B.; Shubin, A. A.; Terskikh, V. V. Solid-State NMR of Oxide-Based Materials. In *Modern Magnetic Resonance*; Webb, G. A., Ed.; Springer International Publishing: Cham, 2016; pp 1–37.

(175) Ashbrook, S. E.; Dawson, D. M. NMR spectroscopy of minerals and allied materials. In *Nuclear Magnetic Resonance*; Ramesh, V., Ed.; Nuclear Magnetic Resonance; Royal Society of Chemistry: Cambridge, 2016; pp 1–52.

(176) Youngman, R. NMR Spectroscopy in Glass Science: A Review of the Elements. *Materials (Basel, Switzerland)* **2018**, *11*.

(177) Walkley, B.; Provis, J. L. Solid-state nuclear magnetic resonance spectroscopy of cements. *Materials Today Advances* **2019**, *1*, 100007.

(178) Souza, F. A. L. de; Ambrozio, A. R.; Souza, E. S.; Cipriano, D. F.; Scopel, W. L.; Freitas, J. C. C. NMR Spectral Parameters in Graphene, Graphite, and Related Materials: Ab Initio Calculations and Experimental Results. *J. Phys. Chem. C* **2016**, *120*, 27707–27716.

(179) Agarwal, N.; Nair, M. S.; Mazumder, A.; Poluri, K. M. Characterization of Nanomaterials Using Nuclear Magnetic Resonance Spectroscopy. *Characterization of Nanomaterials*; Elsevier, 2018; pp 61–102.

(180) Borisov, A. S.; Hazendonk, P.; Hayes, P. G. Solid-State Nuclear Magnetic Resonance Spectroscopy: A Review of Modern Techniques and Applications for Inorganic Polymers. *J Inorg Organomet Polym* **2010**, *20*, 183–212.

(181) Sirusi, A. A.; Ross, J. H. Recent NMR Studies of Thermoelectric Materials; Annual Reports on NMR Spectroscopy; Elsevier, 2017; pp 137–198.

(182) Nagashima, H.; Tricot, G.; Trébosc, J.; Lafon, O.; Amoureux, J.-P.; Pourpoint, F. 3D correlation NMR spectrum between three distinct heteronuclei for the characterization of inorganic samples: Application on sodium alumino-phosphate materials. *Solid state nuclear magnetic resonance* **2017**, *84*, 164–170.

(183) Martineau, C. NMR crystallography: Applications to inorganic materials. *Solid state nuclear magnetic resonance* **2014**, *63-64*, 1–12.

(184) Moran, R. F.; Dawson, D. M.; Ashbrook, S. E. Exploiting NMR spectroscopy for the study of disorder in solids. *International Reviews in Physical Chemistry* **2017**, *36*, 39–115.

(185) Jain, M. G.; Mote, K. R.; Madhu, P. K. NMR Crystallography at Fast Magic-Angle Spinning Frequencies: Application of Novel Recoupling Methods. *Crystals* **2019**, *9*, 231.

(186) Bakhmutov, V. I. *Solid-State NMR in Materials Science: Principles and Applications*, 1st; CRC Press, 2016.

(187) Harris, K. D. M. New in situ solid-state NMR strategies for exploring materials formation and adsorption processes: prospects in heterogenous catalysis. *Appl Petrochem Res* **2016**, *6*, 295–306.

(188) Marchetti, A.; Chen, J.; Pang, Z.; Li, S.; Ling, D.; Deng, F.; Kong, X. Understanding Surface and Interfacial Chemistry in Functional Nanomaterials via Solid-State NMR. *Advanced materials (Deerfield Beach, Fla.)* **2017**, *29*.

(189) Stebbins, J. F. Nuclear magnetic resonance at high temperature. *Chem. Rev.* **1991**, *91*, 1353–1373.

(190) Brus, J.; Dybal, J. Hydrogen-Bond Interactions in Organically-Modified Polysiloxane Networks Studied by 1D and 2D CRAMPS and Double-Quantum 1 H MAS NMR. *Macromolecules* **2002**, *35*, 10038–10047.

(191) Mafra, L.; Rocha, J.; Fernandez, C.; Castro, G. R.; García-Granda, S.; Espina, A.; Khainakov, S. A.; García, J. R. Characterization of Layered γ-Titanium Phosphate (C 2 H 5 NH 3)[Ti(H 1.5 PO 4)(PO 4)] 2 ·H 2 O Intercalate: A Combined NMR, Synchrotron XRD, and DFT Calculations Study. *Chem. Mater.* **2008**, *20*, 3944–3953.

(192) Ganapathy, S.; Fournier, M.; Paul, J. F.; Delevoye, L.; Guelton, M.; Amoureux, J. P. Location of protons in anhydrous Keggin heteropolyacids H(3)PMo(12)O(40) and H(3)PW(12)O(40) by (1)H(31)P/(31)P(1)H REDOR NMR and DFT quantum chemical calculations. *J. Am. Chem. Soc.* **2002**, *124*, 7821–7828.

(193) Li, S.; Deng, F. Recent Advances of Solid-State NMR Studies on Zeolites; Annual Reports on NMR Spectroscopy; Elsevier, 2013; pp 1–54.

(194) Spencer, T. L.; Plagos, N. W.; Brouwer, D. H.; Goward, G. R. The use of 6Li{7Li}-REDOR NMR spectroscopy to compare the ionic conductivities of solid-state lithium ion electrolytes. *Physical chemistry chemical physics : PCCP* **2014**, *16*, 2515–2526.

(195) Rottreau, T. J.; Parlett, C. M. A.; Lee, A. F.; Evans, R. Diffusion NMR Characterization of Catalytic Silica Supports: A Tortuous Path. *J. Phys. Chem. C* **2017**, *121*, 16250–16256.

(196) Engelke, S.; Marbella, L. E.; Trease, N. M.; Volder, M. de; Grey, C. P. Three-dimensional pulsed field gradient NMR measurements of self-diffusion in anisotropic materials for energy storage applications. *Physical chemistry chemical physics : PCCP* **2019**, *21*, 4538–4546.

(197) Dvoyashkina, N.; Freude, D.; Stepanov, A. G.; Böhlmann, W.; Krishna, R.; Kärger, J.; Haase, J. Alkane/alkene mixture diffusion in silicalite-1 studied by MAS PFG NMR. *Microporous and Mesoporous Materials* **2018**, *257*, 128–134.

(198) Lauerer, A.; Kurzhals, R.; Toufar, H.; Freude, D.; Kärger, J. Tracing compartment exchange by NMR diffusometry: Water in lithium-exchanged low-silica X zeolites. *Journal of magnetic resonance (San Diego, Calif. : 1997)* **2018**, *289*, 1–11.

(199) Cho, H. J.; Sigmund, E. E.; Song, Y. Magnetic Resonance Characterization of Porous Media Using Diffusion through Internal Magnetic Fields. *Materials (Basel, Switzerland)* **2012**, *5*, 590–616.

(200) Zhang, Y.; Xiao, L.; Liao, G.; Song, Y.-Q. Direct correlation of diffusion and pore size distributions with low field NMR. *Journal of magnetic resonance (San Diego, Calif. : 1997)* **2016**, *269*, 196–202.

(201) Martineau-Corcos, C.; Dědeček, J.; Taulelle, F. 27Al-27Al double-quantum single-quantum MAS NMR: Applications to the structural characterization of microporous materials. *Solid state nuclear magnetic resonance* **2017**, *84*, 65–72.

(202) Weiland, E.; Springuel-Huet, M.-A.; Nossov, A.; Gédéon, A. 129 Xenon NMR: Review of recent insights into porous materials. *Microporous and Mesoporous Materials* **2016**, *225*, 41–65.

(203) Ashbrook, S. E.; Smith, M. E. Solid state 17O NMR-an introduction to the background principles and applications to inorganic materials. *Chemical Society reviews* **2006**, *35*, 718–735.

(204) Bignami, G. P. M.; Dawson, D. M.; Seymour, V. R.; Wheatley, P. S.; Morris, R. E.; Ashbrook, S. E. Synthesis, Isotopic Enrichment, and Solid-State NMR Characterization of Zeolites Derived from the Assembly, Disassembly, Organization, Reassembly Process. *J. Am. Chem. Soc.* **2017**, *139*, 5140–5148.

(205) Blanc, F.; Sperrin, L.; Jefferson, D. A.; Pawsey, S.; Rosay, M.; Grey, C. P. Dynamic nuclear polarization enhanced natural abundance 17O spectroscopy. *Journal of the American Chemical Society* **2013**, *135*, 2975–2978.

(206) Perras, F. A.; Chaudhary, U.; Slowing, I. I.; Pruski, M. Probing Surface Hydrogen Bonding and Dynamics by Natural Abundance, Multidimensional, 17 O DNP-NMR Spectroscopy. *J. Phys. Chem. C* **2016**, *120*, 11535–11544.

(207) Satterlee, J. D. Fundamental Concepts of NMR in Paramagnetic Systems Part I: The Isotropic Shift. *Concepts Magn. Reson.* **1990**, *2*, 69–79.

(208) Satterlee, J. D. Fundamental Concepts of NMR in Paramagnetic Systems. Part II: Relaxation Effects. *Concepts Magn. Reson.* **1990**, *2*, 119–129.

(209) Roessler, M. M.; Salvadori, E. Principles and applications of EPR spectroscopy in the chemical sciences. *Chemical Society reviews* **2018**, *47*, 2534–2553.

(210) Bertmer, M. Paramagnetic solid-state NMR of materials. *Solid state nuclear magnetic resonance* **2017**, *81*, 1–7.

(211) Nishimura, S.; Takagaki, A.; Ebitani, K. Characterization, synthesis and catalysis of hydrotalcite-related materials for highly efficient materials transformations. *Green Chem.* **2013**, *15*, 2026.

(212) Cavani, F.; Trifirò, F.; Vaccari, A. Hydrotalcite-type anionic clays: Preparation, properties and applications. *Catalysis Today* **1991**, *11*, 173–301.

(213) Sideris, P. J.; Nielsen, U. G.; Gan, Z.; Grey, C. P. Mg/Al ordering in layered double hydroxides revealed by multinuclear NMR spectroscopy. *Science (New York, N.Y.)* **2008**, *321*, 113–117.

(214) Abelló, S.; Medina, F.; Tichit, D.; Pérez-Ramírez, J.; Groen, J. C.; Sueiras, J. E.; Salagre, P.; Cesteros, Y. Aldol condensations over reconstructed Mg-Al hydrotalcites: structure-activity relationships related to the rehydration method. *Chemistry (Weinheim an der Bergstrasse, Germany)* **2005**, *11*, 728–739.

(215) Matzkanin, G. A. A Review of Nondestructive Characterization of Composites Using NMR. In *Nondestructive Characterization of Materials*; Höller, P., Hauk, V., Dobmann, G., Ruud, C. O., Green, R. E., Eds.; Springer Berlin Heidelberg: Berlin, Heidelberg, 1989; pp 655–669.

(216) Martini, F.; Geppi, M.; Borsacchi, S. NMR Spectroscopy of Clay–Polymer Nanocomposites. *Clay-Polymer Nanocomposites*; Elsevier, 2017; pp 307–325.

(217) Bonhomme, C.; Gervais, C.; Laurencin, D. Recent NMR developments applied to organic-inorganic materials. *Progress in Nuclear Magnetic Resonance Spectroscopy* **2014**, *77*, 1–48.

(218) Sutrisno, A.; Huang, Y. Solid-state NMR: a powerful tool for characterization of metal-organic frameworks. *Solid state nuclear magnetic resonance* **2013**, *49-50*, 1–11.

(219) Grekov, D.; Vancompernolle, T.; Taoufik, M.; Delevoye, L.; Gauvin, R. M. Solid-state NMR of quadrupolar nuclei for investigations into supported organometallic catalysts: scope and frontiers. *Chemical Society reviews* **2018**, *47*, 2572–2590.

(220) Copéret, C.; Allouche, F.; Chan, K. W.; Conley, M. P.; Delley, M. F.; Fedorov, A.; Moroz, I. B.; Mougel, V.; Pucino, M.; Searles, K. *et al.* Bridging the Gap between Industrial and Well-Defined Supported Catalysts. *Angewandte Chemie (International ed. in English)* **2018**, *57*, 6398–6440.

(221) Basset, J.-M.; Gates, B. C.; Candy, J.-P.; Choplin, A.; Leconte, M.; Quignard, F.; Santini, C. *Surface Organometallic Chemistry: Molecular Approaches to Surface Catalysis*; Springer Netherlands: Dordrecht, 1988.

(222) Basset, J. M.; Ugo, R. On the Origins and Development of“Surface Organometallic Chemistry”. In *Modern Surface Organometallic Chemistry*; Basset, J.-M., Psaro, R., Roberto, D., Ugo, R., Eds.; Wiley-VCH Verlag GmbH & Co. KGaA: Weinheim, Germany, 2009; pp 1–21.

(223) Pucino, M.; Mougel, V.; Schowner, R.; Fedorov, A.; Buchmeiser, M. R.; Copéret, C. Cationic Silica-Supported N-Heterocyclic Carbene Tungsten Oxo Alkylidene Sites: Highly Active and Stable Catalysts for Olefin Metathesis. *Angewandte Chemie (International ed. in English)* **2016**, *55*, 4300–4302.

(224) Pucino, M.; Inoue, M.; Gordon, C. P.; Schowner, R.; Stöhr, L.; Sen, S.; Hegedüs, C.; Robé, E.; Tóth, F.; Buchmeiser, M. R. *et al.* Promoting Terminal Olefin Metathesis with a Supported Cationic Molybdenum Imido Alkylidene N-Heterocyclic Carbene Catalyst. *Angewandte Chemie (International ed. in English)* **2018**, *57*, 14566–14569.

(225) Ong, T.-C.; Liao, W.-C.; Mougel, V.; Gajan, D.; Lesage, A.; Emsley, L.; Copéret, C. Atomistic Description of Reaction Intermediates for Supported Metathesis Catalysts Enabled by DNP SENS. *Angewandte Chemie (International ed. in English)* **2016**, *55*, 4743–4747.

(226) Ashbrook, S. E.; Griffin, J. M.; Johnston, K. E. Recent Advances in Solid-State Nuclear Magnetic Resonance Spectroscopy. *Annual review of analytical chemistry (Palo Alto, Calif.)* **2018**, *11*, 485–508.

(227) Férey, G.; Haouas, M.; Loiseau, T.; Taulelle, F. Nanoporous Solids: How Do They Form? An In Situ Approach. *Chem. Mater.* **2014**, *26*, 299–309.

(228) Haouas, M. Nuclear Magnetic Resonance Spectroscopy for In Situ Monitoring of Porous Materials Formation under Hydrothermal Conditions. *Materials (Basel, Switzerland)* **2018**, *11*.

(229) Hu, J. Z.; Hu, M. Y.; Zhao, Z.; Xu, S.; Vjunov, A.; Shi, H.; Camaioni, D. M.; Peden, C. H. F.; Lercher, J. A. Sealed rotors for in situ high temperature high pressure MAS NMR. *Chemical communications (Cambridge, England)* **2015**, *51*, 13458–13461.

(230) Hughes, C. E.; Williams, P. A.; Harris, K. D. M. "CLASSIC NMR": an in-situ NMR strategy for mapping the time-evolution of crystallization processes by combined liquid-state and solid-state measurements. *Angewandte Chemie (International ed. in English)* **2014**, *53*, 8939–8943.

(231) Harris, K. D. M.; Hughes, C. E.; Williams, P. A.; Edwards-Gau, G. R. `NMR Crystallization': in-situ NMR techniques for time-resolved monitoring of crystallization processes. *Acta crystallographica. Section C, Structural chemistry* **2017**, *73*, 137–148.

(232) Odin, C. NMR Studies of Phase Transitions; Annual Reports on NMR Spectroscopy; Elsevier, 2006; pp 117–205.

(233) BIELECKI, A.; Burum, D. P. Temperature Dependence of 207 Pb MAS Spectra of Solid Lead Nitrate. An Accurate, Sensitive Thermometer for Variable-Temperature MAS. *Journal of Magnetic Resonance, Series A* **1995**, *116*, 215–220.

(234) Beckmann; Dybowski. A thermometer for nonspinning solid-state NMR spectroscopy. *Journal of magnetic resonance (San Diego, Calif. : 1997)* **2000**, *146*, 379–380.

(235) Bernard, G. M.; Goyal, A.; Miskolzie, M.; McKay, R.; Wu, Q.; Wasylishen, R. E.; Michaelis, V. K. Methylammonium lead chloride: A sensitive sample for an accurate NMR thermometer. *Journal of magnetic resonance (San Diego, Calif. : 1997)* **2017**, *283*, 14–21.

(236) Zhang, W.; Xu, S.; Han, X.; Bao, X. In situ solid-state NMR for heterogeneous catalysis: a joint experimental and theoretical approach. *Chemical Society reviews* **2012**, *41*, 192–210.

(237) Wang, X. L.; Liu, W.; Yu, Y.-Y.; Song, Y.; Fang, W. Q.; Wei, D.; Gong, X.-Q.; Yao, Y.-F.; Yang, H. G. Operando NMR spectroscopic analysis of proton transfer in heterogeneous photocatalytic reactions. *Nature communications* **2016**, *7*, 11918.

(238) Leutzsch, M.; Sederman, A. J.; Gladden, L. F.; Mantle, M. D. In situ reaction monitoring in heterogeneous catalysts by a benchtop NMR spectrometer. *Magnetic resonance imaging* **2019**, *56*, 138–143.

(239) Paul, G.; Bisio, C.; Braschi, I.; Cossi, M.; Gatti, G.; Gianotti, E.; Marchese, L. Combined solid-state NMR, FT-IR and computational studies on layered and porous materials. *Chemical Society reviews* **2018**, *47*, 5684–5739.

(240) Mori, H.; Kono, H.; Terano, M.; Nosov, A.; Zakharov, V. A. In situCP MAS NMR spectroscopy under continuous-flow conditions to monitor real time dynamics during propene polymerization over a supported Ziegler catalyst. *Macromol. Rapid Commun.* **1999**, *20*, 536–540.

(241) Haven, J. J.; Junkers, T. Online Monitoring of Polymerizations: Current Status. *Eur. J. Org. Chem.* **2017**, *2017*, 6474–6482.

(242) Hughes, C. E.; Walkley, B.; Gardner, L. J.; Walling, S. A.; Bernal, S. A.; Iuga, D.; Provis, J. L.; Harris, K. D. M. Exploiting in-situ solid-state NMR spectroscopy to probe the early stages of hydration of calcium aluminate cement. *Solid state nuclear magnetic resonance* **2019**, *99*, 1–6.

(243) Pecher, O.; Vyalikh, A.; Grey, C. P. Challenges and new opportunities of in situ NMR characterization of electrochemical processes. In ; Author(s), 2016; p 20011.

(244) Hu, J. Z.; Jaegers, N. R.; Hu, M. Y.; Mueller, K. T. In situ and ex situ NMR for battery research. *Journal of physics. Condensed matter : an Institute of Physics journal* **2018**, *30*, 463001.

(245) Pecher, O.; Carretero-González, J.; Griffith, K. J.; Grey, C. P. Materials' Methods: NMR in Battery Research. *Chem. Mater.* **2017**, *29*, 213–242.

(246) Griffin, J. M.; Forse, A. C.; Grey, C. P. Solid-state NMR studies of supercapacitors. *Solid state nuclear magnetic resonance* **2016**, *74-75*, 16–35.

(247) Richter, J. B.; Eßbach, C.; Senkovska, I.; Kaskel, S.; Brunner, E. Quantitative in situ13C NMR studies of the electro-catalytic oxidation of ethanol. *Chemical communications (Cambridge, England)* **2019**, *55*, 6042–6045.

Index

O

P

Q

R

S

T

U

V